DISSERTATION

IN VITRO AND IN SITU PROPERTIES OF CANINE NEURAL PRECURSOR CELLS WITH RESPECT TO TRANSPLANTATION POTENTIAL

Submitted by

Raquel M. Walton

Department of Microbiology, Immunology, and Pathology

In partial fulfillment of the requirements

for the Degree of Doctor of Philosophy

Colorado State University

Fort Collins, Colorado

Spring 2006

COLORADO STATE UNIVERSITY

December 21, 2005

WE HEREBY RECOMMEND THAT THE DISSERTATION PREPARED UNDER OUR SUPERVISION BY Raquel M. Walton ENTITLED In Vitro and In Situ Properties of Canine Neural Precursor Cells with Respect to Transplantation Potential BE ACCEPTED AS FULFILLING IN PART REQUIREMENTS FOR THE DEGREE OF DOCTOR OF PHILOSOPHY.

Committee on Graduate Work

R A Bowen

Edward A. Hoover

Mary Anna Thrall
Advisor

Co-Advisor

Department Head

ABSTRACT OF DISSERTATION

IN VITRO AND IN SITU PROPERTIES OF CANINE NEURAL PRECURSOR CELLS WITH RESPECT TO TRANSPLANTATION POTENTIAL

Neurodegenerative diseases represent a broad spectrum of genetic and acquired processes that would benefit from CNS transplantation therapy. The lysosomal storage disease Mucopolysaccharidosis VII (MPS VII) is an inherited disorder caused by ß-glucuronidase (GUSB) enzyme deficiency whose signs include mental retardation due to neurodegenerative disease. The existence of both small and large animal homologues of human MPS VII make this disease a valuable model for transplantation therapy of storage diseases. The studies described herein focused upon the characterization of canine neural precursor cells (CNPCs) for CNS transplantation therapy in an animal model of MPS VII.

Canine NPCs were isolated from three neurogenic regions of the postnatal brain: the olfactory bulb, cerebellum and striatal subventricular zone (SVZ). The growth, expansion, and multipotency of CNPCs from unaffected and MPS VII dogs were compared. There were no differences attributable to CNPC genotype. Cerebellar-derived CNPCs grew more slowly than those from other brain regions. Cells obtained from all regions could be expanded ex vivo nearly 600-fold. Independent of genotype or region, undifferentiated CNPCs were immunopositive for nestin and glial fibrillary acidic protein (GFAP), and could be

differentiated into neurons, astrocytes and oligodendrocytes.

Neurogenic regions within the canine brain were evaluated for two candidate NPC cell surface markers, CD15 and CD133. We evaluated the immunophenotype of cells in the ventricular/subventricular zone and the cerebellum. CD15 immunoreactivity in the postnatal cerebellum was present in white matter tracts of folia. The embryonic ventricular zone and postnatal SVZ stained positively for CD15, but were immunonegative for CD133. The proportion of CD15-positive cells in the canine SVZ was 6.6 ± 2.2%. When cells from the SVZ were sorted into CD15-positive and negative populations, both populations could be expanded in response to basic fibroblast growth factor (bFGF) and epidermal growth factor (EGF), although CD15-positive cells more consistently so.

Efficient transduction of CNPCs was achieved with lentiviral and modified, selectable retroviral vectors containing the human GUSB gene and promoter. Transplantation of the lentivirus transduced CNPCs into a xenograft model (the neonatal SCID mouse) resulted in sparse but consistent GUSB-positive cell engraftment up to six weeks post-transplantation primarily in regions immediately adjacent to the lateral ventricles, especially white matter tracts. Xenografts of cells transduced with the retroviral vector showed robust GUSB expression at 1 week post-transplantation, but significant loss of GUSB activity was observed after 4 weeks.

In allograft transplants of lentivirus transduced cells, small numbers of GUSB-positive cells were detected in the canine striatum and thalamus up to the

latest time-point evaluated, 4 weeks post-transplantation. At 2 weeks post-transplantation, small numbers of nestin-positive and GFAP-positive graft cells were identified, but no graft cells stained with neuronal markers.

The data describe a population of postnatal cells in the dog that possess characteristics of neural precursor cells. These cells have at least limited self-renewal ability and are multipotent. It is hoped that CNPC characterization will afford a valuable model of therapeutic cellular transplantation in a large animal model of genetic neurodegenerative disease.

Raquel M. Walton
Department of Microbiology, Immunology, and Pathology
Colorado State University
Fort Collins, CO 80523
Spring 2006

ACKNOWLEDGMENTS

I would like to thank my advisor, Dr. Mary Anna Thrall, for her support and guidance in an unconventional graduate student arrangement. Thank you also to my co-advisor, Dr. John Wolfe, for his mentorship and knowledge. Dr. Wolfe provided me with the opportunity and the facilities in which to pursue research that was intellectually stimulating and of clinical significance. He also ensured that I received excellent guidance and training as a graduate student. The opportunity to do my doctoral research at the University of Pennsylvania afforded unique and invaluable collaborations with the Department of Radiology of the Hospital of the University of Pennsylvania and the Center for Comparative Medical Genetics, University of Pennsylvania School of Veterinary Medicine. It is due to the cooperation and mentorship of my advisor and co-advisor that I was able to complete the work necessary for my dissertation. My thanks also to the other members of my committee, Drs. Edward Hoover and Richard Bowen, for sharing their expertise and constructive criticisms.

Thank you to the members of the Wolfe laboratory, especially Aracelis Polesky, Erlinda Cabacungan, and Trena Clarke for their excellent technical assistance, readiness to help, and good company. I owe a debt of gratitude to Dr. Mark Haskins for his learned advice and support. Patty O'Donnell willingly provided expert technical assistance and moral support with the canine surgeries

and post-mortems. Drs. Harish Poptani and Sergey Magnitsky were an invaluable and productive collaborative team, without whom the imaging studies could not have been performed. Thank you to Dr. Gabi Seiler for her help in the ultrasound-guided canine neural precursor cell implantations; her expertise afforded a unique opportunity to image and target our transplantations.

Finally, a great amount of gratitude is owed to the animals that were sacrificed for these studies or that contributed neural tissue post-mortem. The animals were the most valuable part of these studies and it is hoped that the data obtained by their sacrifice will contribute to the development of an effective therapy for the many who suffer from neurodegenerative disease. All of the research was performed with the support of an NIH institutional training grant for post-graduate veterinarians from the NCRR.

TABLE OF CONTENTS

INTRODUCTION

The lysosomal storage diseases (LSDs) comprise a group of diseases whose etiology is due to a single enzyme deficiency within the cellular lysosome. There are over fifty acid hydrolases within lysosomes [46]. To date, there are over forty storage diseases that are attributable to a genetic defect coding for a single acid hydrolase [46, 180]. The lysosomal acid hydrolases catabolize various cellular macromolecules in a sequential fashion. At the end of the degradative sequence, the macromolecules may be recycled back into organelles. A defect in the enzymatic breakdown produces a buildup of the substrate that fails to be catabolized. The clinical manifestation of a LSD is dependent upon the type and location of substrate accumulation [73, 180]. Although every cell accumulates substrate, clinical manifestations of LSDs are highly variable [46, 73]. However, many LSDs have a significant neurologic component that is characterized by neurodegeneration [183, 73].

Mucopolysaccharidosis VII (MPS VII) is a neurodegenerative LSD that first manifests in early childhood [164]. Animal models of MPS VII exist in mice, cats, and dogs [59, 11, 52, 24, 47]. MPS VII is characterized by lysosomal ß-glucuronidase enzyme deficiency. Multiple organ failure and mental retardation succeed the accumulation of undegraded glycosaminoglycans in cellular

lysosomes [164]. MPS VII is a rare heritable disease, however, it serves as a paradigm for lysosomal storage diseases, which in aggregate occur in approximately one out of every five thousand births [7, 100]. MPS VII is a valuable paradigm for exploring lysosomal storage disease therapy because small and large animal models exist and there are sensitive molecular, biochemical, and histochemical reagents for the ß-glucuronidase enzyme [53, 164, 59, 193].

Therapeutic strategies for MPS VII include enzyme replacement, bone marrow transplantation, cellular implantation, and somatic cell gene therapy. Because of the blood-brain barrier, expression of ß-glucuronidase outside of the central nervous system (CNS) does not treat disease within the brain or spinal cord. With bone marrow transplantation, too few bone marrow cells enter into the brain to impact upon CNS disease. Thus, only direct CNS somatic cell gene therapy and cellular implantation show promise for treating CNS disease.

A significant challenge to the correction of inherited metabolic diseases via gene therapy is the need for global distribution of enzyme. However, MPS VII, like other lysosomal storage diseases, is particularly suited to gene and cellular implantation therapies due to the phenomenon of cross-correction [115]. Cross-correction occurs because lysosomal proteins such as ß-glucuronidase are post-translationally modified with mannose-6-phosphate residues. Mannose-6-phosphate moieties bind to receptors in a late Golgi compartment and dissociate in the acidic prelysosomal compartment. Due to receptor binding inefficiency, some lysosomal enzyme is secreted. A calcium-independent mannose-6-

phosphate receptor on the cell surface binds extracellular mannose-6-phosphate-containing enzymes and transfers them into a prelysosomal compartment via endocytosis. Thus, transduced or implanted cells can function as enzyme 'pumps,' secreting enzyme that can be delivered to nearby cells via cell surface mannose-6-phosphate receptors. Recent studies have shown that within the CNS correction can also occur in sites distal from transduced regions via axonal enzyme transport [163, 128, 96]. The effect of cellular transplants or cellular transduction may therefore be greatly amplified locally and distally via enzyme diffusion and axonal transport, respectively. For these reasons, treatment of lysosomal storage disorders with gene or cellular therapy may be feasible despite the global requirement for enzyme distribution.

Cellular therapy for Mucopolysaccharidosis VII

Gene transfer of lysosomal enzyme to the central nervous system has been accomplished using cellular therapy and direct viral transduction of neural cells [191, 167, 87, 163, 195, 84, 14, 74, 128, 132, 101, 148, 161]. Although non-neural cells such as fibroblasts and amniotic epithelial cells have been used for transplantation within the CNS [176], the use of neural stem/progenitor cells (NPCs) for cellular therapy could provide benefits beyond the expression of a single deficient protein. For example, NPCs can elaborate trophic factors to rescue dysfunctional endogenous neurons, inhibit inflammation, or replace dead and dying cells by differentiating into neurons and glia [166, 167, 144, 41, 44, 121, 175, 37, 131]. Moreover, unlike other cellular implants that may potentially

cause a space-occupying mass and disrupt neuronal connections, studies have shown that NPCs can integrate into the existing neural architecture and express a tissue-appropriate phenotype [167, 97, 172, 41, 44, 122, 175]. For the specific treatment of lysosomal storage diseases, transduced NPCs [87, 41, 14, 101, 161] or NPCs from normal mice [167, 195] can supply therapeutically relevant levels of a required protein.

Neural precursor cells

Neural stem cells (NSCs) are rigorously defined as multipotent, capable of extended self-renewal, and able to generate a large number of progeny [139]. Cells that demonstrate only multipotency, or are bi- or unipotent, are more appropriately termed 'neural progenitor cells'. For the purposes of this dissertation, the term 'neural precursor cell' (NPC) will be used to include both neural stem and progenitor cell populations. To date, NPCs have been isolated from mice, rats, pigs, dogs, sheep and primates [140, 105, 126, 200, 23, 124, 165, 35, 119]. During fetal development, neural stem cells are present in the neuroepithelium of the developing neural tube ventricular zone; these cells have a radial morphology and express markers of radial glial cells such as vimentin, RC1, RC2, nestin, and glial fibrillary acidic protein (GFAP; in primates only) [116, 134, 177]. Radial glia have been shown to differentiate into both neurons and glia [50, 116, 134, 177]. Indeed, lineage studies of SVZ radial glial cells have shown they can differentiate into astrocytes (including the astrocytic NPCs of the SVZ), neurons, oligodendrocytes, and ependymal cells [102]. After birth, radial

glia disappear, 'differentiating' into astrocytes. It was thought that with their disappearance, the ability for neurogenesis was lost. Only within the past fifteen years has it been established that neural stem cells and neurogenesis persist into adulthood.

In the 1960s, Altman was among the first to document neurogenesis within the postnatal CNS [2, 3]. Thirty years after the first report suggesting the possibility of postnatal neurogenesis, neural stem cells were isolated from the brains of adult mice [140, 142]. In vivo and in vitro studies show that adult NPCs are identified as GFAP-positive astrocytic cells in the subventricular zone (SVZ) and hippocampal subgranular zone [32, 88, 157, 70, 108, 51]. It is of interest to note that the radial glia-derived astrocytes of the SVZ share some of the molecular markers and structural features of radial glia, such as the presence of GFAP, contact with the ventricle, and a single cilium extended into the ventricle [134, 177]. Thus, the neural stem cell in both developing and adult vertebrates is a cell with markers and structural characteristics of an astrocyte. One emerging theory posits that the origin of adult NPCs is the ventricular zone neuroepithelial cells. In this view, neural stem cells persist from development through adulthood, undergoing a morphologic transformation from neuroepithelial cell to radial glial cell to astrocyte [30].

Neural precursor cells isolated from the developing and postnatal brain were first identified by their *in vitro* response to growth factors known to stimulate precursor proliferation in the developing neuroepithelium [140, 142, 137, 141]. In these studies, NPCs proliferated in response to epidermal growth factor (EGF) or

basic fibroblast growth factor (bFGF) with heparin. Basic fibroblast growth factor requires heparin to potentiate its action; heparin also prevents the degradation of bFGF *in vitro* [118, 18]. Subsequently, it was shown that NPCs in the mouse embryonic telencephalic germinal zone are responsive to FGF as early as embryonic day 8.5 (E8.5), but EGF responsiveness does not occur until E14.5 [178]. This study also suggested that EGF-responsive NPCs were lineage descendants of the FGF-responsive NPCs. Indeed, later studies showed that FGF upregulates EGF receptor expression in NPCs [92, 21].

Neural precursor cells grow as free-floating cellular clusters termed 'neurospheres' or as adherent cell cultures [140, 142, 137, 126]. Neurospheres may contain both neural stem cells as well as progenitor cells. It was widely held that a neurosphere represented the clonal expansion of a single stem cell, however, there is evidence that neurospheres may also be generated by progenitor cells [139]. Thus, the standard neurosphere assay that assesses the ability of single cells to form neurospheres overestimates the proportion of true stem cells in a population [139].

Protocols for *in vitro* NPC culture differ with respect to concentrations and combinations of growth factors and substrate [140, 142, 78, 137, 48, 110, 126, 23, 88]. There is ample evidence that NPC response to growth factors varies not only with developmental stage, but also with factor and concentration [189, 202]. For example, although NPCs grown in either EGF or bFGF with heparin were multipotential, two separate studies showed a preferential gliogenic effect from EGF-derived cultures and a neurogenic effect in cultures derived from bFGF and

heparin, [189, 202]. In one study [202], this effect was noted in NPCs derived from embryonic and early postnatal rats but not in adults, whereas a second group reported these results for adult rat NPCs [189]. The combination of EGF and bFGF with heparin, rather than either alone, was shown to have a synergistic effect with embryonic rat and human NPCs, and with adult mouse subventricular NPCs [20, 58, 181, 18]. Culture conditions affect not only NPC proliferation rate and proportion of progeny type, but even cell migration. Epidermal growth factor generated NPCs were shown to migrate further on a poly-D-lysine substrate (PDL) than bFGF generated NPCs [202]. Similarly, the substrate on which NPCs are grown can also affect cell growth and behavior. In a study of the effect of three extracellular matrix components on cerebellar-derived neurospheres, fibronectin and laminin enhanced neurosphere motility and migration; chondroitin sulfate proteoglycan inhibited sphere migration and velocity [77]. In light of these findings, direct comparisons of neural precursor cells grown under variable culture conditions must consider the conditions under which the cells are grown. Moreover, optimal growth conditions must be determined for NPCs according to developmental stage and intended use.

Phenotypic characterization of NPCs will aid in the identification of true stem cells, allow their prospective isolation and enrichment for therapeutic purposes, and help in elucidating the mechanisms by which the nervous system develops and regenerates. Among the first neural stem/progenitor cell markers identified were nestin and vimentin, which are intracellular intermediate filamentous proteins [64, 90]. Vimentin and nestin are not ideal NPC markers

because their expression is not restricted to NPCs. Vimentin is present in many other cell types in the CNS besides NPCs, and nestin is expressed in fibroblastic cell lines, reactive astrocytes, and muscle [156, 147, 171]. Moreover, neural progenitor/stem cells have been identified that do not express nestin [85].

Work in the past six years has shown that NPCs in the developing fetus and in neurogenic regions of the postnatal brain express glial fibrillary acidic protein (GFAP) [32, 157, 116, 70, 108, 102]. The astrocytic type B cell identified as the neural stem cell in the adult mouse subventricular zone is both GFAP- and nestin-positive [33]. Like nestin and vimentin, GFAP is an intracellular filamentous protein and is expressed in non-precursor cells as well as NPCs. There is evidence that GFAP-positive cells from neurogenic and non-neurogenic regions are NPCs and astrocytes, respectively [71]. In rodent neurogenic regions, the GFAP-positive cells with NPC ability represent a morphologically distinct population of cells with bipolar or unipolar morphology [51]. Subsequent studies demonstrated that GFAP-positive cells cultured with leukemia inhibitory factor have a bipolar/tripolar morphology and possess NPC markers and differentiation ability, whereas bone morphogenetic protein-generated GFAP-positive cells are astrocytes [12].

Although none of these proteins alone is a definitive NPC marker, labelling for combinations of markers in conjunction with cellular morphology may serve to accurately identify neural precursor cells. While the use of intracellular NPC markers is a valuable tool for *in situ* studies of neural development and

regeneration, prospective isolation and enrichment of NPCs for *in vitro* and transplantation studies requires a cell surface marker.

Candidate cell surface markers that have been used to enrich for NPCs include Lewis X antigen (CD15), CD133, and differential binding of peanut agglutinin and heat-stable antigen [179, 143, 22, 89]. The cell surface antigen CD133 and the differential binding of peanut agglutinin and heat-stable antigen have been used to fractionate human and murine hematopoietic stem cells, respectively. In one study, approximately 80% of the cells from the ependyma/subependyma of adult mice that had poor peanut agglutinin binding and expressed very low levels of heat-stable antigen were capable of forming neurospheres; this represents nearly a 250-fold enrichment of NPC activity compared to unsorted cells [143]. The cell surface marker CD133 selected for a nearly 24-fold increase of NPC activity from human fetal brain tissue [179]; Lewis X antigen (CD15) was useful in enriching adult mouse NPCs from the subependyma up to 25-fold [22]. CD133 has also been used to prospectively identify a multipotent NPC in the postnatal mouse cerebellum [89]. In addition, three other cell surface markers have proved useful in enriching for embryonic mouse NPCs, though to a lesser degree. It was shown that selecting for Notch-1, syndecan-1, and ß1-integrin in single cell suspensions from cultured neurospheres gave a two- to three-fold NPC enrichment [113]. Double positive combinations of these three markers produced 6.1- to 7.6-fold enrichment of neurosphere-forming ability when primary embryonic tissue was used as a source [113].

Investigators have borrowed from the vast amount that is known about hematopoietic stem cells for another method of neural stem cell purification, namely, side-population analysis [56]. It was discovered that hematopoietic stem cells excluded the nuclear dye Hoechst 33342, resulting in the presence of a side-population of cells with low fluorescence emission [56]. Differential dye efflux was shown to be a property of NPCs as it is with hematopoietic stem cells [68, 79]. In the side-population derived from embryonic neurospheres there was a 278-fold increase in NPC activity, whereas the side-population derived from adult neurospheres showed a 7.5-fold enrichment [79]. Moreover, combining side-population analysis with CD15 labelling further enriched for neural stem cell activity beyond that achieved by side-population analysis alone. This enrichment was much more pronounced with embryonic neural precursor cells (38% enrichment) than with adult NPCs (10% enrichment) [79].

Neural precursor cell transplantation and the dog as a large animal model

Sources of postnatal multipotent NPCs are found in the regions of the brain where postnatal neurogenesis occurs: the hippocampus, cerebellum, olfactory bulb, and subventricular zone (SVZ) of the striatum [140, 166, 126, 124, 57, 154, 94]. It is of interest that non-neurogenic regions of the postnatal brain containing glial NPCs have yielded multipotent NPCs when cultured in the presence of EGF and/or bFGF [125, 83, 117]. This suggests that the potency of neural progenitor cells is determined by the environment in which they reside. Thus, manipulation of the NPC niche may endow at least one stem cell quality

(multipotency) on what are normally progenitor cells. Although in one study, the ubiquitous population of postnatal NG2 proteoglycan progenitors showed an immediate multipotency, i.e., one that is not dependent upon long-term growth factor exposure, which argues for an intrinsic ability rather than reprogramming in vitro [8].

Of the four sites in which multipotent NPCs are found in vivo, the cerebellum and olfactory bulb are the most readily accessible as an autologous source of NPCs. Autologous transplants of corrected (transduced) NPCs into affected patients would obviate the need for long-term immunosuppressive therapy required with allogeneic transplantation procedures. In a study performed in Australia, the median age of diagnosis for lysosomal storage diseases was 2.7 years [100]. Thus, treatment for most lysosomal storage diseases is usually initiated in young children. Cerebellar progenitor cells persist in the external germinal layer (EGL) of the child up to 2 years of age [133]. However, studies within the past ten years have shown that multipotential NPCs actually reside and migrate through the white matter tracts of the postnatal cerebellum in rats and mice, and not in the EGL as was once thought [197, 198, 82, 89]. It has been shown that cerebellar NPCs are present even in adult mice [82]. It is not known if humans are similar to mice in this respect, and, therefore, whether there are multipotent NPCs in the cerebellum of children beyond the disappearance of the EGL. Olfactory bulb NPCs can be isolated into adulthood in humans and rodents [124, 94].

If NPC transplants are to be explored for children, the dog is a good model for testing transplantation strategies. The dog brain is similar in both structure and size to a human child's, and the EGL of the cerebellum serves as a source of neural precursors in the dog up to 70 days after birth [130]. In light of the recent evidence of multipotent NPCs in murine cerebellar white matter tracts, canine cerebellar NPCs may remain after the disappearance of the EGL at around postnatal day 70. While to date there are no published characterizations of canine olfactory bulb NPCs, the persistence of NPCs in the adult rodent and human olfactory bulb suggests that the postnatal canine olfactory bulb will also provide a source of NPCs. Indeed, we have successfully isolated multipotent NPCs from the postnatal canine OB that show at least limited self-renewal capability. The olfactory bulb and cerebellum can be surgically accessed in the dog to serve as autologous sources of NPCs [6, 54]. Thus, canine MPS VII, a homologue of the human disease, is a valuable model to explore the potential of NPCs for gene/cellular therapy of a neurodegenerative disorder.

There are two published reports of canine NPCs [105, 200]. One study focused on canine oligodendroglial progenitors [200]. In the second study, multipotent canine NPCs with a broader differentiation capability were isolated from the embryonic and early postnatal midbrain [105]. The focus of both of these studies was transplantation therapy and there is relatively little information on the primary characteristics of canine NPCs, such as growth rate, expansion potential, self-renewal ability, or a quantitative assessment of multipotency. One of the studies showed that canine NPCs (CNPCs) were multipotent and reported

the ability to culture embryonic-derived CNPCs for up to six months *in vitro* [105]. Long-term proliferative capacity *in vitro* would support the criterion of self-renewal, and together with multipotency, the two major criteria of stem cells are met [155]. However, no information on the longevity of postnatal-derived CNPC cultures was reported.

Embryonic-derived canine neural precursor cells were transplanted into the spinal cord of two animal models of myelin disease, the myelin-deficient (*md*) rat and shaking dog (*sh*). A proportion of the transplanted CNPCs differentiated into oligodendrocytes, and produced myelin in both the *md* rat and *sh* dog models. To date, there are no reports of CNPC transplants into the brain. Determining the extent to which NPCs can engraft and migrate in the brain in both the early postnatal period and in adult animals is essential information for treatment strategies.

In rodents, intraventricular injection of NPCs into the developing brain results in widespread engraftment throughout the entire brain, whereas transplant into the adult brain shows a more restricted engraftment pattern [49, 167, 97, 93, 41, 44, 60, 122, 14, 175]. Some of the differences in engraftment between developing and adult brains may be due to changes in polysialylated neural cell adhesion molecule (PSA-NCAM) expression or changes in other extracellular matrix components [60, 77, 21]. It is unknown whether NPC engraftment throughout the entire brain occurs with intraventricular injection in neonatal dogs as it does in rodents, because dogs are more developmentally advanced at birth. There is a possibility that intraventricular injection and

widespread engraftment may be achieved in neonatal diseased dog brains despite the advanced developmental stage.

Recent studies have shown that intraventricular injection of embryonic mouse NPCs into adult rats with localized ischemic striatal injury can result in engraftment and migration to the ischemic site [75]. Ischemic injury is necessary for the NPC migration, however, because only very limited engraftment into the SVZ was noted after intraventricular injections in non-injured adult rats [75]. Similarly, intraventricular injections of NPCs into adult murine models of experimental autoimmune encephalitis also resulted in widespread NPC engraftment [37, 131]. Intraventricular injection into juvenile or adult models of lysosomal storage disease (LSD) has not been reported, so it is unknown whether neurodegenerative disease will stimulate NPC engraftment and migration as in ischemic/inflammatory disease.

It is also not known whether canine NPC transplantation into selected neural regions in adult dogs will result in engraftment and migration beyond the injection site. In adult rats, targeted xenograft injections to neurogenic regions such as the dentate gyrus and lateral ventricular wall resulted in human fetal NPC migration within the subgranular zone and along the rostral migratory stream to the olfactory bulb, respectively [44]. Similar results were reported with syngeneic NPC transplants into the adult rat dentate gyrus and lateral ventricular wall [172]. In a non-neurogenic region of the adult rat striatum, human fetal NPC migration was seen up to 1.5 mm from the graft center [44]. Likewise, syngeneic adult NPCs grafted into the non-neurogenic adult rat cerebellum migrated about

1 mm [172]. In another xenograft transplantation study, human fetal NPCs engrafted into the non-neurogenic adult rat striatum migrated along the corpus callosum rostrally into the forceps minor and frontal cortex and caudally along the internal capsule into the cerebellar peduncle and midbrain [38]. Thus, in rodents, there is potential for cell migration beyond the injection site even in adult animals. It is unknown whether these results will be seen in a large animal model such as the dog.

The principle of cross-correction permits a therapeutic effect that extends beyond the immediate cellular graft in cellular therapy of MPS VII and other lysosomal storage diseases. Cells that express ß-glucuronidase will secrete the protein into the extracellular environment, thereby transferring the enzyme via cross-correction to neighboring endogenous cells. In this manner, a 'sphere of correction' is achieved beyond the grafted cells [176, 163]. The greater the migration and spread of engrafted cells following injection, the wider the sphere of correction that can be achieved. In larger brains, engraftment with a robust migratory pattern will provide multiple sources of extracellular enzyme resulting in overlapping spheres of correction that may provide nearly global correction.

Factors that affect the migratory ability of NPCs are under study. Greater migratory capacity has been reported with undifferentiated versus pre-differentiated neurosphere grafts [19]. Epidermal growth factor-generated NPCs were shown to migrate further on a poly-D-lysine substrate (PDL) than bFGF-generated NPCs, and EGF infusion greatly increased migration and proliferation of embryonic mouse NPCs grafted into the adult rat striatum, as well as

endogenous mouse subventricular NPCs [29, 202, 45]. Subsequently, Boockvar et al. [13] utilized a constitutively active EGF receptor (EGFR) that acted independently of EGF to enhance migration and motility in a clonal mouse NPC line. Thus, NPC migration and motility may be enhanced with select culture conditions or manipulation of cell surface ligands.

Transduction of neural precursor cells for gene therapy

Neural stem cells have been engineered to provide protein correction in protein deficiency disorders, to produce trophic factors necessary for repair, or to deliver cytotoxic agents to brain tumors [87, 41, 146, 195, 1, 9, 14]. Successful introduction of genetic material requires the appropriate receptors for vector entry into the cell. Lentiviral, retroviral, adenoviral, and adeno-associated viral (AAV) vectors [40, 67, 123, 194, 135] have been used to transduce NPCs in vitro with variable results that may be attributable to differences in species, culture conditions, and multiplicity of infection. Unlike adenoviral, retroviral, or AAV vectors, lentiviruses transduce non-dividing cells and integrate into the cellular genome [114]. Retroviral pseudotyping permits targeting of specific cellular populations by varying the surface proteins of enveloped retroviruses [17]. Transduction of CNS cells could be achieved with self-inactivating (SIN) HIV vectors pseudotyped with envelope glycoproteins from the vesicular stomatitis virus (VSV-G), lymphocytic choriomeningitis virus (LCMV), Mokola virus, and amphotropic murine leukemia virus (MuLV) [186]. In vivo studies of lentiviral transduction have shown that pseudotyped feline immunodeficiency virus (FIV)

and human immunodeficiency virus (HIV) vectors transduce neural progenitor/stem cell populations in mice [26, 170]. While both VSV-G and LCMV pseudotypes transduced NPCs in vivo, LCMV glycoproteins preferentially transduced astrocytic cells, including NPCs, whereas VSV-G transduction was more widespread in the CNS [26, 170].

Postnatal-derived primary neural precursor cell transplantation

There is relatively little in the current literature concerning transplantation of primary, ex vivo expanded, postnatal NPCs into the postnatal brain. Most transplantation studies aimed at therapy have utilized fetal or immortalized NPCs [167, 173, 105, 168, 181, 195, 120, 111]. While the therapeutic use of immortalized NPCs is attractive because of the ease of expansion and potentially unlimited supply of cells, immortalized cells will likely face greater resistance for use in clinical trials because of the presence of an introduced oncogene. Apart from the moral and ethical implications that the use of embryonic tissue poses, its availability is limited. Postnatal NPCs not only provide a more readily available source of cells for transplantation, but also allow for autologous transplantation strategies, i.e., ex vivo gene therapy.

Studies exploring the behavior of postnatal NPCs have evaluated adult rat hippocampal- and spinal cord-derived NPCs for transplantation into neurogenic and non-neurogenic regions of healthy rodents [49, 172, 160]. The adult-derived NPCs engrafted and differentiated into neurons, astrocytes and oligodendrocytes in a site appropriate manner. Another study evaluated the behavior of postnatal

cerebellar-derived NPCs when transplanted into the cerebellum of a normal neonatal mouse, but only with respect to differentiation ability [89]. Two groups have assessed the engraftment potential of adult SVZ-derived NPCs into the normal mouse brain, however SVZ explants were used for transplantation rather than cultured cells [93, 129]; thus, results from these studies cannot necessarily be extrapolated to ex vivo expanded NPCs.

Therapeutic transplantation studies of postnatal NPCs were performed by two groups using postnatal murine neurospheres [37, 131]. Postnatal NPCs were injected into the lateral ventricles of rodent models of acute and chronic experimental autoimmune encephalitis (EAE). In both models, there was widespread engraftment and migration of the postnatal NPCs with resultant amelioration of disease. In the acute model, in the areas of engrafted NPCs there was a significant decrease in perivascular inflammatory cell infiltrates and down regulation of the inflammatory markers intercellular adhesion molecule-1 (ICAM-1) and lymphocyte function-associated antigen-1 (LFA-1) [37]. In the chronic EAE model, NPC transplantation resulted in areas of remyelination [131].

To date, only one study has assessed the potential of primary postnatal NPCs for therapy of a lysosomal storage disease [161]. Neural precursor cells derived from adult mouse whole brain were transduced ex vivo to express the human acid sphingomyelinase (ASM) protein. The transduced NPCs were transplanted into the hippocampus, thalamus and striatum of the ASM knockout mouse, a model of human Type A Niemann-Pick disease. The transplanted cells produced sufficient levels of enzyme to clear storage lesions in the regions in

which they engrafted. Other studies did evaluate NPC transplantation for treatment of MPS VII, however, immortalized NPCs were used [167, 101]. One group used immortalized postnatal-derived murine NPCs expressing normal levels of ß-glucuronidase (GUSB) [167], whereas the second group genetically modified an immortalized human fetal NPC clonal line to over-express human GUSB [101]. In both studies, after intraventricular injection into neonatal MPS VII-affected mice the NPCs engrafted and expressed GUSB at therapeutic levels in all brain regions.

Non-invasive monitoring of neural precursor cell engraftment

If stem cell therapy is to become a viable treatment for neurodegenerative diseases, a non-invasive method of monitoring cellular engraftment and migration will be necessary. Magnetic resonance imaging (MRI) shows promise in detecting NPCs following transplantation into the rodent brain [16, 91, 15, 107, 201]. Progenitor cells may be labelled with superparamagnetic iron oxide (SPIO) microparticles by targeting the particles to the transferrin receptor [16], by derivatizing the particles with a membrane translocation signal (HIV tat) [91], or by using non-specific endocytic uptake [15]. Superparamagnetic iron oxide particles accumulate in phagocytic vacuoles in the cell. These SPIO particles serve as contrast agents by producing a hypointense area on MR images that co-registers with labelled cells on histologic sections [15, 36, 98]. The nature of superparamagnetic particles is that they have a high relaxivity thereby producing a large effect on signal intensity because the homogeneity of the magnetic field is

disrupted disproportionately to particle size [159]. With a T^*_2-weighted 3-D gradient echo technique (susceptibility-based), contrast is enhanced to produce a 'blooming effect' that allows detection of even small numbers of labelled cells [15]. As few as five hundred cells labelled with a relatively low concentration of SPIO particles on a clinical strength 4.7 Tesla magnet can be detected in vitro [98]. In vivo MRI of three cells/voxel has been reported with an 8.5 Tesla magnet [80] and single cell imaging was achieved in the microcirculation of the brain with a 1.5T magnet [62].

There are few studies assessing the sensitivity of high resolution MRI in detecting engraftment and migration of SPIO-labelled cells [196, 62, 169] and only one study evaluating SPIO-labelled NPCs in mouse brains [98]. To date, most of the published studies have been performed in the larger rat brain [16, 15, 65, 107, 201, 72]. High resolution MRI in the mouse brain is a valuable tool given that mice are a much more useful species as a genetic disease model than the rat. Currently, there are no published MRI studies of magnetically-labelled NPCs in a large animal model such as the dog.

CHAPTER ONE: In Vitro Characterization of Canine Neural Precursor Cells

Introduction

The observation that there was evidence of neurogenesis in the postnatal brain marked the beginning of the search for neural precursor cells (NPCs) in the developed central nervous system [2, 3]. Neural precursor cells were originally isolated from the adult rodent brain by selective response to epidermal growth factor (EGF) or basic fibroblast growth factor (bFGF) [140, 142]. To date, NPCs have been successfully isolated from rodents, primates, sheep, pigs, and dogs [140, 105, 126, 200, 23, 124, 165, 35, 119]. Much of the impetus to isolate and characterize NPCs from different species has been a direct result of therapeutic studies for human neurologic diseases that have specific animal models.

The existence of large and small animal models of mucopolysaccharidosis VII (MPS VII) [59, 11, 52, 24] affords a unique therapeutic research opportunity for the treatment of neurodegeneration associated with lysosomal enzyme deficiency. In this manner, MPS VII serves as a therapeutic paradigm for lysosomal storage diseases in which there is a significant neurologic component and for which there may not be animal models. MPS VII, or Sly disease, is the consequence of a deficiency of the lysosomal acid hydrolase, ß-glucuronidase (GUSB), which results in the accumulation of heparan and chondroitin sulfate glycosaminoglycans within lysosomes [164, 193]. Because of the presence of the blood-brain barrier, enzyme replacement and bone marrow transplantation

therapy do not significantly impact on CNS disease. Thus, specific CNS-directed therapy is required.

Neural precursor cell therapy for lysosomal storage diseases with CNS pathology has been successful for mouse models of Niemann-Pick A and MPS VII. Transplantation of NPCs into the brain resulted in therapeutic levels of enzyme expression with resultant clearance of cell storage material in the regions of engraftment [167, 101, 161]. These studies are proof of principle that NPC transplantation is therapeutically effective for treatment of CNS disease associated with lysosomal enzyme deficiency. However, the brain of a human child is architecturally more complex and almost 2000-fold larger than that of a mouse. Modelling cell transplantation therapy in the dog brain would allow for the architectural complexities of the human brain with a difference in brain size of only 10-fold. To that end, we isolated and expanded postnatal canine NPCs (CNPCs) from unaffected and MPS VII dogs for characterization.

Apart from the ethical and moral implications associated with embryonic NPCs, postnatal NPCs are more readily available and afford the opportunity for autologous transplants. Canine NPCs have been isolated from the embryonic and neonatal ventral mesencephalon and striatal subventricular zone (SVZ) [105, 200]. In the developed brain, multipotent NPCs reside in the SVZ and its rostral and caudal extensions into the olfactory bulb and hippocampus, as well as within the white matter tracts of the rodent cerebellum [95, 197, 198, 126, 94, 82, 89]. In addition, glial progenitors in non-neurogenic regions can become multipotent when exposed to the appropriate growth factors in vitro [125, 83, 8, 117].

However, there is a paucity of studies that directly compare the properties of NPCs from different regions of the developed brain.

While much has been learned about the genetic and molecular bases of the mucopolysaccharidoses, the pathogenesis of neurodegeneration is unknown [183, 184]. In MPS VII-affected individuals, there are no abnormalities associated with brain structure attributable to defective embryonic neural development. However, more subtle defects in postnatal neurogenesis within regions such as the olfactory bulb and subgranular layer of the hippocampus have not been evaluated. It is possible that the accumulating heparan sulfate and chondroitin sulfate glycosaminoglycans do not affect neurogenesis or gliogenesis until the postnatal period.

Our study assessed postnatal CNPC growth rate, expansion potential, and multipotency for three separate aims. First, we compared CNPCs from MPS VII-affected and unaffected dogs to determine whether there were intrinsic differences attributable to disease phenotype. The second aim was to comparatively assess CNPCs from three different postnatal brain regions for differences attributable to site of origin. Finally, we evaluated three different methods of cell culture to determine optimal growth conditions for CNPCs derived from one of the regions, the olfactory bulb.

Materials and Methods

Experimental animals. Dogs were raised in the animal colony at the University of Pennsylvania School of Veterinary Medicine according to NIH and USDA guidelines for the use of animals in research and were approved by the Institutional Animal Care and Use Committee of the University of Pennsylvania. Screening for MPS VII dogs was performed by evaluating Wright-Giemsa-stained blood films for the presence of storage granules in white blood cells. Normal, carrier, or MPS VII genotype was then established by polymerase chain reaction for the mutation [136].

Isolation of canine neural precursor cells. Three unaffected and four MPS VII-affected dogs ranging in age from nineteen to twenty-three days of age were humanely euthanized by intravenous injection of a barbituate solution. The brain was removed, placed into a balanced salt solution, and then dissected grossly. The olfactory bulbs, cerebellum, and rostral one-third of the brain located just caudal to the olfactory bulbs and rostral to the hippocampus were separated from the brain and from each other. The rostral one-third of the brain was further dissected to leave primarily the tissue surrounding the lateral ventricles (including parts of the corpus callosum, caudate putamen, and septae). Half of the vermis and half of a lobule were removed from the cerebellum. The resultant tissues from the striatal SVZ and cerebellum, as well as the olfactory bulbs, were minced separately and then digested in 0.25% trypsin (Worthington) in a 37°C water bath for 45 minutes to 1 hour. The enzymatic digestion was stopped with addition of fetal bovine serum (FBS; Hyclone). The tissues were

then incubated with DNAse I (Sigma) for fifteen minutes in a 37°C water bath and triturated to a single cell suspension with successively smaller diameter pipettes, ending at a flame-polished Pasteur pipette. The cell suspensions were centrifuged at 700 rpm at 4°C for 8 minutes, resuspended in 10% FBS plating medium (see below), and triturated. The total number of viable cells was determined by manual count on a hemacytometer; cell viability was assessed using trypan blue exclusion (0.4%; Sigma).

Neural precursor cell culture and expansion. The NPCs were plated at a concentration of $4x10^4/cm^2$ in 10% serum-containing plating medium consisting of DMEM:F12 (1:1 ratio; GibcoBRL) supplemented with 10% FBS, 1% N2 supplement (GibcoBRL), 1% antibiotic-antimycotic (PSF)(100 U/mL penicillin; 100 µg/mL streptomycin; 0.25 µg/mL amphotericin B; GibcoBRL), and 1% L-glutamine (2mM; GibcoBRL). After 24-48 hours, the medium was changed to a serum-free feeding medium consisting of DMEM:F12 supplemented with 1% N2 supplement, 1% PSF, and 1% L-glutamine. The standard combination of growth factors consisted of 20 ng/mL epidermal growth factor (EGF) (recombinant murine; Roche), 20 ng/mL basic fibroblast growth factor (bFGF) (recombinant human; Promega), and heparin (5 µg/mL; Sigma). For a subset of cultures, 10 ng/mL leukemia inhibitory factor (LIF) (recombinant human; Chemicon) was added along with the standard growth factor combination. The NPC cultures were maintained at 37°C in humidified 5% CO_2 tissue culture incubators. Cultures were fed every 3-5 days by changing half of the medium and adding fresh growth factors. The NPCs were plated into 25 cm^2 tissue culture flasks

(Corning) coated with 10 µg/mL poly-D-lysine (Sigma), poly-D-lysine with 5 µg/mL fibronectin (0.1% bovine; Sigma), or poly-D-lysine with 10 µg/mL laminin (mouse; GibcoBRL). Cultures were passaged at approximately 90% confluence by trypsinizing (0.05% trypsin-EDTA; GibcoBRL) and replating at a concentration of $4x10^4/cm^2$.

Immunocytochemistry. Cultures were differentiated by plating in the absence of growth factors in an 8-well chamber slide (Lab-Tek II; Nalge Nunc) at a concentration of 4×10^4 cells/well in feeding medium supplemented with 1% FBS. Undifferentiated NPCs were plated at a concentration of $2x10^4$/well onto poly-D-lysine-coated 8-well glass slides (Cel-Line, Erie Scientific) and allowed to attach overnight in feeding medium containing growth factors. Differentiated and undifferentiated NPC cultures were processed for immunocytochemistry after 10-12 days and 24 hours, respectively.

The polyclonal primary antibodies used were rabbit polyclonal anti-nestin, *1:60* dilution (rabbit 130; kind gift of R. McKay, NIH) and rabbit polyclonal anti-glial fibrillary acidic protein (GFAP), *1:100* dilution (Chemicon). Primary monoclonal antibodies consisted of rat anti-GFAP, *1:1* dilution (IgG; kind gift of V. Lee); mouse anti-ßtubulin III, *1:300* dilution (IgG; Chemicon); mouse anti-MAP2ab, *1:300* dilution (IgG; Chemicon); mouse anti-O4, *1:3* dilution (IgM); and mouse anti-galactocerebroside, *1:1* dilution (IgG3) (both oligodendrocyte markers were generous gifts of J. Grinspan). Secondary fluorescent antibodies used were goat anti-mouse IgG/IgM FITC, *1:300* dilution (Chemicon); goat anti-rabbit IgG 594 Alexa fluor, *1:300* dilution (Molecular Probes); goat anti-rabbit IgG 488

Alexa fluor, *1:300* dilution (Molecular Probes); and goat anti-mouse IgM Alexa fluor 488, *1:300* dilution (Molecular Probes).

For all intracellular markers, cells were rinsed in Tris-buffered saline (TBS) (50 mM Tris-base, 0.15M NaCl; pH 7.6), fixed for 10 minutes in 4% paraformaldehyde (Sigma), rinsed three times with TBS, blocked in 5% goat serum (GibcoBRL) with 0.1% Triton X-100 (Sigma) for 40 minutes, and then incubated with primary antibody in 1% goat serum with 0.02% Triton X-100 for 1 hour at room temperature or overnight at 4°C. After three TBS washes, the secondary antibody was applied for 1 hour at room temperature or overnight at 4°C. Cell surface marker staining was performed on live cells. The cells were rinsed in TBS, incubated with primary antibody diluted in TBS for 30 minutes, rinsed briefly with TBS, incubated with secondary antibody for 40 minutes, rinsed with TBS, and then fixed for 10 minutes in 4% paraformaldehyde. All slides were washed three times with TBS before mounting in Vectashield containing 4',6 diamidino-2-phenylindole (DAPI; Vector Laboratories).

Quantitation of immunofluorescence. A minimum of 10 fields for each marker was photographed using a SPOT RT camera (Diagnostic Instruments). An effort was made to sample representatively; when differentiation was not uniformly distributed, similar numbers of fields without positive staining were analyzed. The DAPI-stained nucleus was used to count the total number of cells in all fields using a manual tag with Image-Pro Plus software (version 4.0; Media Cybernetics). The percentage of cells that stained positively for an

immunofluorescent marker was obtained using the average of positive cells and total cells for all fields.

NPC population parameters and statistics. For each cell culture, the number of cells plated at the beginning and harvested at the end of each passage was recorded. Cultures were plated in triplicate for comparison of unaffected and MPS VII NPCs from the cerebellum, olfactory bulb, and subventricular zone. For comparison of growth on fibronectin, laminin, and in the presence of leukemia inhibitory factor, canine olfactory bulb NPCs (OB-CNPC) derived from three unaffected dogs were evaluated in duplicate for each condition. The total potential cell number generated was calculated by multiplying the total number of viable cells harvested after each passage by the ratio of the total cells harvested to the total cells plated. The product for each passage was added to the subsequent passage to produce the total potential cells generated if all cells harvested were plated [141]. Cell doubling time was determined from the standard formula: doubling time= [(log *P*- log *H*)/ log 2]/ *D*; where *P*= the number of cells plated, *H*= the number of cells harvested, and *D*= the days between plating and harvest [61].

Statistical analysis was performed to determine whether there was a difference in population doubling times and differentiation ability between NPCs derived from MPS VII and unaffected dogs in each region using an unpaired Welch's *t* test. Comparisons between the growth parameters of multiple brain regions were performed using the Kruskal-Wallis non-parametric analysis of variance and, where appropriate, the Dunn's multiple comparisons test. The

three culture conditions were evaluated using the Friedman nonparametric repeated measures test.

Results

Comparison of CNPC growth parameters from three different brain regions of MPS VII-affected and unaffected dogs. The SVZ has been well characterized as a source of NPCs in rodents [33, 32, 108]. In addition, we decided to evaluate CNPCs derived from the olfactory bulb and cerebellum because both sites are surgically accessible in humans and dogs for potential autologous transplantation therapy. The NPCs were selected by epigenetic stimulation in a serum-free medium and grown as an adherent monolayer on a poly-D-lysine substrate in the presence of EGF and bFGF with heparin. There was no significant difference in the morphology of CNPCs in culture regardless of disease phenotype or region of derivation (Fig. 1.1). The cells were primarily bipolar or unipolar, fusiform, and grew in a lacey, interconnected fashion. Neurospheres occasionally formed from dense adherent cell clusters and floated free or remained attached to the cellular substratum. The populations became more morphologically homogenous with successive passages.

Cultures were established in triplicate for each region in three independent isolations from both MPS VII-affected and unaffected dogs. Because NPC proliferation in response to basic fibroblast growth factor (bFGF) is potentiated by cell surface heparan sulfates [118, 20, 18], defects in heparan sulfate catabolism may alter growth parameters. We therefore evaluated the population doubling

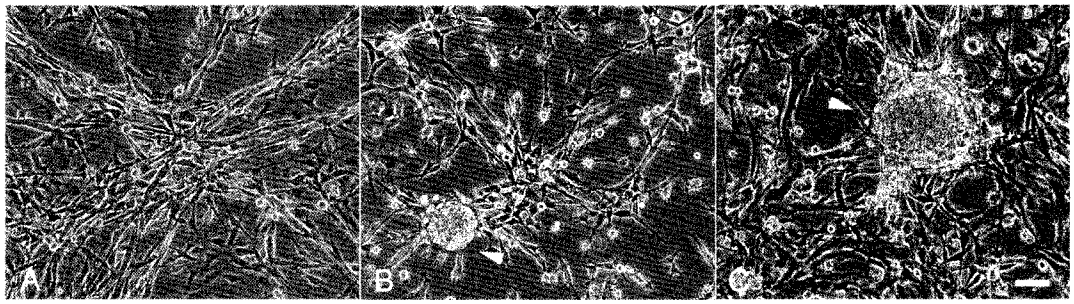

Figure 1.1 Canine NPC morphology in culture. Phase contrast photomicrographs at the primary passage for (A) MPS VII Cb-CNPC; (B) unaffected OB-CNPC; and (C) unaffected SVZ-CNPC. Arrowheads point to neurospheres. SVZ-CNPC, canine subventricular zone NPC; OB-CNPC, canine olfactory bulb NPC; Cb-CNPC, canine cerebellar NPC. Bar= 25μm.

times over the course of ten passages for each region of origin (Table 1.1). We also determined the total potential numbers of cells generated if all cells had been plated after each passage (Figure 1.2).

Most of the CNPCs were actively proliferating at the end of passage 10, corresponding to around 80 days in vitro. Population doubling time for actively proliferating cultures ranged from 1 to 18 days. There was no statistical difference in population doubling or total cell expansion number between MPS VII and unaffected NPC cultures. The doubling time for cerebellar-derived NPC cultures was significantly slower compared with those from subventricular zone (SVZ) and olfactory bulb NPCs. This was true for both unaffected and MPS VII NPCs.

Immunophenotype and morphology of undifferentiated CNPC cultures. Aliquots of cultures from each genotype (diseased and unaffected) and from each region were plated overnight in the presence of growth factors for analysis of the undifferentiated phenotype. Immunophenotyping was performed for all regions at passage 1 and passage 10; olfactory-bulb-derived NPCs (OB-CNPCs) were also assessed at passage 5 (Tables 1.2-1.4).

Glial fibrillary acidic protein (GFAP) is a marker of both differentiated astrocytes and neural stem cells [32, 88, 104, 108]. Nestin is used as a marker of neural precursor cells [64, 43, 90]. The neural stem cells of the SVZ are reported to be both nestin- and GFAP-positive [33]. The undifferentiated CNPC phenotype was similar for both unaffected and MPS VII NPC cultures, and for all

Doubling times (days) for unaffected and MPS VII-affected NPCs. The mean for each region is the average for ten passages, each passage cultured in triplicate (except passage 1, which represents a single culture). There was no statistical difference between unaffected and MPS VII-affected NPC doubling time for each site (p values ranged from 0.1 to 0.3). Within each genotype, there was a significant difference between Cb-CNPC doubling time and SVZ-CNPC and OB-CNPC doubling time (indicated by asterisks; p <0.0001). In a multiple comparisons test, Cb-CNPC doubling time was significantly slower than SVZ-CNPC and OB-CNPC doubling time independent of disease state (p <0.001). [a]SVZ-CNPC, canine subventricular zone NPC; [b]OB-CNPC, canine olfactory bulb NPC; [c]Cb-CNPC, canine cerebellar NPC.

Table 1.1 Comparison of unaffected and MPS VII-affected doubling times from CNPCs derived from three different brain regions.

	SVZ-CNPC[a]			OB-CNPC[b]			Cb-CNPC[c]		
Passage	**Dog 1**	**Dog 2**	**Dog 3**	**Dog 1**	**Dog 2**	**Dog 3**	**Dog 1**	**Dog 2**	**Dog 3**
Unaffected									
1	2.2	3.5	1.3	2.8	3.2	1.0	3.3	3.9	2.3
2	1.7	4.3	2.5	4.3	4.5	2.5	2.7	6.7	2.8
3	3.6	3.0	3.7	4.1	5.1	2.9	2.4	2.8	2.4
4	4.4	1.9	3.5	2.0	2.1	3.1	1.9	2.4	2.1
5	2.9	1.5	4.1	1.7	1.7	2.0	4.3	2.3	3.3
6	2.0	1.8	2.9	2.3	1.5	2.8	21.8	6.3	2.5
7	1.5	1.9	1.7	2.0	1.9	2.3	6.7	4.9	2.2
8	2.0	14.4	1.8	3.5	3.4	2.2	7.4	6.3	1.7
9	2.7	43.1	1.8	3.4	3.2	2.2	12.0	5.6	5.7
10	5.6	6.2	2.9	3.2	3.7	2.2	25.2	9.9	10.9
Mean±SEM	2.9±0.4	8.2±4.1	2.6±0.3	2.9±0.3	3.0±0.4	2.3±0.2	8.8±2.7	5.1±0.8	3.6±0.9
REGION Mean±SEM		**3.4±0.3**			**2.8±0.1**			**6.0±0.7***	
MPS VII									
1	5.7	3.4	3.4	3.3	5.1	3.5	3.2	3.5	2.6
2	2.5	2.0	1.9	2.5	2.5	14.7	2.5	20.2	1.8
3	3.3	3.4	2.4	2.7	4.7	9.2	4.3	2.7	2.0
4	2.3	5.9	2.3	4.4	2.5	2.0	5.9	2.0	3.4
5	1.7	3.0	2.2	3.2	1.8	3.0	10.8	2.7	3.5
6	1.8	2.1	2.4	1.8	1.6	8.4	6.7	3.4	2.8
7	2.6	1.9	1.8	2.6	1.7	2.1	8.1	5.5	1.9
8	2.5	2.8	1.9	2.5	1.7	2.0	17.4	3.3	2.9
8	5.8	3.5	2.1	2.0	1.6	2.6	5.3	2.6	3.9
10	2.3	10.2	2.3	2.2	2.3	3.8	6.3	3.6	5.3
Mean±SEM	3.1±0.5	3.8±0.8	2.3±0.1	2.7±0.2	2.6±0.4	5.1±1.4	7.1±1.4	5.0±1.7	3.0±0.3
REGION Mean±SEM		**3.0±0.2**			**3.4±0.4**			**5.1±0.6***	

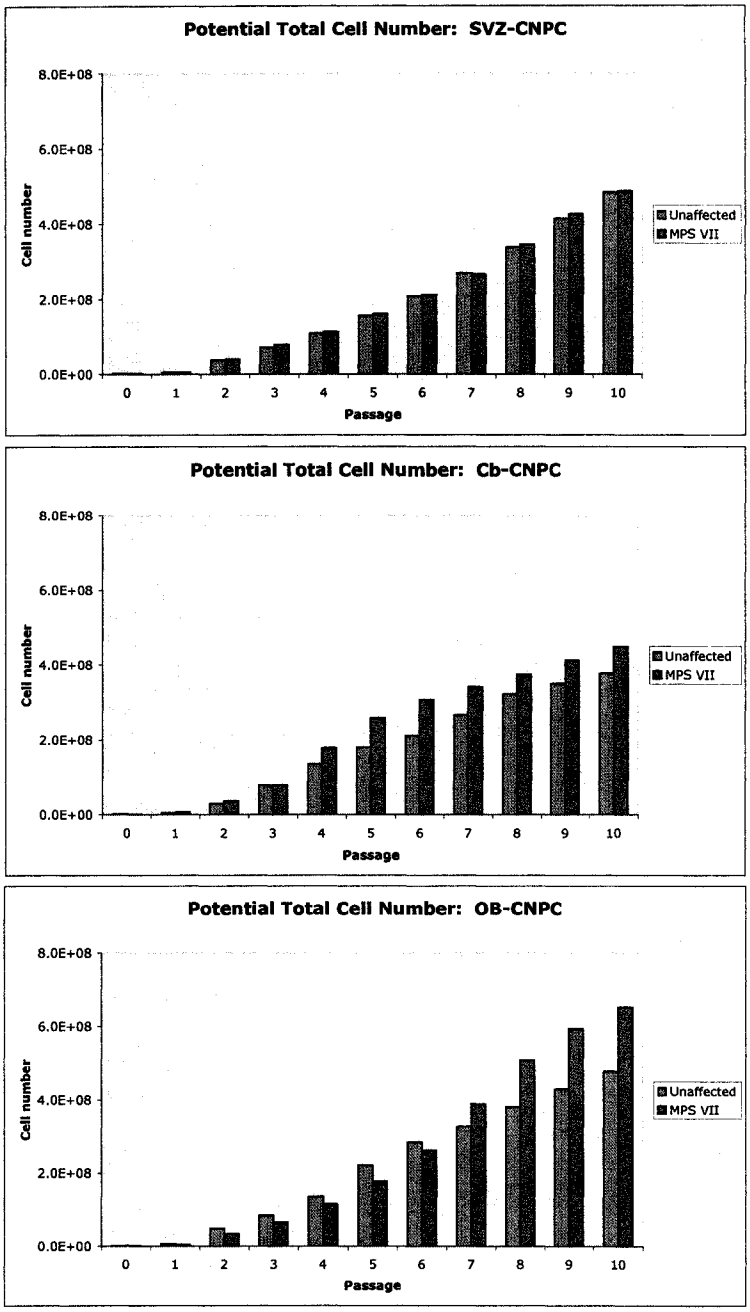

Figure 1.2 The calculated number of total CNPCs produced after ten passages if all the cells generated had been plated. Starting at a concentration of $1x10^6$ at passage 0, after ten passages nearly (A) $5x10^8$, (B) $4x10^8$, and (C) $6x10^8$ cells would have been produced for SVZ-, cerebellar-, and olfactory bulb-derived NPCs, respectively. The data represent the mean of triplicate cultures for three unaffected dogs and four MPS VII-affected dogs (except for Cb-CNPC, where n=3 affected dogs). SVZ-CNPC, canine subventricular zone NPC; Cb-CNPC, canine cerebellar NPC; OB-CNPC, canine olfactory bulb NPC.

Table 1.2 Phenotype (%) of undifferentiated and differentiated OB-CNPCs.

Undifferentiated

Unaffected Passage	Dog	Nestin	GFAP Immature/Mature		ß-Tubulin	Map2ab	O4	GalC
1	1	NA	NA		NA	NA	NA	NA
	2	57.6	13.6	20.1	0	0	1.0	0
	3	64.8	61.5	11.5	0	0	0	0
Mean±SEM		**61.2±3.6**	**37.6±24.0**	**15.8±4.3**	**0**	**0**	**0.5±0.5**	**0**
5	1	99.2	93.2	6.8	0	13.3	0	0
	2	94.2	86.5	9.5	0	0	0	0
	3	92.2	79.8	11.0	0	0	0	0
Mean±SEM		**95.2±2.1**	**86.5±3.9**	**9.1±1.2**	**0**	**4.4±4.4**	**0**	**0**
10	1	NA	NA		NA	NA	NA	NA
	2	97.2	98.8	0	0	0	0	0
	3	92.2	90.0	0	0	0	0	0
Mean±SEM		**94.7±2.5**	**94.4±4.4**	**0**	**0**	**0**	**0**	**0**

MPS VII Passage	Dog	Nestin	GFAP Immature/Mature		ß-Tubulin	Map2ab	O4	GalC
1	1	NA	NA		NA	NA	NA	NA
	2	77.7	34.8	3.1	0	0.9	0	0
	3	91.1	97.7	1.7	0	0	0	2.5
Mean±SEM		**84.4±6.7**	**66.3±31.5**	**2.4±0.7**	**0**	**0.5±0.5**	**0**	**1.3±1.3**
5	1	100.0	100.0	0	0	0	0	0
	2	97.6	96.4	3.6	0	0	0	0
	3	100.0	96.2	0	0	0	0	0
Mean±SEM		**99.2±0.8**	**97.5±1.2**	**1.2±1.2**	**0**	**0**	**0**	**0**
10	1	NA	NA		NA	NA	NA	NA
	2	98.0	99.2	0	0	0	0	0
	3	98.1	99.2	0	0	0	0	0
Mean±SEM		**98.1±0.1**	**99.2±0.0**	**0**	**0**	**0**	**0**	**0**

Values represent the mean percentage of positive staining ± SEM for three independent isolations except where noted. NA, not available.

Table 1.2 Phenotype (%) of undifferentiated and differentiated OB-CNPCs.

Differentiated

Unaffected Passage	Dog	Nestin	GFAP Immature/Mature		ß-Tubulin	Map2ab	O4	GalC
1	1	57.0	16.7	5.0	4.6	0	1.3	0
	2	28.8	3.1	37.8	18.3	1.8	0	0
	3	17.8	6.1	22.1	19.7	3.1	7.5	1.4
Mean±SEM		**34.5±11.7**	**8.6±4.1**	**21.6±9.5**	**14.2±4.8**	**1.6±0.9**	**2.9±2.3**	**0.5±0.5**
5	1	94.1	88.4	8.8	0	5.8	0	0
	2	95.0	38.0	25.0	9.0	0	5.8	0
	3	67.7	14.7	51.4	8.0	13.8	0	0
Mean±SEM		**85.6±9.0**	**47.0±21.8**	**28.4±12.4**	**5.7±2.9**	**6.5±4.0**	**1.9±1.9**	**0**
10	1	77.5	29.9	69.4	0	0	0	0
	2	99.1	66.4	23.5	0	0	0	0
	3	97.8	62.8	2.3	0	0	0	0
Mean±SEM		**91.5±7.0**	**53.0±11.6**	**31.7±19.8**	**0**	**0**	**0**	**0**

MPS VII Passage	Dog	Nestin	GFAP Immature/Mature		ß-Tubulin	Map2ab	O4	GalC
1	1	94.7	38.2	6.8	0.7	0	0	0
	2	61.0	7.7	16.2	0	0	0	0
	3	72.8	46.9	31.1	15.4	0	8.6	0
Mean±SEM		**76.2±9.9**	**30.9±11.9**	**18.0±7.1**	**5.4±5.0**	**0**	**2.9±2.9**	**0**
5	1	98.2	67.7	30.4	0	0	0	0
	2	94.4	42.6	11.2	1.4	1.5	0	0
	3	86.9	13.0	2.8	0	4.0	0	0
Mean±SEM		**93.2±3.3**	**41.1±15.8**	**14.8±8.2**	**0.5±0.5**	**1.8±1.2**	**0**	**0**
10	1	78.6	57.0	35.7	0	0	0	0
	2	98.3	60.0	40.0	0	0	0	0
	3	98.4	65.2	15.0	0	0	0	0
Mean±SEM		**91.8±6.6**	**60.7±2.4**	**30.2±7.7**	**0**	**0**	**0**	**0**

Values represent the mean percentage of positive staining ± SEM for three independent isolations. There was no significant difference with respect to differentiation ability between unaffected and MPS VII NPCs for neuronal or mature astrocytic markers at P1 or P5 (p ranges from 0.21 to 0.78).

Table 1.3 Phenotype (%) of undifferentiated and differentiated SVZ-CNPCs.

Undifferentiated

Unaffected Passage	Dog	Nestin	GFAP Immature/Mature		ß-Tubulin	Map2ab	O4	GalC
1	1	NA	NA		NA	NA	NA	NA
	2	NA	NA		NA	NA	NA	NA
	3	98.1	72.8	20.1	0	0	6.7	1.1
Mean±SD		**61.2±3.6**	**37.6±24.0**	**15.8±4.3**	**0**	**0**	**6.7±10.4**	**1.1±2.5**
10	1	NA	NA		NA	NA	NA	NA
	2	91.2	98.9	0	0	12.6	0	0
	3	92.0	97.1	0	0	0	0	0
Mean±SEM		**91.6±0.4**	**98.0±0.9**	**0**	**0**	**6.3±6.3**	**0**	**0**

MPS VII Passage	Dog	Nestin	GFAP Immature/Mature		ß-Tubulin	Map2ab	O4	GalC
1	1	NA	NA		NA	NA	NA	NA
	2	68.7	67.2	9.7	20.6	8.2	0	0
	3	92.2	47.9	31.3	0	0	0	1.3
Mean±SEM		**80.5±11.8**	**57.6±9.7**	**20.5±10.8**	**10.3±10.3**	**4.1±4.1**	**0**	**0.7±0.7**
10	1	96.6	100.0	0	0	0	0	0
	2	94.8	100.0	0	0	3.1	0	0
	3	100.0	98.7	0	0	5.5	0	0
Mean±SEM		**97.1±1.5**	**99.6±0.4**	**0**	**0**	**2.9±1.6**	**0**	**0**

Values represent the mean percentage of positive staining ± SEM for three independent isolations except where noted (standard deviation (SD) was used when only a single culture was analyzed). NA, not available.

Table 1.3 Phenotype (%) of undifferentiated and differentiated SVZ-CNPCs.

Differentiated

Unaffected Passage	Dog	Nestin	GFAP Immature/Mature		ß-Tubulin	Map2ab	O4	GalC
1	1	98.2	4.8	39.2	14.0	0	3.2	0
	2	77.5	13.9	64.4	46.4	0	11.6	8.9
	3	71.9	25.2	58.3	41.5	0	15.3	9.1
Mean±SEM		**82.5±8.0**	**14.6±5.9**	**54.0±7.6**	**34.0±10.1**	**0**	**10.0±3.6**	**6.0±3.0**
10	1	93.0	70.6	26.3	0	0	0	0
	2	95.5	96.8	1.9	0	0	0	0
	3	97.2	79.4	20.6	0	0	0	0
Mean±SEM		**95.2±1.2**	**82.3±7.7**	**16.3±7.4**	**0**	**0**	**0**	**0**

MPS VII Passage	Dog	Nestin	GFAP Immature/Mature		ß-Tubulin	Map2ab	O4	GalC
1	1	76.2	12.1	32.2	14.7	0	0	0
	2	71.3	21.0	13.0	7.9	0	3.0	0
	3	52.9	16.7	61.1	19.6	0	0	0
Mean±SEM		**66.8±7.1**	**16.6±2.6**	**35.4±14.0**	**14.1±3.4**	**0**	**1.0±1.0**	**0**
10	1	83.9	94.1	4.6	0	0	0	0
	2	73.2	67.2	32.0	0	0	0	0
	3	98.3	68.9	26.2	0	0	0	0
Mean±SEM		**85.1±7.3**	**76.7±8.7**	**20.9±8.3**	**0**	**0**	**0**	**0**

Values represent the mean percentage of positive staining ± SEM for three independent isolations. There was no significant difference with respect to differentiation ability between unaffected and MPS VII NPCs for neuronal or mature astrocytic markers at P1 (p ranges from 0.21 to 0.33).

Table 1.4 Phenotype (%) of undifferentiated and differentiated Cb-CNPCs.

Undifferentiated

Unaffected Passage	Dog	Nestin	GFAP Immature/Mature		ß-Tubulin	Map2ab	O4	GalC
1	1	NA	NA		NA	NA	NA	NA
	2	NA	NA		NA	NA	NA	NA
	3	52.3	5.9	4.5	6.5	0	4.4	0
Mean±SD		**52.3±4.6**	**5.9±3.8**	**4.5±4.3**	**6.5±6.3**	**0**	**4.4±4.3**	**0**
10	1	92.6	98.1	0	0	0	0	0
	2	98.6	100.0	0	0	27.7	0	0
	3	97.6	99.8	0	0	18.7	0	0
Mean±SEM		**96.3±1.9**	**99.3±0.6**	**0**	**0**	**15.5±8.2**	**0**	**0**

MPS VII Passage	Dog	Nestin	GFAP Immature/Mature		ß-Tubulin	Map2ab	O4	GalC
1	1	NA	NA		NA	NA	NA	NA
	2	100.0	98.3	0	0	0	0	0
	3	93.7	96.5	0	0	0	0	0
Mean±SEM		**96.9±3.2**	**97.4±0.9**	**0**	**0**	**0**	**0**	**0**
10	1	96.1	99.3	0	0	0	0	0
	2	97.1	100.0	0	0	39.0	0	0
	3	96.8	100.0	0	0	0	0	0
Mean±SEM		**96.7±0.3**	**99.8±0.2**	**0**	**0**	**13.0±13.0**	**0**	**0**

Values represent the mean percentage of positive staining ± SEM for three independent isolations except where noted (standard deviation (SD) was used when only a single culture was analyzed). NA, not available.

Table 1.4 Phenotype (%) of undifferentiated and differentiated Cb-CNPCs.

Differentiated

Unaffected Passage	Dog	Nestin	GFAP Immature/Mature		ß-Tubulin	Map2ab	O4	GalC
1	1	97.0	32.4	41.7	3.1	0	0	0
	2	72.2	32.4	42.7	19.8	0	17.8	0
	3	90.6	33.3	66.7	9.1	0	0	0
Mean±SEM		**86.6±7.4**	**32.7±0.3**	**50.4±8.2**	**10.7±4.9**	**0**	**5.9±5.9**	**0**
10	1	78.4	44.7	55.3	0	12.1	0	0
	2	98.6	13.3	87.0	0	0	0	0
	3	99.7	74.4	6.8	0	2.2	0	0
Mean±SEM		**92.2±6.9**	**44.1±17.6**	**49.7±23.3**	**0**	**4.8±3.7**	**0**	**0**

MPS VII Passage	Dog	Nestin	GFAP Immature/Mature		ß-Tubulin	Map2ab	O4	GalC
1	1	NA	NA		0	0	0	0
	2	NA	NA		0	0	0	0
	3	82.7	39.4	54.5	2.2	0	2.0	0
Mean±SD		**82.7±11.1**	**39.4±23.5**	**54.5±23.5**	**0.7±0.7***	**0**	**0.7±0.7***	**0**
10	1	88.0	61.7	38.3	2.2	18.9	0	0
	2	97.1	73.9	20.4	0	0	0	0
	3	93.7	61.7	38.3	0	11.8	0	0
Mean±SEM		**92.9±2.7**	**65.8±4.1**	**32.3±6.0**	**0.7±0.7**	**10.2±5.5**	**0**	**0**

Values represent the mean percentage of positive staining ± SEM for three independent isolations except where noted (standard deviation (SD) was used when only a single culture was analyzed). There was no significant difference with respect to differentiation ability between unaffected and MPS VII NPCs for neuronal or mature astrocytic markers at P1 (p ranges from 0.18 to 0.66). *Indicates SEM. NA, not available.

regions. The majority of cells stained positively for GFAP and nestin. The GFAP-positive cells were divided into two groups based on cellular morphology and staining. Cells with the following characteristics were considered 'immature' or undifferentiated: Small nucleus; unipolar or bipolar; round or fusiform shape; and a non-filamentous, diffuse GFAP staining pattern. In contrast, cells with larger nuclei, a stellate or flattened, epithelioid morphology with increased cytoplasmic to nuclear ratio (relative to undifferentiated cells), and a filamentous staining pattern, were considered 'mature' because this morphology is consistent with mature astrocytes [152] (Figure 1.3).

One study reported that GFAP staining in embryonic human neuroepithelial cells was likely an artifact due to cross-reactivity to vimentin or nestin [199]. In this study, human NPCs stained positively with polyclonal GFAP antiserum, but were negative for GFAP with a monoclonal anti-GFAP antibody. To verify that the GFAP staining in the CNPC cultures was specific, we co-stained both undifferentiated and differentiated cultures with a polyclonal rabbit GFAP antiserum and a rat monoclonal anti-GFAP antibody. The polyclonal and monoclonal anti-GFAP antibodies stained the same cells (Figure 1.4). In addition, the same two types of staining patterns in immature and mature cells—diffuse and filamentous, respectively—were observed.

Consistent with selection for NPCs over time, the proportion of mature GFAP cells decreased, and immature GFAP-positive cells and nestin-positive cells increased with passage number. For the neuronal markers (ß-tubulin and

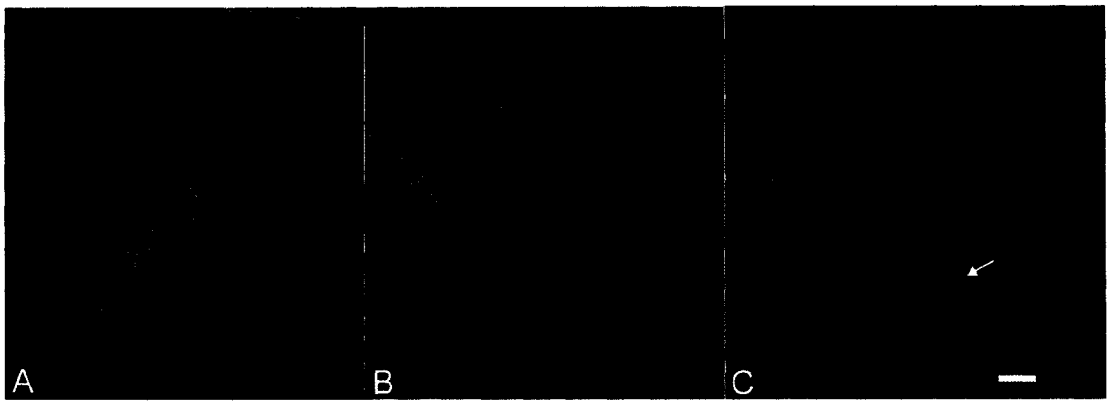

Figure 1.3 Glial fibrillary acidic protein (GFAP)-positive cells showed two types of morphology and staining. (A) The majority of cells grown in the presence of growth factor were small, round or fusiform, and stained diffusely for GFAP. (B) Some cells grown under differentiating conditions developed the morphology and filamentous GFAP staining of 'mature' differentiated astrocytes (arrow). (C) Both 'undifferentiated' (arrow) and 'mature' GFAP-positive cells were present in differentiation cultures. (A,B) Bar= 25μm; (C) Bar= 50μm.

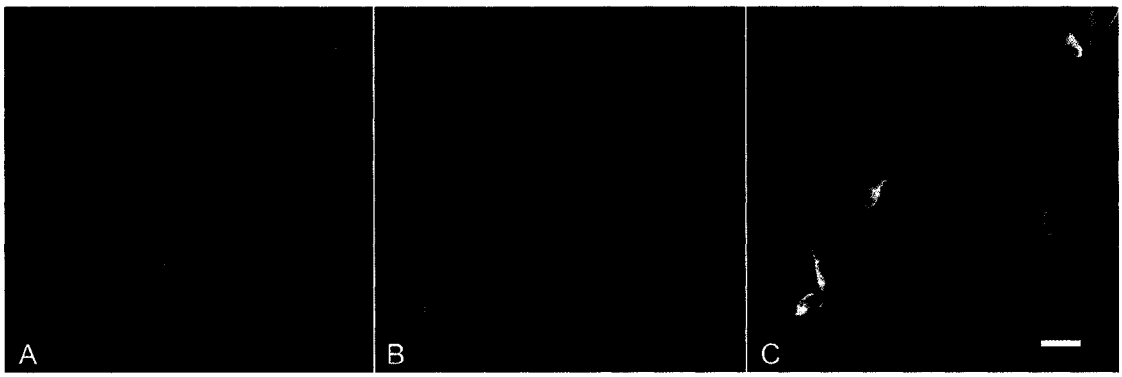

Figure 1.4 Anti-GFAP staining of CNPCs using polyclonal and monoclonal antibodies. (A) Rabbit polyclonal anti-GFAP with a secondary Alexa fluor 594 antibody (red). (B) Rat monoclonal anti-GFAP with a FITC secondary antibody. (C) Merged image showing co-staining of GFAP-positive cells with both primary antibody types. Note the two types of GFAP staining: Diffuse and filamentous. Bar= 25μm.

Map2ab) and the oligodendrocyte markers (O4 and galactocerebroside), a small proportion of positive staining (≤10%) was seen at passage 1(P1). Over successive passages, the cultures maintained in growth factors developed a more homogeneous, immature phenotype with the exception of Map2ab staining. At P5 and P10, there was Map2ab-staining in the undifferentiated cultures from the olfactory bulb, and the SVZ and cerebellum, respectively. However, the cellular morphology of the Map2ab-positive cells was consistently immature (small cells with bipolar, fusiform shape), unlike the morphology of Map2ab-positive cells in the differentiated cultures.

Immunophenotype and morphology of differentiated CNPC cultures. For analysis of the differentiated phenotype, aliquots were plated for 10-12 days in 1% serum-supplemented medium in the absence of growth factors. In the differentiation assay, the greatest amount of spontaneous differentiation was observed at the primary passage. At P1 and P5, after withdrawal of growth factors, cells stained positively for neuronal, astrocytic, and oligodendrocytic markers, in addition to displaying a phenotype-appropriate morphology (Figure 1.5). At P1 and P5, markers of differentiated neurons, astrocytes and oligodendrocytes were observed for all cultures. In addition, the proportion of nestin-positive and immature GFAP-positive cells was lower than the undifferentiated (growth factor-maintained) phenotype for the same passages.

At P10, there appeared to be a decrease in spontaneous differentiation after growth factor withdrawal that was uniform across CNPC disease status and

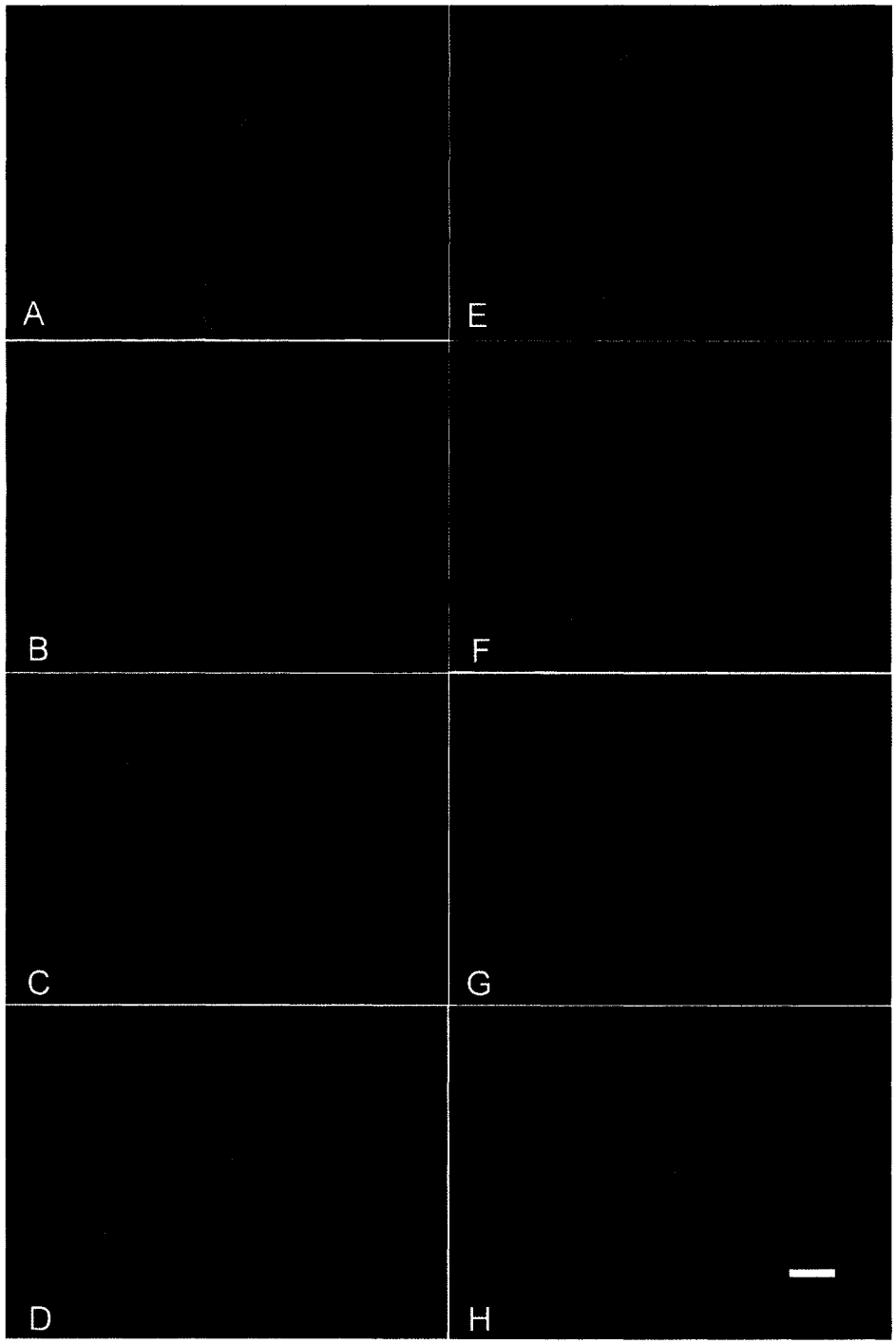

Figure 1.5 Immunophenotyping of OB-CNPCs. (A, E) The majority of cells stained positively for nestin and GFAP in undifferentiated cultures. (B,F) Nestin and GFAP staining changes in intensity and cellular morphology is less mature in differentiating conditions. (C,G) OB-CNPCs stain positively for neuronal markers ß-tubulin III and Map2ab, and (D,H) oligodendrocytic markers O4 and GalC after growth factor withdrawal. The appropriate morphology for astrocytes (F), neurons (C,G) and oligodendrocytes (D,H) is observed. Bar= 25µm.

site of origin. Many fewer cells stained positively for differentiation markers, and the proportion of nestin-positive and GFAP-positive cells with immature morphology increased relative to P1. Moreover, the GFAP-positive cells with mature morphology consistently stained with an immature, diffuse pattern rather than a filamentous one. Unaffected and MPS VII CNPCs were evaluated for differences in proportions of neuronal and mature astrocytic markers at P1 and P5 because there were the greatest numbers of cells with mature staining at these time points. Oligodendrocytes were proportionately too few to be evaluated. There was no statistically significant difference between unaffected and MPS VII CNPCs with respect to neuronal or astrocytic markers at either passage evaluated.

Comparison of OB-CNPC growth parameters under three different culture conditions. In order to determine whether different culture conditions would affect CNPC cell growth, phenotype, or differentiation, normal cells from olfactory bulb NPC isolations were subjected to two experimental variables. Olfactory bulb NPCs (OB-CNPCs) from three different unaffected dogs were plated onto poly-D-lysine (PDL) and fed with the standard medium. For the experimental groups, the OB-CNPCs were either plated onto PDL with fibronectin and fed with the standard medium, or plated onto PDL and fed with leukemia inhibitory factor (LIF)-supplemented medium. Leukemia inhibitory factor has been shown to maintain human fetal NPCs in an undifferentiated state

and to increase cell expansion number relative to NPCs grown with the standard growth factors [23].

Cultures from each dog were plated in duplicate for each variable. Population doubling times and cell expansion were determined over the course of ten passages. Cell expansion represents the total theoretical number of cells produced if all cells were plated after each passage. There was no statistical difference between population doubling times with respect to substrate, but culture with LIF significantly lengthened doubling time (Table 1.5). In addition, there was also a significant difference in the total number of potential cells generated. Neural precursor cell cultures supplemented with LIF produced fewer total cells (Fig 1.6).

In vivo studies of the SVZ showed that neural stem cells have a much longer doubling time than progenitor cells [109]. Thus, a slower doubling time may reflect a more undifferentiated precursor. We therefore evaluated CNPC phenotype and differentiation potential to determine whether substrate (fibronectin) or addition of LIF significantly affected either (Table 1.6). Parameters were assessed at P5 and P10 to allow sufficient time for effect.

Regardless of experimental variable, the undifferentiated CNPCs were primarily nestin-positive and GFAP-positive (immature morphology). Little to no staining for mature markers was present with the exception of Map2ab. The morphology of the Map2ab-positive cells in undifferentiated cultures was consistently immature (small, bipolar and fusiform cells). When growth factors were withdrawn, spontaneous differentiation was observed. At P5, cells stained

Table 1.5 Population doubling times for OB-CNPCs cultured under varied growth conditions.

	Dog 1			Dog 2			Dog 3		
Passage	**Fibro[a]**	**LIF[b]**	**PDL[c]**	**Fibro**	**LIF**	**PDL**	**Fibro**	**LIF**	**PDL**
2	2.9	3.6	4.5	2.1	2.6*	4.3	5.0	4.0	2.5
3	6.2	8.3	5.1	5.1	1.6	4.1	4.2	8.3	2.9
4	3.3	5.0	2.1	3.6	6.9	2.0	2.7	3.8	3.1
5	1.6	2.1	1.7	2.7	19.6	1.7	1.5	2.5	2.0
6	2.5	1.8	1.5	1.3	3.8	2.3	1.4	1.8	2.8
7	5.2	3.9	1.9	5.0	-47.7*	2.0	2.4	2.1	2.3
8	3.3	5.0	3.4	9.8	8.5*	3.5	14.3	3.3	2.2
9	3.2	5.2	3.2	4.2	NA	3.4	6.4	6.5	2.2
10	6.7	4.5	2.7	10.8	NA	3.2	2.0	4.9	2.2
Mean±SEM	**3.9±0.6**	**4.3±0.6**	**2.9±0.4**	**5.0±1.1**	**NA**	**2.9±0.3**	**4.4±1.4**	**4.1±0.7**	**2.5±0.1**

Doubling time (days) for OB-CNPCs derived from three unaffected dogs. The mean represents duplicate cultures over nine passages except where noted (*single culture). There was a significant difference in doubling time between CNPCs cultured with leukemia inhibitory factor (LIF) and those cultured with the standard growth factors on different substrates (p= 0.03). OB-CNPC, canine olfactory bulb NPC; [a]Fibro, poly-D-lysine and fibronectin substrate with standard growth factors; [b]LIF, poly-D-lysine substrate with standard growth factors and leukemia inhibitory factor (LIF); [c]PDL, poly-D-lysine substrate with standard growth factors.

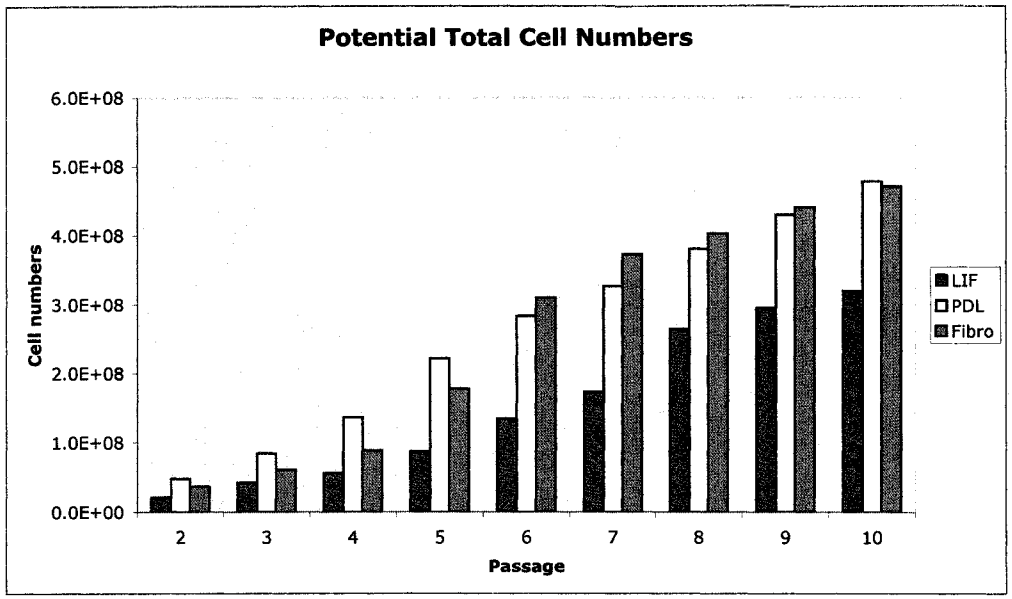

Figure 1.6 The calculated number of total CNPCs produced after ten passages if all the cells generated had been plated. Starting at passage 2, after eight passages nearly $5x10^8$ cells would have been produced for OB-CNPCs grown on either PDL or PDL-fibronectin. Addition of LIF produced fewer total theoretical cells (~$3x10^8$). The data represent the mean ± SEM of duplicate cultures for three unaffected dogs (except for PDL, where cultures were done in triplicate). LIF, leukemia inhibitory factor; PDL, poly-D-lysine substrate; Fibro, PDL-fibronectin substrate.

Table 1.6 Phenotype (%) of undifferentiated and differentiated OB-CNPCs cultured under varied growth conditions.

Undifferentiated

PDL Passage	Dog	Nestin	GFAP Immature / Mature		ß-Tubulin	Map2ab	O4	GalC
5	1	99.2	93.2	6.8	0	13.3	0	0
	2	94.2	86.5	9.5	0	0	0	0
	3	92.2	79.8	11.0	0	0	0	0
Mean±SEM		**95.2±2.1**	**86.5±3.9**	**9.1±1.2**	**0**	**4.4±4.4**	**0**	**0**
10	1	NA	NA		NA	NA	NA	NA
	2	97.2	98.8	0	0	0	0	0
	3	92.2	90.0	0	0	0	0	0
Mean±SEM		**94.7±2.5**	**94.4±4.4**	**0**	**0**	**0**	**0**	**0**
Fibronectin Passage								
5	1	98.5	85.1	6.3	0	0	0	0
	2	96.3	88.3	3.8	3.6	0	0	0
	3	96.7	81.9	14.2	2.1	11.7	0	0
Mean±SEM		**97.2±0.7**	**85.1±1.9**	**8.1±3.1**	**1.9±1.0**	**3.9±3.9**	**0**	**0**
10	1	97.0	99.5	0	0	0	0	0
	2	97.5	98.8	1.2	0	0	0	0
	3	98.2	98.9	0	0	0	0	0
Mean±SEM		**97.6±0.3**	**99.1±0.2**	**0.4±0.4**	**0**	**0**	**0**	**0**
LIF Passage								
5	1	NA	NA		NA	NA	NA	NA
	2	97.2	96.1	3.2	0	9.8	0	0
	3	88.4	41.5	14.2	1.5	5.2	0	0
Mean±SEM		**92.8±4.4**	**68.8±27.3**	**8.7±5.5**	**0.8±0.8**	**7.5±2.3**	**0**	**0**
10	1	NA	NA		NA	NA	NA	NA
	2	97.2	99.0	0	0	0	0	0
	3	92.2	87.6	0	0	11.8	0	0
Mean±SEM		**94.7±2.5**	**93.3±5.7**	**0**	**0**	**5.9±5.9**	**0**	**0**

Values represent the mean percentage of positive staining ± SEM for three independent isolations except where noted. NA, not available.

Table 1.6 Phenotype (%) of undifferentiated and differentiated OB-CNPCs cultured under varied growth conditions.

Differentiated

PDL Passage	Dog	Nestin	GFAP Immature / Mature		ß-Tubulin	Map2ab	O4	GalC
5	1	94.1	88.4	8.8	0	5.8	0	0
	2	95.0	38.0	25.0	9.0	0	5.8	0
	3	67.7	14.7	51.4	8.0	13.8	0	0
Mean±SEM		**85.6±9.0**	**47.0±21.8**	**28.4±12.4**	**5.7±2.9**	**6.5±4.0**	**1.9±1.9**	**0**
10	1	77.5	29.9	69.4	0	0	0	0
	2	99.1	66.4	23.5	0	0	0	0
	3	97.8	62.8	2.3	0	0	0	0
Mean±SEM		**91.5±7.0**	**53.0±11.6**	**31.7±19.8**	**0**	**0**	**0**	**0**
Fibronectin Passage								
5	1	94.8	14.0	20.1	3.9	1.6	2.4	3.8
	2	91.7	38.0	13.6	5.4	21.3	2.6	4.2
	3	88.7	33.0	18.8	0	8.7	1.5	0
Mean±SEM		**91.7±1.8**	**28.3±7.3**	**17.5±2.0**	**3.1±1.6**	**10.5±5.8**	**2.2±0.3**	**2.7±1.3**
10	1	93.9	94.2	5.8	0	0	0	0
	2	95.8	88.6	10.8	0	13.8	0	0
	3	97.8	79.6	20.7	0	2.7	0	0
Mean±SEM		**95.8±1.1**	**87.5±4.3**	**12.4±4.4**	**0**	**5.5±4.2**	**0**	**0**
LIF Passage								
5	1	99.2	73.3	7.8	0	5.8	0	0
	2	79.5	37.2	35.3	6.7	19.8	9.2	0
	3	60.8	2.6	76.8	20.6	7.3	4.8	2.5
Mean±SEM		**79.8±11.1**	**37.7±20.4**	**40.0±20.1**	**9.1±6.1**	**11.0±4.4**	**4.7±2.7**	**0.8±0.8**
10	1	NA	NA		NA	NA	NA	NA
	2	96.1	90.4	11.6	0	0	0	0
	3	95.4	59.3	40.7	0	4.2	0	0
Mean±SEM		**95.8±0.4**	**74.9±15.6**	**26.2±**	**0**	**2.1±2.1**	**0**	**0**

Values represent the mean percentage of positive staining ± SEM for three independent isolations except where noted. There was no significant difference between the three culture conditions with respect to differentiation based on staining for neuronal or mature astrocytic markers at P5 (p= 0.944).

positively for neuronal, astrocytic, and oligodendrocytic markers and expressed marker-appropriate morphology. By P10, spontaneous differentiation markedly decreased and the GFAP-positive cells with mature morphology stained with an immature, diffuse pattern rather than a filamentous one. Relative to P5, the proportion of nestin-positive and immature GFAP-positive cells was increased. There was no statistically significant difference between the undifferentiated or differentiated phenotypes of CNPCs cultured under these three conditions.

Discussion

It is important to choose appropriate models for transplantation therapy prior to clinical human trials. While rodents are invaluable models for many genetic and acquired neurologic diseases, the differences in the size and architecture of the murine and human brain are vast. The MPS VII dog model is a homologue of human Sly disease that is a much better paradigm for therapeutic and autologous transplantation strategies than the mouse. Previous studies have characterized CNPCs from the embryonic and neonatal dog ventral mesencephalon and caudate nucleus/subventricular zone as multipotent [105, 203]. Embryonic CNPCs could be expanded for up to six months ex vivo [105]. Thus, embryonic CNPCs fulfill two minimal criteria for neural stem cells: multipotency and self-renewal ability [4, 155]. However, a quantitative evaluation of growth rate, expansion potential, and multipotency was not reported. The authors also do not discuss specific properties of postnatal CNPCs.

To appropriately model transplantation strategies in the dog, it is important to characterize canine neural precursor cells with respect to precursor cell qualities. Two of the criteria that define stem cells fulfill desirable qualities of cells for transplantation. The ability to generate large numbers of progeny and to differentiate into glia and neurons are advantageous features of transplantation cells. In this study we wanted to determine whether NPCs obtained from surgically accessible sites in the postnatal brain could be expanded ex vivo to generate large numbers of progeny and, in so doing, demonstrate properties of stem or progenitor cells. Postnatal CNPCs could be expanded ex vivo for at least 10 passages, producing a 10^2-fold increase in cell number. One study reported a 10^7-fold increase in cells generated over 10 passages (10 weeks), however, mouse embryonic NPCs were evaluated [141]. Another study using human embryonic NPCs showed a 10^7-fold expansion over the course of a year; a 10^2-fold increase was obtained after approximately 50-70 days, similar to our findings for CNPCs [23]. The doubling time for CNPCs is also similar to that obtained for postnatal mouse NPCs and human embryonic NPCs. Mean CNPC doubling times ranged from 2.8 to 6.0 days. Mean doubling times for postnatal mouse NPCs ranged from 3.2 to 9.0 days and human embryonic NPC doubling times were reported as 7-10 days [23, 61]. Although mean doubling times were comparable to human and rodent NPCs, there was a difference between growth rates from different sites. Our findings support the use of olfactory bulb NPCs over cerebellar-derived NPCs for transplantation. Olfactory bulb NPCs had a shorter expansion time and generated greater numbers of cells.

The ability to self-renew, to generate large numbers of progeny, and to differentiate into multiple lineages are hallmark characteristics of neural stem cells [4, 155, 55]. Neural progenitor cells have only limited self-renewal ability and produce only glia or neurons. We and others [105, 200] have demonstrated that CNPC cultures can give rise to cells of all three neural lineages and can be expanded and maintained in culture for months. However, the true test of a neural stem cell is the ability of a single cell to proliferate and give rise to glia and neurons and to duplicate itself. While the proliferation of CNPCs for up to 3 months in culture is support for self-renewal capability, a longer period in culture than was performed in these studies would provide more evidence of self-renewal. Canine NPCs have yet to be clonally assayed for multipotency. It is possible that the CNPC cultures are comprised of separate glial and neuronal progenitors, rather than stem cells. Until a clonal assay is performed, canine NPCs cannot be characterized as stem cells.

The undifferentiated phenotype of CNPCs was nestin-positive and GFAP-positive. Because polyclonal antibodies to GFAP have been reported to show spurious positive staining as a result of cross-reaction with other proteins [199, 34], we confirmed GFAP-positive staining with a monoclonal anti-GFAP antibody. Although GFAP-positive cells have been shown to be stem cells in vivo [32, 157, 108, 51], reports of GFAP staining in undifferentiated human and mouse NPCs ranges from absent to high [126, 23, 103, 61, 8, 153]. Nestin immunopositivity is consistently high in all reports. The presence of Map2ab-positive cells in phenotypically immature cultures, is puzzling. These cells also have an

immature morphology despite staining for a mature neuronal marker. Interestingly, Schinstine et al. [152] reported Map2 and *Tau* immunopositivity in EGF-maintained mouse NPCs and in nascent astrocytes derived from the mouse NPCs. These astrocytes were GFAP-positive, nestin-positive, Map2-positive and *Tau*-positive. Map2 and *Tau* are microtubule-associated proteins that are present in neurons. The authors noted that the EGF-generated NPCs, that also were Map2 and *Tau* immunoreactive, were bipotential. They then speculated that the nestin-positive, GFAP-positive, and Map2-positive 'astrocyte' represents a transitional cell whose cytoskeleton requires the stability of a microtubule-associated protein until it develops other microtubule-associated proteins present in mature astrocytes. Certainly, despite the Map2ab immunoreactivity in canine NPCs, the immature cellular morphology makes it unlikely that these cells represent mature neurons. The interpretation of immunoreactivity is greatly aided by the recognition of cellular morphology.

Canine NPC differentiation assays demonstrated positive staining for neuronal, astrocytic, and oligodendrocytic markers at P1 and P5. However, by P10, there was less immunopositivity for mature markers and an increase in immature morphology. It is possible that after prolonged growth factor exposure the withdrawal of growth factors and exposure to low serum concentration were insufficient stimuli for differentiation. Differentiation in retinoic acid, forskolin, or ciliary neurotrophic factor (CNTF) would determine whether this were the case; these factors have been shown to stimulate differentiation of all three neural cell types[126, 189]. It seems unlikely that the decreased staining for mature

markers is due to a lack of progenitors because one would expect that the undifferentiated cultures would then be composed largely of mature, differentiated cells, which is not the case.

The growth rate, expansion, and differentiation potential of normal CNPCs are comparable to human and postnatal mouse NPCs. The pathogenesis of neurodegeneration in MPS VII, as for most LSDs, is unclear. The response of neural precursor cells to bFGF, EGF, and other morphogens in vivo such as sonic hedgehog and bone morphogenetic proteins-2 (BMP-2) and BMP-4, is dependent upon the heparan sulfate glycosaminoglyan [10]. Proteins such as laminin, fibronectin, and chondroitin sulfate proteoglycan contribute to the maintenance of the neural stem cell niche and modulate neuronal migration and axonal guidance [190, 69, 31, 77, 21]. In MPS VII, GUSB deficiency results primarily in lysosomal accumulation of heparan and chondroitin sulfates [193, 138]. Although there are no gross defects in neural structures attributed to the accumulation of substrate during development, it is possible there are postnatal effects of the accumulating substrates. We previously hypothesized that defects in heparan sulfate catabolism may directly impact upon the ability of NPCs to respond to certain morphogens and the extracellular environment [61].

In the mouse model of MPS VII, there was no evidence that the disease phenotype affected either growth rate or neuronal differentiation of NPCs [61]. In this study, unaffected and MPS VII NPCs from postnatal day 1-3 mice were evaluated. Developmentally, a postnatal day 3 mouse is comparable to a human fetus in the early second trimester. Assuming the dog is developmentally similar

to the cat, a 21-day old dog is neurally equivalent to a human fetus in its early third trimester [25]. Thus, we were interested in evaluating diseased NPCs from a later developmental stage. Our data from a large animal model of MPS VII at a later developmental stage did not show any differences between diseased and unaffected CNPCs with respect to growth potential, or neuronal or astrocytic differentiation.

To determine whether CNPC proliferation could be enhanced, we evaluated two variables that have been shown to maintain neural precursor cell qualities in vitro. Fibronectin and leukemia inhibitory factor (LIF) have both been in the culture of NPCs. Fibronectin is an important part of the extracellular matrix and is present in the ventricular and subventricular zones of postnatal rats and mice [69, 21]. When used to facilitate NPC retroviral transduction, it was shown to increase NPC proliferation [135]. Leukemia inhibitory factor is essential to the maintenance of embryonic stem cell cultures and was shown to increase NPC proliferation rate and longevity [23]. Leukemia inhibitory factor receptor (LIFR) deficient mice have a reduced number of adult neural stem cells [162]. When normal canine olfactory bulb-derived NPCs were cultured on fibronectin or in the presence of LIF, there was no difference with respect to differentiation ability. Neural precursor cells grown with LIF had a significantly slower doubling time and generated fewer cells than NPCs grown without LIF. However, the effects of LIF on NPC growth were not apparent until 50-60 days in culture in one study using human fetal NPCs [23]. For transplantation purposes, the delay in growth noted with LIF-supplemented cultures is not advantageous.

Fibronectin did not enhance growth rate or expansion of CNPCs as it did for neonatal mouse NPCs [135]. Whittemore et al. [189] compared the growth rate of adult rat SVZ-derived NPCs with different combinations of substrates and growth factors. They found that cells grown on polyornithine-fibronectin with bFGF and heparin did not proliferate more than the other substrates used. However, the addition of EGF with bFGF and heparin in our cultures makes it difficult to compare results with those of this group because different combinations of growth factors can affect differentiation ability or growth [189, 202].

Other than slower expansion potential in cells derived from cerebellum or cultured with LIF, our data show no difference between CNPCs from different brain regions, from MPS VII-affected or unaffected dogs, or between cells cultured with fibronectin versus PDL. However, whether these results translate to in vivo behavior is unknown. A comparative transplantation study of CNPCs from different brain regions and cultured under different conditions would be more informative. The characterization of canine neural precursor cells from surgically accessible sites in the postnatal brain will aid in the development of a transplantation model for neurodegenerative disease in a brain that is scaled to that of a human's. Furthermore, the use of NPCs from the olfactory bulb and cerebellum will help pave the way for autologous transplantation studies.

CHAPTER TWO: Lewis X Antigen (CD15) as a Cell Surface Marker for Canine Neural Precursor Cells

Introduction

It has only been a little over a decade that there was widespread acceptance that neural stem cells were responsible for neurogenesis in selected regions of the developed mammalian brain [140, 95, 109, 125, 126, 39, 124]. Neural stem and progenitor cells (NPCs) have been retrospectively identified in vitro by their proliferation in response to growth factors [140, 125, 126, 83, 145, 117]. In vivo, markers of proliferation such as tritiated thymidine and bromodeoxyuridine, were used to identify precursor cells and their derived progeny [2, 3, 95, 109, 39]. Proliferative markers do not unambiguously identify neural precursor cells because they incorporate into the DNA and are present in progeny as well as parent. Intracellular markers such as nestin and glial fibrillary acidic protein (GFAP) have been shown to identify NPCs [64, 90, 32, 157]. The subsequent use of nestin and GFAP promoters for targeted ablation or reporter gene expression has greatly aided in the identification and localization of neural precursor cells in situ [145, 151, 70, 108, 51]. For prospective enrichment of NPCs, intracellular markers preclude the isolation of viable cells. A precursor cell-specific surface marker is ideal for the prospective identification and isolation of NPCs.

The search for a definitive marker of the hematopoietic stem cell (HSC) produced a prodigious list of cell surface antigens that, when expressed in conjunction, served to unambiguously identify HSCs [188]. The true HSC was

identified primarily by the absence of lineage commitment markers. A similar approach for prospective enrichment and identification of adult mouse NPCs in situ has been reported [143]. Positive surface markers for human and rodent NPC selection have included Lewis X antigen (CD15), CD133, Notch-1, ß1-integrin, and syndecan-1 [76, 179, 81, 22, 21, 89]. Additionally, side-population analysis using differential cellular uptake of the nuclear dye Hoeschst 33342 has shown promise for enrichment [68, 79].

Prospective enrichment of neural precursor cells is advantageous for transplantation biology as well as stem cell studies. Neural precursor cell transplantation for neurodegenerative and neoplastic disease is being actively explored [167, 173, 195, 1, 9, 37, 101, 131, 161]. Lysosomal storage diseases are inherited lysosomal enzyme deficiencies, many of which display neurodegenerative disease [115, 183, 46, 184, 73, 180]. The existence of a canine model of the lysosomal storage disease Mucopolysaccharidosis VII (Sly disease) [59] affords the opportunity to model NPC transplantation in a large animal model. Multipotent canine NPCs have been isolated from embryonic and postnatal dogs [105, 200]. To date, canine NPCs are not fully characterized. This study evaluated the use of two cell surface antigens for the prospective identification and isolation of postnatal canine neural precursor cells.

Materials and Methods

Experimental animals. Dogs were raised in the animal colony at the University of Pennsylvania School of Veterinary Medicine according to NIH

and USDA guidelines for the use of animals in research and were approved by the Institutional Animal Care and Use Committee of the University of Pennsylvania. Screening for MPS VII dogs was performed by evaluating Wright-Giemsa-stained blood films for the presence of storage granules in white blood cells. Normal, carrier, or MPS VII genotype was then established by polymerase chain reaction for the mutation [136].

Isolation of canine neural precursor cells. Three unaffected dogs ranging nineteen days of age were humanely euthanized by intravenous injection of a barbituate solution. The brain was removed, placed into a balanced salt solution, and then dissected grossly. The cerebellum and rostral one-third of the brain located just caudal to the olfactory bulbs and rostral to the hippocampus were separated from the brain and from each other. The rostral one-third of the brain was further dissected to leave primarily the tissue surrounding the lateral ventricles (including parts of the corpus callosum, caudate putamen, and septae). Half of the vermis and half of a lobule were removed from the cerebellum. The resultant tissues from the striatal SVZ and cerebellum were minced separately, then digested in 0.25% trypsin (Worthington) in a 37°C water bath for 45 minutes to 1 hour. The enzymatic digestion was stopped with addition of fetal bovine serum (FBS; Hyclone). The tissues were then incubated with DNAse I (Sigma) for fifteen minutes in a 37°C water bath and triturated to a single cell suspension with successively smaller diameter pipettes, ending at a flame-polished Pasteur pipette. The cell suspensions were centrifuged at 700 rpm at 4°C for 8 minutes, resuspended in 10% FBS plating medium (see below), and triturated. The total

number of viable cells was determined by manual count on a hemacytometer; cell viability was assessed using trypan blue exclusion (0.4%; Sigma).

Neural precursor cell culture and expansion. The NPCs were plated at a concentration of $4x10^4/cm^2$ in 10% serum-containing plating medium consisting of DMEM:F12 (1:1 ratio; GibcoBRL) supplemented with 10% FBS, 1% N2 supplement (GibcoBRL), 1% antibiotic-antimycotic (PSF)(100 U/mL penicillin; 100 µg/mL streptomycin; 0.25 µg/mL amphotericin B; GibcoBRL), and 1% L-glutamine (2mM; GibcoBRL). After 24-48 hours, the medium was changed to a serum-free feeding medium consisting of DMEM:F12 supplemented with 1% N2 supplement, 1% PSF, and 1% L-glutamine. The standard combination of growth factors consisted of 20 ng/mL epidermal growth factor (EGF) (recombinant murine; Roche), 20 ng/mL basic fibroblast growth factor (bFGF) (recombinant human; Promega), and heparin (5 µg/mL; Sigma). The NPC cultures were maintained at 37°C in humidified 5% CO_2 tissue culture incubators. Cultures were fed every 3-5 days by changing half of the medium and adding fresh growth factors. The NPCs were plated into 25 cm^2 tissue culture flasks (Corning) coated with 10 µg/mL poly-D-lysine (Sigma). Cultures were passaged at approximately 90% confluence by trypsinizing (0.05% trypsin-EDTA; GibcoBRL) and replating at a concentration of $4x10^4/cm^2$.

Preparation of the brain. Four dogs 19-23 days of age (MPS VII, n=3; unaffected, n=1) and two dogs 3 and 5 days of age (unaffected and MPS VII, respectively) were humanely euthanized with an intravenous injection of a barbituate solution. Immediately before death, the dogs were anesthetized and

given intravenous heparin (1000U/mL). After death, intracardiac perfusion with cold 0.9% saline followed by 4% paraformaldehyde solution was performed. The brains were removed and fixed in 4% paraformaldehyde for 24 hours prior to dehydration in 30% sucrose solution. The rostral brain was transversely sectioned caudal to the olfactory bulbs and rostral to the hippocampus, and the cerebellum was separated from the brainstem. These sections were then frozen in optimal cutting temperature (OCT) embedding medium and stored at -80°C.

An embryonic dog at day 28 of gestation was obtained from a pregnant dam. The dam was anesthetized and a caeserian section was performed using sterile surgical practice according to the guidelines of the Institutional Animal Care and Use Committee. The pup was removed and humanely euthanized with an intraperitoneal injection of barbituate. The head was removed and placed into 4% paraformaldehyde for 24 hours. After fixation and dehydration in 30% sucrose solution, the tissue was frozen in OCT.

Immunohistochemistry. The frozen brain regions were sectioned into 20 µm slices on a cryotome and subjected to immunohistochemical staining. The polyclonal primary antibodies used were rabbit polyclonal anti-nestin, *1:20* dilution (rabbit 130; kind gift of R. McKay, NIH) and rabbit polyclonal anti-glial fibrillary acidic protein (GFAP), *1:100* dilution (Chemicon). Primary monoclonal antibodies consisted of rat anti-GFAP, *1:1* dilution (IgG; kind gift of V. Lee); mouse anti-human CD133/1 and CD133/2 (clones AC133 and 293C3, respectively), *1:50* dilution (IgG; Miltenyi Biotec); and mouse anti-human CD15, *1:20* dilution (IgM; BD PharMingen). Secondary fluorescent antibodies used

were goat anti-mouse IgG/IgM FITC, *1:300* dilution (Chemicon); goat anti-rabbit IgG 594 Alexa fluor, *1:300* dilution (Molecular Probes); goat anti-rabbit IgG 488 Alexa fluor, *1:300* dilution (Molecular Probes); and goat anti-mouse IgM Alexa fluor 488, *1:300* dilution (Molecular Probes).

Tissue sections were thawed, then blocked for 1 hour in 10% goat serum (GibcoBRL) with 0.2% Triton X-100 (Sigma) in PBS. Sections labelled with antibodies against cell surface antigens did not receive a blocking step. Primary antibody incubation was performed for 2 hours at room temperature or overnight at 4°C in PBS with 2% goat serum and 0.2% Triton X-100 (Triton X-100 was not used for cell surface marker labelling). The sections were washed three times in PBS and then incubated with secondary antibody in PBS for 1 hour at room temperature or overnight at 4°C. After another 3 PBS washes, the slides were mounted in Vectashield containing 4',6 diamidino-2-phenylindole (DAPI; Vector Laboratories).

Canine neurospheres from CNPC cultures were washed in PBS, suspended in 4% paraformaldehyde for 10 minutes, dehydrated in 30% sucrose solution for 4 hours, and frozen in OCT. Cryosections of neurospheres (20 μm) were then subjected to immunofluorescent staining as above.

Fluorescence activated cell sorting (FACS). Single cell suspensions from three separate isolations of acutely dissociated striatal subventricular zone tissue and from a single isolation of dissociated cerebellar tissue were used. The cells were obtained from 19 day-old unaffected dogs. Aliquots of $5x10^6$ cells were rinsed in PBS after centrifugation at 700 rpm for 8 minutes at 4°C. The

cells were then incubated in a 1:50 dilution of anti-human CD15 (BD Pharmingen) in 2% bovine serum albumin (BSA; GibcoBRL) for 25 minutes at 4°C. The cells were washed twice in 2% BSA and resuspended in a 1:500 dilution of goat anti-mouse IgM Alexa fluor 488 (Molecular Probes) for 20 minutes at 4°C. Control aliquots were incubated only with the secondary antibody. After a final two washes, cells were resuspended in 2% BSA for FACS analysis. Alexa fluor 488+ cells were sorted using a FACSVantage SE cell sorter (BD Biosciences) at a rate of 5000 events/second. The cells were collected into N2 medium supplemented with 10% FBS and plated at a density of $4x10^4/cm^2$ into PDL-coated wells.

Confocal analysis. Immunolabelled sections were scanned with a Leica DM IRE2 HC fluo TCS 1-B-UV microscope coupled to a Leica TCS SP2 spectral confocal system/UV. The three fluorochromes were then sequentially scanned.

Immunocytochemistry. Cultures were differentiated by plating in the absence of growth factors in an 8-well chamber slide (Lab-Tek II; Nalge Nunc) at a concentration of 4×10^4 cells/well in feeding medium supplemented with 1% FBS. Undifferentiated NPCs were plated at a concentration of $2x10^4$/well onto poly-D-lysine-coated 8-well glass slides (Cel-Line, Erie Scientific) and allowed to attach overnight in feeding medium containing growth factors. Differentiated and undifferentiated NPC cultures were processed for immunocytochemistry after 10-12 days and 24 hours, respectively.

The polyclonal primary antibodies used were rabbit polyclonal anti-nestin, *1:60* dilution (rabbit 130; R. McKay, NIH) and rabbit polyclonal anti-GFAP, *1:100*

dilution (Chemicon). Primary monoclonal antibodies consisted of rat anti-GFAP, *1:1* dilution (IgG; V. Lee); mouse anti-human CD15, *1:50* dilution (IgM; BD PharMingen); mouse anti-ßtubulin III, *1:300* dilution (IgG; Chemicon); mouse anti-MAP2ab, *1:300* dilution (IgG; Chemicon); mouse anti-O4, *1:3* dilution (IgM); and mouse anti-galactocerebroside, *1:1* dilution (IgG3) (both oligodendrocyte markers were generous gifts of J. Grinspan). Secondary fluorescent antibodies used were goat anti-mouse IgG/IgM FITC, *1:300* dilution (Chemicon); goat anti-rabbit IgG 594 Alexa fluor, *1:300* dilution (Molecular Probes); goat anti-rabbit IgG 488 Alexa fluor, *1:300* dilution (Molecular Probes); and goat anti-mouse IgM Alexa fluor 488, *1:300* dilution (Molecular Probes).

For all intracellular markers, cells were rinsed in Tris-buffered saline (TBS) (50 mM Tris-base, 0.15M NaCl; pH 7.6), fixed for 10 minutes in 4% paraformaldehyde (Sigma), rinsed three times with TBS, blocked in 5% goat serum (GibcoBRL) with 0.1% Triton X-100 for 40 minutes, and then incubated with primary antibody in 1% goat serum with 0.02% Triton X-100 for 1 hour at room temperature or overnight at 4°C. After three TBS washes, the secondary antibody was applied for 1 hour at room temperature or overnight at 4°C. Cell surface marker staining was performed on live cells. The cells were rinsed in TBS, incubated with primary antibody diluted in TBS for 30 minutes, rinsed briefly with TBS, incubated with secondary antibody for 40 minutes, rinsed with TBS, and then fixed for 10 minutes in 4% paraformaldehyde. All slides were washed three times with TBS before mounting in Vectashield containing DAPI (Vector Laboratories).

Results

Canine neurospheres are CD15-immunopositive. We evaluated postnatal canine NPCs cultured with EGF and bFGF/heparin for reactivity to Lewis X antigen (CD15) and CD133. Cryosections of canine neurospheres maintained in growth factors were immunophenotyped for intracellular neural precursor cell markers, as well as the cell surface molecules CD15 and CD133 (Figure 2.1). The spheres stained positively for nestin, glial fibrillary acidic protein (GFAP), and CD15. No immunoreactivity to CD133 was observed (data not shown). Positive GFAP-staining with polyclonal GFAP antiserum was confirmed with a monoclonal anti-GFAP antibody. Cross-reactivity to proteins other than GFAP has been reported with polyclonal GFAP antiserum [199, 34].

Immunolabelling of the canine neuroepithelium and subventricular zone. In order to determine whether CD15 or CD133 would be appropriate markers for canine neural precursor cells, we evaluated a known region of postnatal neurogenesis, the striatal subventricular zone [95, 109, 149], and its embryonic precursor, the ventricular neuroepithelium. Cryosections of the head of an embryonic day 28 (E28) dog and the striatal SVZ of postnatal day 3 (P3) and P21 dogs were examined. All sections were assayed for nestin, GFAP, CD133 and CD15 immunoreactivity (Figure 2.2). Positive staining for nestin and CD15 was observed in the neuroepithelial cells of the ventricular zone. No staining for GFAP or CD133 was seen in the E28 ventricular zone or the surrounding area (data not shown). The subventricular zone of the P3 and P21

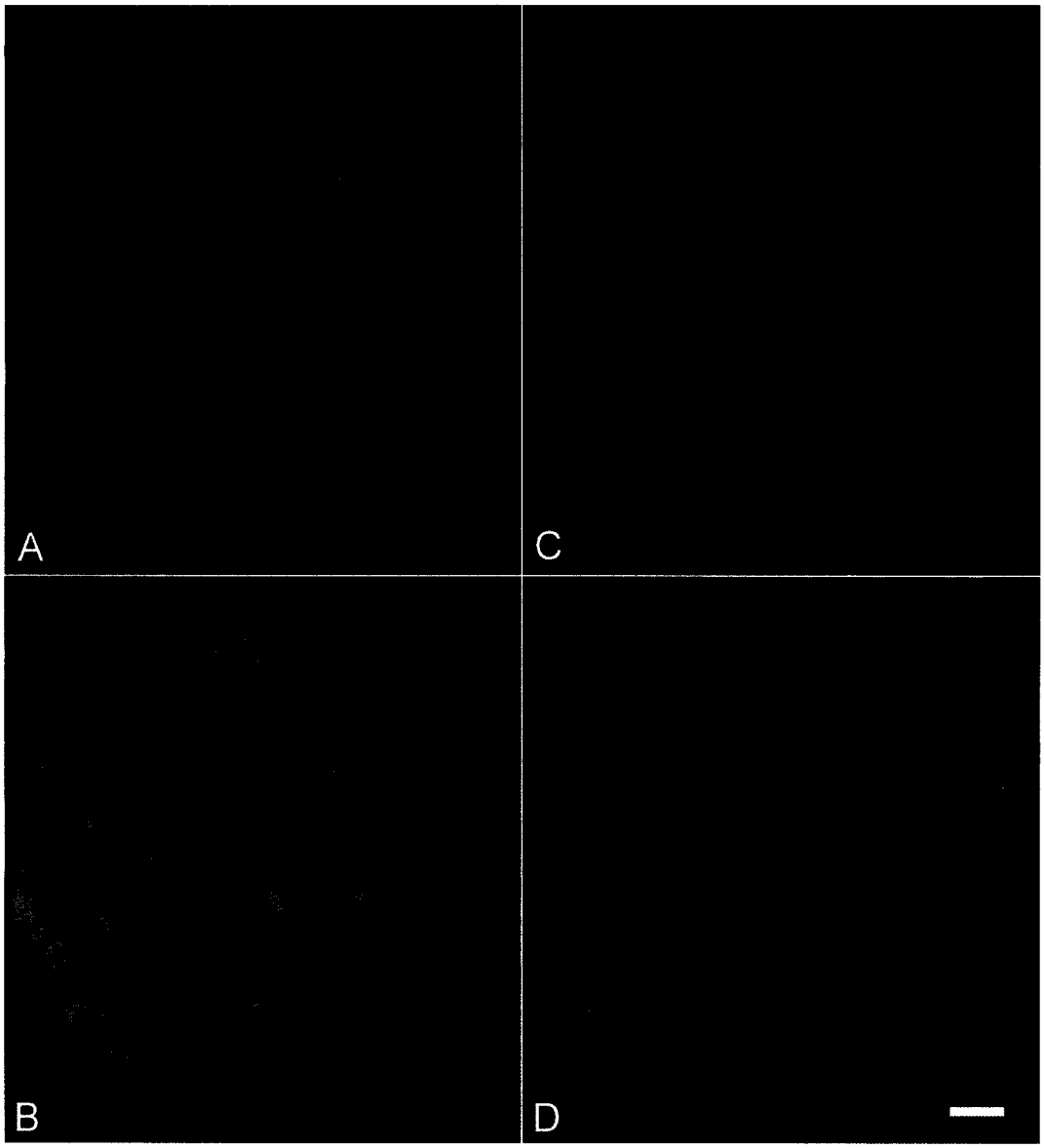

Figure 2.1 Cryosections of canine neurospheres immunolabelled with (A) CD15 (green); (B) GFAP (monoclonal anti-GFAP antibody); (C) control section labelled only with secondary antibody; and (D) nestin (red). Bar= 25μm.

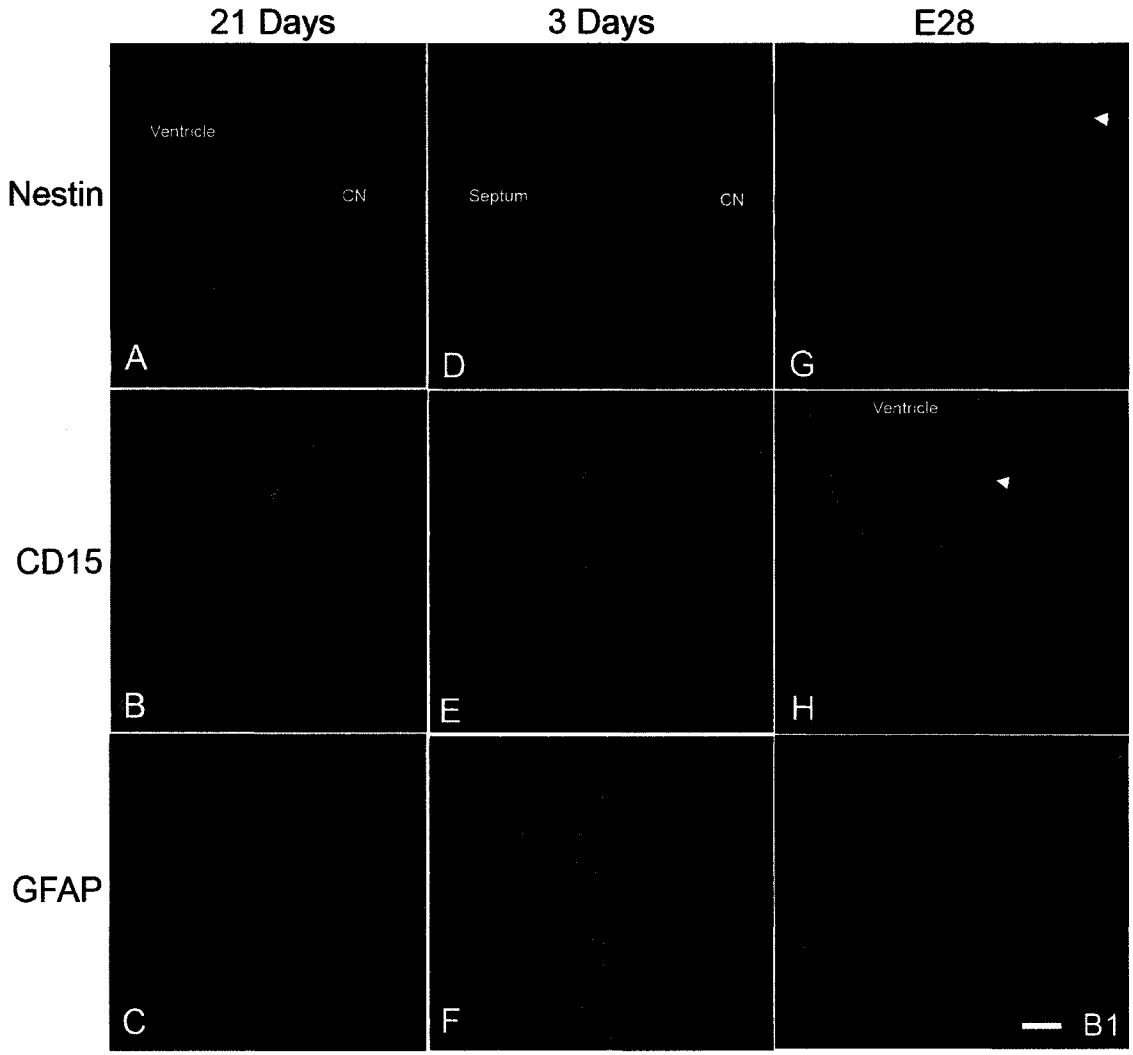

Figure 2.2 In situ immunophenotype of the canine ventricular and subventricular zones. (A-C) The striatal (caudate nucleus) SVZ of a P21 dog. (D-F) The ventricle with septum and caudate nucleus of a P3 dog. (G, H) The telencephalic vesicle (ventricle) and neuroepithelium of an E28 dog. Immunostaining for nestin (A, D, G); CD15 (B, E, H); and GFAP (C, F). A higher magnification view of the CD15-positive cells in the striatal SVZ is shown in (B1). The ventricular neuroepithelial cells are marked by arrowheads (G, H). CN, caudate nucleus. (A-H) Bar= 50μm; (B1) Bar= 25μm.

dogs stained positively for nestin, GFAP, and CD15, but was negative for CD133. In the P3 dog, CD15 staining was restricted to the septal SVZ, whereas in the P21 dog, CD15 staining was evident in both the striatal and septal SVZ (Figure 2.2 and Figure 2.3). The nestin, GFAP and CD15 staining appeared to co-localize in some areas. To confirm double staining of nestin-positive and GFAP-positive cells, sections from the P3 and P21 dogs were analyzed using confocal microscopy. In the regions analyzed, small numbers of nestin and GFAP double positive cells were seen within the ependymal and subependymal layers for both P3 (data not shown) and P21 dogs (Figure 2.4).

Immunolabelling of the canine P21 cerebellum. In the dog, the external granular layer (EGL) of the cerebellum is composed of actively proliferating cells and is maintained until around 70 days of age [130]. The cerebellum from a 21-day old dog was evaluated for CD15 immunoreactivity. We hypothesized that the EGL, a known location of neuronal progenitors, would stain positively for CD15. Strong staining was observed in the white matter tracts of cerebellar folia (Figure 2.5). There were no CD15-positive cells observed in the EGL. We were interested to learn whether nestin-positive cells would also be found in the white matter tracts. Serial sections from the same dog were evaluated for nestin immunoreactivity. Nestin-positive cells were present within the white matter (Figure 2.6).

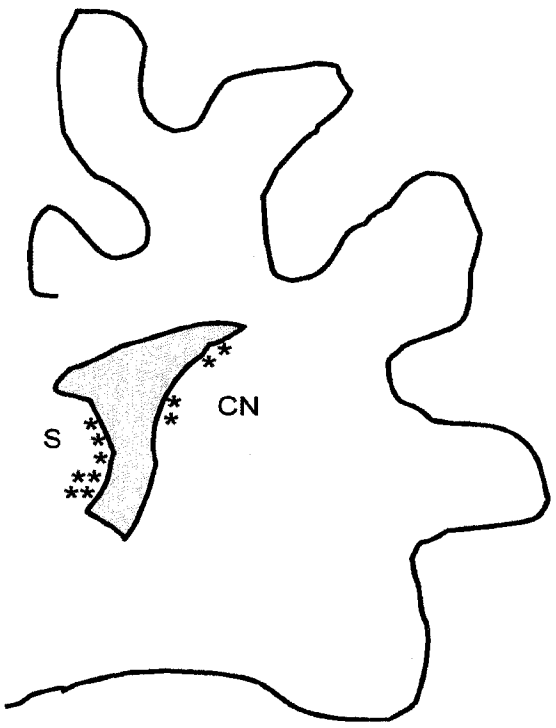

Figure 2.3 Schematic of the right side of the P21 canine brain at the level of the striatal SVZ (caudate nucleus). The asterisks denote regions in which CD15 immunostaining was observed. CN, caudate nucleus; S, septum.

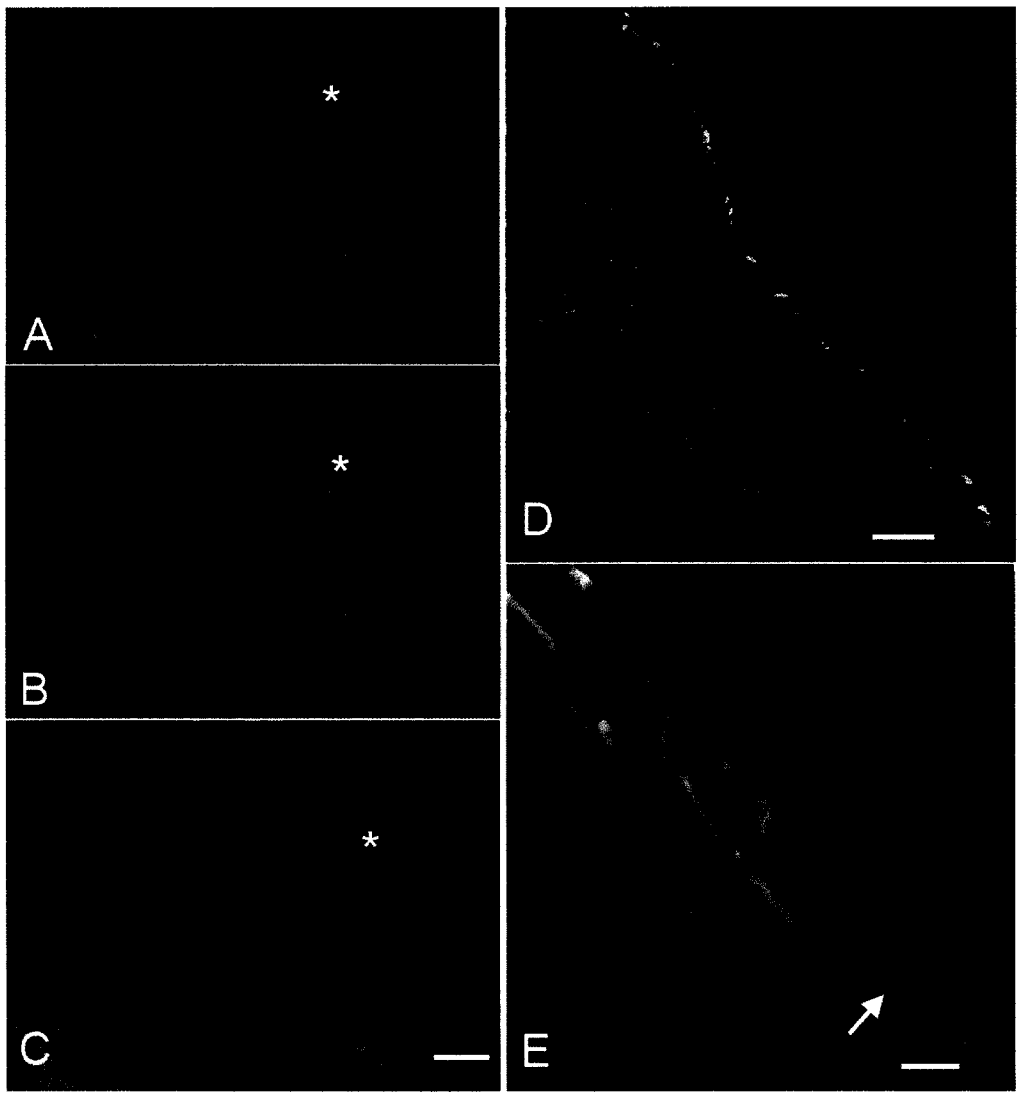

Figure 2.4 The canine septal SVZ. Immunostaining for (A) nestin; (B) GFAP; and (C) CD15. The asterisks mark the ependymal layer. Bar= 20μm. (D) Confocal z-stack of the area depicted in (A-C). Note that there is co-localization of nestin and GFAP staining (yellow) in the processes that run nearly parallel to the ventricle. Bar= 50μm. (E) Confocal z-stack image of the same area at high magnification. The arrow points to one of the double-labelled processes extending to the ventricular surface. A step size of 0.2 μm was used. Bar= 10μm.

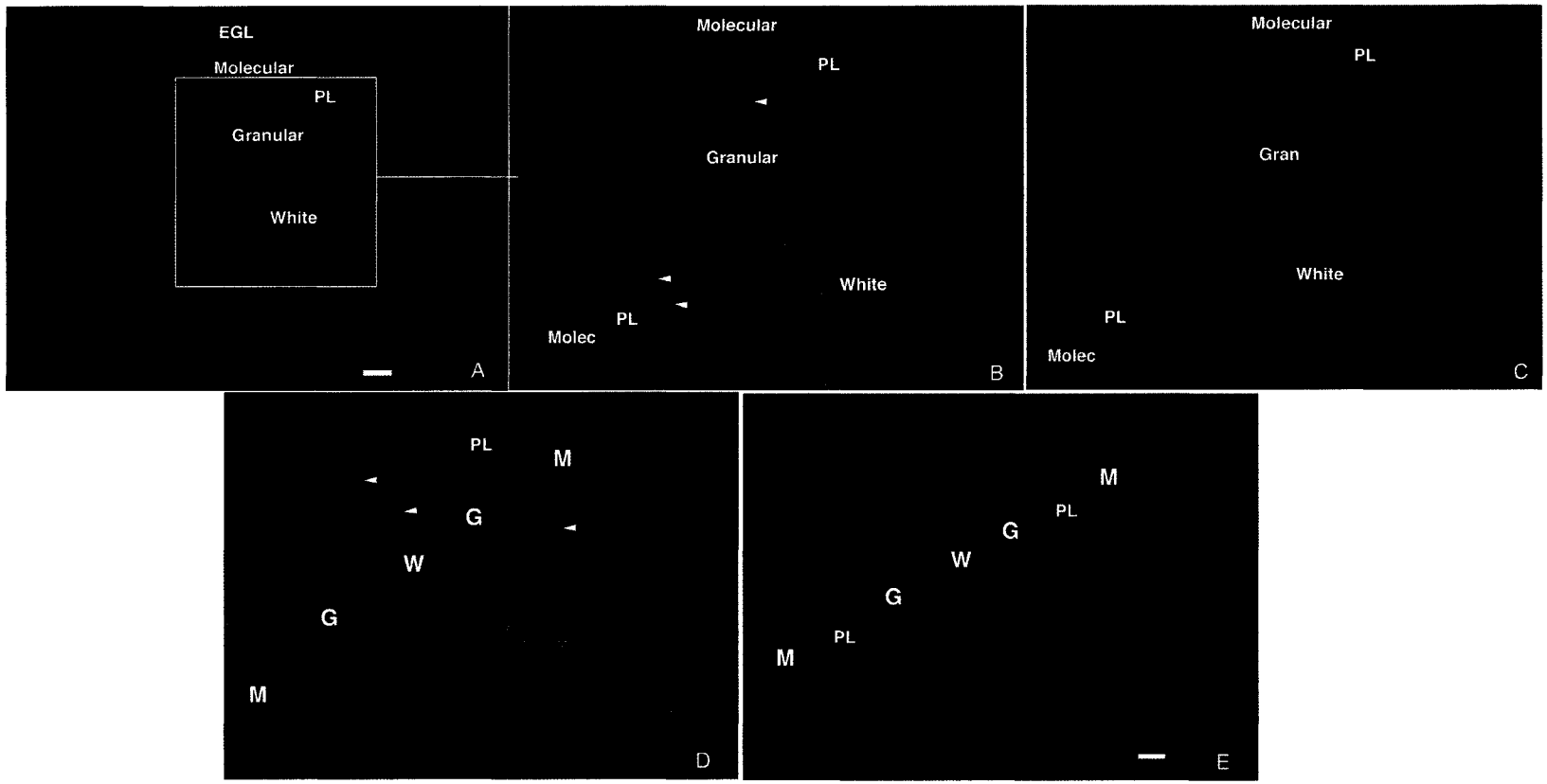

Figure 2.5 CD15 immunostaining of the white matter tracts of the canine P21 cerebellum. (A) DAPI stain showing location of cell nuclei. Bar= 200μm. (B) Higher magnification view of boxed area in A. Note the presence of CD15+ cells in the area corresponding to white matter. (C) Control section for non-specific secondary antibody staining of the same area in B. (D) CD15+ cells concentrated within the white matter tract of a cerebellar folium. Arrowheads in B and D mark CD15+ cells between the white matter and the molecular layer. (B-E) Bar= 50μm. EGL, external granular layer; PL, Purkinje layer; M, molecular layer; G, granular layer; W, white matter.

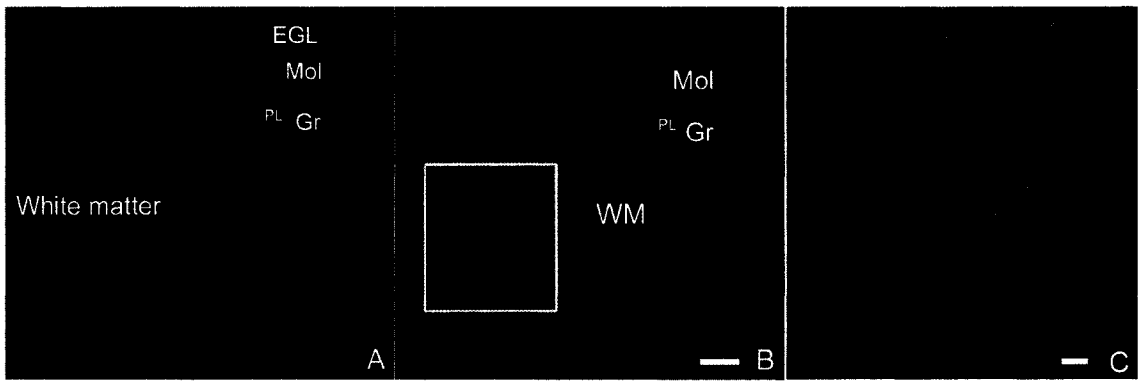

Figure 2.6 Nestin immunoreactivity in the white matter tracts of cerebellar folia. (A) DAPI stain showing location of cell nuclei. (B) Nestin-positive cells are detected within the white matter. (C) High magnification view of the box in B. (A,B) Bar= 100μm; (C) Bar= 20μm. EGL, external granular layer; Mol, molecular layer; PL, Purkinje layer; Gr, granular layer; WM, white matter.

Isolation of CD15+ cells from the canine striatal SVZ. The presence of CD15-positive cells in regions in which neural precursor cells are known to reside supported the use of CD15 as a potential marker for NPC enrichment. Consequently, acute dissociations of the striatal SVZ were performed for three dogs ranging in age from 19 to 23 days. Single cell suspensions were labelled anti-CD15 antibodies and sorted for immunoreactivity with flow cytometry. The mean proportion of SVZ-derived CD15-positive cells from three independent isolations was 6.6 ± 2.2%. A single isolation from the cerebellum of one of these dogs yielded 8.3% CD15-positive cells.

The CD15-positive and CD15-negative cell populations were plated separately into NPC medium with growth factors to assay for proliferation and multipotency. The CD15-negative population was evaluated for CD15-staining immediately post-sorting and was indeed negative. In one of the isolations, neither the CD15-positive nor CD15-negative cells could be expanded beyond passage four. In both of the remaining two isolations, the CD15-positive cell population proliferated, whereas CD15-negative cells were successfully expanded in only one out of the two. Although passage ten was the endpoint of this study, the cells were still proliferating at the end of the experiment.

We evaluated the morphology of CD15-positive and CD15-negative cell populations to determine if there was evidence of maturation in the CD15-negative cells. The morphology of the NPCs was similar regardless of the initial CD15 status (Figure 2.7). Neurospheres were present in both sorted cell categories. The CD15-positive and negative NPCs maintained in growth factors

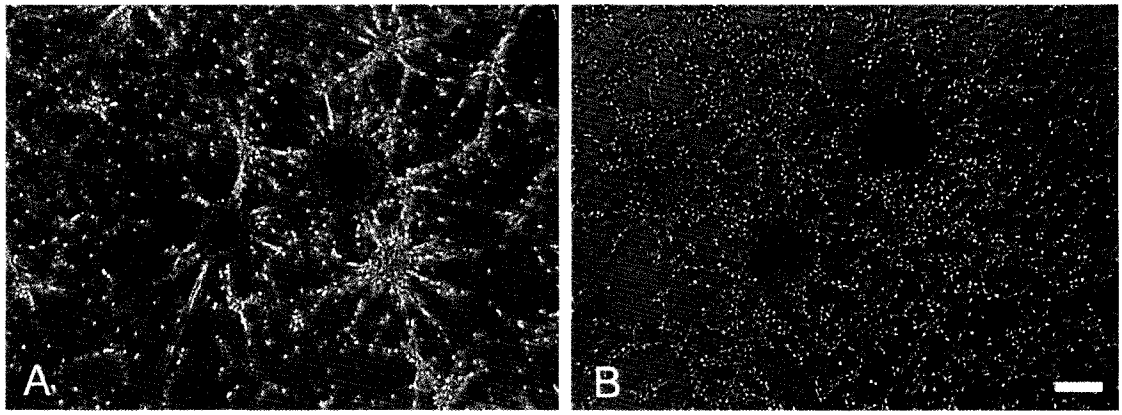

Figure 2.7 Morphology of canine SVZ-derived NPCs sorted for CD15 immunoreactivity in culture. (A) CD15-positive NPCs. (B) CD15-negative NPCs. Both sorted populations generated neurospheres.

were immunophenotyped using a panel of markers for mature and undifferentiated neural cells (Figure 2.8). Both populations of NPCs were nestin-positive and GFAP-positive. The majority of the GFAP-positive cells had an immature, undifferentiated morphology and a diffuse, non-filamentous GFAP staining pattern. The undifferentiated cellular morphology was characterized by small cells with either a unipolar or bipolar, fusiform shape. The diffuse, non-filamentous staining was observed with both polyclonal GFAP antiserum and with monoclonal anti-GFAP antibody. Staining for neuronal markers (ß-tubulin III and Map2ab) and oligodendrocytic markers (O4 and galactocerebroside) was absent. Interestingly, both populations contained a small number of cells that stained positively for CD15.

We next sought to determine whether CD15 distinguished between multipotent neural precursors and lineage-restricted progenitors, by plating the cells for differentiation when sufficient numbers were available. Maturation of GFAP-positive cells from an immature morphology to a mature, large, flattened or stellate cell with a filamentous staining pattern was noted for differentiation cultures derived from both the CD15-positive and CD15-negative populations (Figure 2.9). The CD15-positive-derived differentiation cultures also showed rare (<1%) O4-positive and galactocerebroside-positive cells with marker-appropriate morphology and small numbers (<10%) of faintly positive Map2ab cells. The differentiation culture derived from the CD15-negative NPCs showed fewer than 10% faintly staining ß-tubulin III cells and no positive staining for oligodendrocyte markers.

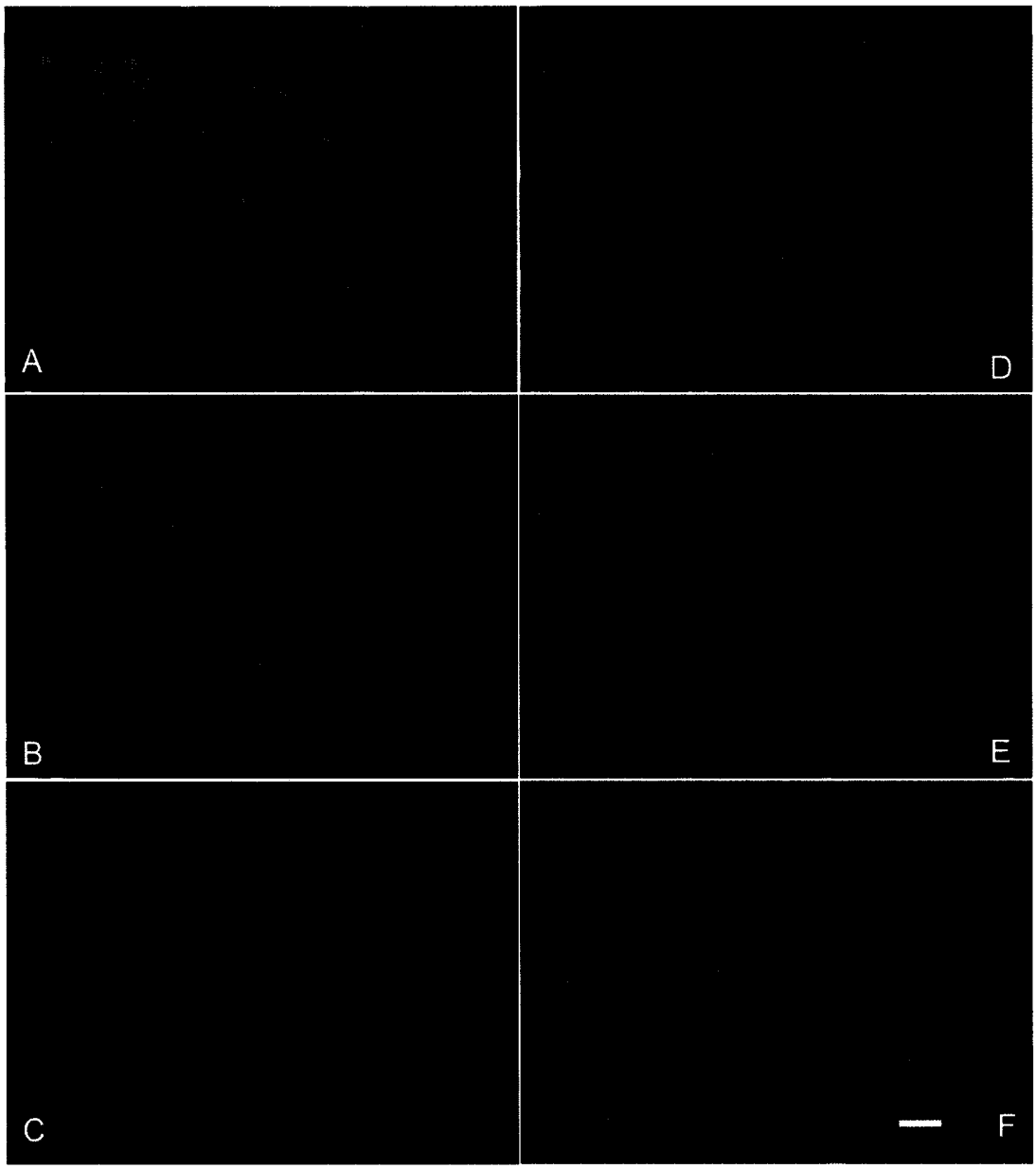

Figure 2.8 Immunophenotype of undifferentiated SVZ-derived canine CD15-postive (A-C) and CD15-negative (D-F) NPCs. The panels represent immunostaining for nestin (A,D), GFAP (B,E) and CD15 (C,F). Bar= 25μm.

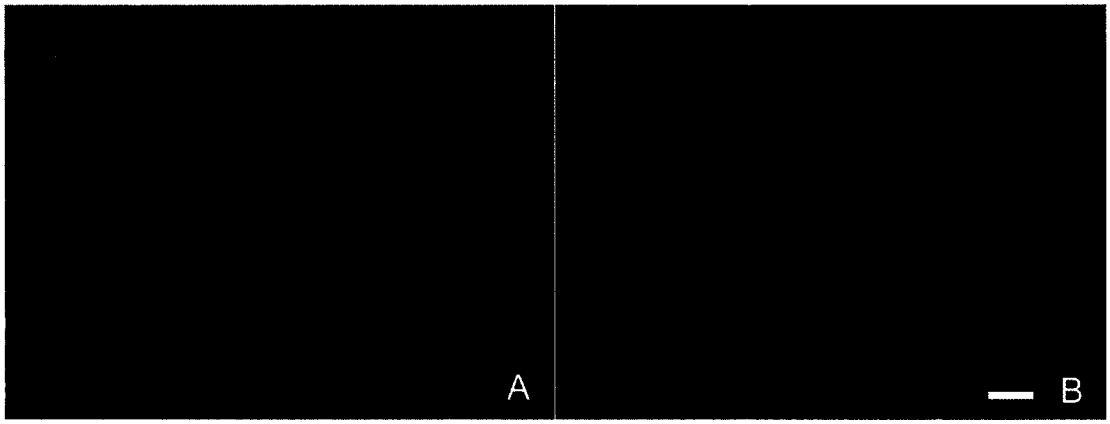

Figure 2.9 Astrocytic cells in differentiation cultures derived from canine CD15-positive NPCs (A), and CD15-negative NPCs (B). Note the change from a diffuse to a filamentous GFAP staining pattern. Bar= 25μm.

Discussion

Cell surface markers permit the selection and sorting of viable cells for in vitro expansion. Lewis X antigen (CD15) is a carbohydrate surface moiety that is associated with primordial germ cells and multipotential stem cells in both the mouse and human [112]. CD133 is the human homologue of prominin, a mouse cell surface glycoprotein that has been used to purify hematopoietic stem cells [27]. Both ligands were shown to be markers for neural precursor cells. CD15 immunoreactivity was present in adult mouse subventricular zone-derived neural precursor cells [179, 22] and CD133 was expressed in embryonic human NPCs [179]. We evaluated both cell surface markers for their potential to prospectively identify canine NPCs.

Our assessment of these two markers was initiated with growth factor-maintained canine neurospheres. While CD15 staining was present on the surface of cells within and at the margins of the spheres, no CD133 staining was observed. We then examined the neuroepithelium of the ventricular zone and the subventricular zone (SVZ) of the caudate nucleus in embryonic and postnatal dogs, respectively. The embryonic ventricular zone and postnatal SVZ are known to be sites in which multipotent neural precursor cells reside [95, 109, 177, 149]. CD15 staining was observed in the neuroepithelium of the embryonic canine ventricular zone as has been reported for the neuroepithelium of the embryonic human and mouse ventricular zones [5, 42]. CD15 immunostaining was also observed in the postnatal canine SVZ, however, there was a difference in the distribution of immunoreactivity between 3- and 21-day old dogs. The

CD15 staining was restricted to the septal SVZ in 3-day old dogs, whereas CD15 staining was present in both the striatal and septal SVZ in 21-day old dogs.

The lack of immunoreactivity to CD133 seen in the postnatal neurospheres was recapitulated in situ for both embryonic and postnatal dogs. The absence of CD133 staining in both embryonic and postnatal tissues precluded developmental stage-specific expression of the marker. Furthermore, CD133/prominin immunoreactivity has been reported for embryonic human NPCs and murine neuroepithelium [179, 151], as well as for adult hematopoietic stem cells and postnatal mouse cerebellar NPCs [27, 89]. It seems likely that species differences in the antigenicity of a putative canine prominin/CD133 ligand account for the lack of immunoreactivity with the anti-human CD133 antibodies. The least amount of conservation between mouse prominin and human CD133 (48-57%) is in the extracellular domain that is recognized by antibodies [27]. The anti-human CD133 antibody AC133 recognizes an epitope that is glycosylated and is detected only in certain stages of cellular differentiation [28]. However, canine tissue was evaluated with both AC133 and 293C3 antibodies; 293C3 is not reported to be influenced by glycosylation. To date, prominin/CD133 has not been reported in the dog, however, given the conservation of the ligand type from rodent to human, it is very likely that a similar glycoprotein is present in the dog.

We also evaluated two intracellular markers associated with NPCs, nestin and GFAP. The embryonic canine neuroepithelium showed strong nestin immunoreactivity, but no filamentous GFAP staining was observed. Strong nestin staining concentrated in the embryonic neuroepithelium has also been

shown for the mouse [151]. The majority of the cells in the postnatal neurospheres and SVZ were immunoreactive for both GFAP and nestin. We were able to co-localize GFAP and nestin staining in small numbers of SVZ cells. These findings are similar to the mouse SVZ in which GFAP/nestin double-positive cells were demonstrated to represent the astrocytic neural stem cell [33].

In the postnatal SVZ, the mean proportion of CD15-positive cells from three independent isolations was 6.6 ± 2.2%. This is similar to the proportion reported for the adult mouse striatal SVZ (4.3 ± 0.2%) [22]. The isolation and expansion of CD15-positive cells for up to three months (10 passages) and the demonstration of multipotency in a differentiation assay with CD15-positive-derived neural cells suggests that CD15 is expressed on canine neural precursor cells. Furthermore, these cells were phenotypically consistent with an NPC phenotype (GFAP-positive and nestin-positive). However, CD15-negative cells from the two isolations evaluated also expressed a GFAP/nestin double-positive phenotype. In addition, one of the three CD15-negative sorted SVZ isolations was expanded for the same amount of time as the CD15-positive cells and expressed markers and morphology of both neurons and mature astrocytes when grown under differentiating conditions. It is possible that the CD15 surface marker comprises a multipotent NPC, whereas the CD15-negative cell population includes unipotent or bipotent progenitors. Too few cells with differentiation markers were obtained in the differentiation assays to determine the full range of potency for CD15-positive and negative populations. Use of factors to promote

cellular differentiation such as retinoic acid, forskolin, or ciliary neurotrophic factor would help in the characterization of potency [126, 189].

The cerebellum is an additional site of postnatal neurogenesis [133, 197, 198, 89]. We anticipated that the source of proliferating cells obtained in canine cerebellar NPC cultures was the external granular layer (EGL). The EGL remains proliferative for weeks to years after birth, depending upon the species and was thought to account for the interneurons of the granular and molecular layers [133, 130, 48]. It was recently shown that NPCs residing in white matter tracts are the source of molecular layer interneurons; EGL granule cell precursors were shown to be restricted to the generation of granule cell neurons [198]. Furthermore, the white matter NPCs were also shown to generate oligodendrocytes and astrocytes [197]. In support of these findings, another study has identified two groups of neural precursors in the cerebellum: bFGF-responsive and bFGF-non-responsive cells [89]. The bFGF non-responsive cells were granule cell precursors (GCPs) of the EGL identified by reporter gene expression driven by a GCP-specific promoter. None of the bFGF-responsive cells represented GCPs and approximately 30% of these cells stained positively for prominin. Of the prominin-positive cells that expressed no markers of differentiation, ~20% stained positively for nestin. Prominin was then used to successfully identify and isolate multipotent postnatal mouse cerebellar precursor cells [89]. Interestingly, in situ hybridization for prominin mRNA and prominin immunoreactivity was restricted to the white matter tracts of cerebellar folia and not in the EGL [89]. Our data showing CD15-positive cells and nestin-positive

cells within the canine cerebellar white matter suggests that CNPCs are also present within the postnatal canine cerebellum. In previous work, we have successfully isolated and propagated canine cerebellar NPCs in bFGF/heparin and EGF. These canine NPC populations were demonstrated to be multipotent. Because bFGF-responsive cells in the mouse cerebellum are not derived from the EGL [89], it is possible that canine cerebellar cells expanded in bFGF/heparin are also derived from the white matter rather than the EGL. Further studies are necessary to determine whether the CD15-positive cells from the canine cerebellar white matter are equivalent to the prominin-positive, bFGF-responsive cells reported in the mouse cerebellum.

The results of this study demonstrate that CD15-positive cells do include NPCs capable of expansion and differentiation into glia and neurons. However, it is not certain that CD15 staining enriches for neural precursors because similar findings were obtained for the population of CD15-negative cells. The presence of CD15 immunoreactivity in putative CD15-negative cultures would suggest that the sort did not fully separate the two populations. Although the CD15-negative population was evaluated under immunofluorescence immediately post-sorting and found to be negative, it is possible that there were weakly positive CD15 cells that could not be detected with the human eye. Alternatively, it is possible that CD15 is not present on all canine NPCs. Further studies of CD15 expression in canine NPCs are needed.

CHAPTER THREE: Transplantation of Canine Neural Precursor Cells in Xenograft and Allograft Models

Introduction

The isolation of neural stem/progenitor cells that could be expanded ex vivo while still maintaining the ability to self-renew and generate mature progeny opened the way to transplantation therapy for central nervous system (CNS) diseases [43, 140, 142, 166, 137, 23, 181]. The first transplantation studies of ex vivo expanded neural precursor cells (NPCs) showed that NPCs were capable of integrating into the existing neuroarchitecture [167, 41, 44, 195, 122, 37, 131]. Moreover, NPCs could be expanded several logs in vitro, providing a large supply of cells for transplantation [141, 23]. The discovery that multipotent NPCs existed within the postnatal brain [2, 3, 140, 95, 126, 39, 94] broached the concept of autologous cell transplantation that would preclude the need for the immunosuppressive therapy accompanying transplantation procedures.

Neurodegenerative diseases represent a broad spectrum of genetic and acquired processes that would benefit from CNS transplantation therapy. The lysosomal storage diseases (LSDs) are genetic diseases due to a single lysosomal enzyme deficiency. The LSDs occur in as many as 1 in 7000 births [100] and many of them have a significant neurologic component that is characterized by neurodegeneration [183, 73]. The distribution of neurodegeneration within the brain is nearly global [183, 46, 73, 180]. However, because of the nature of lysosomal enzymes, the LSDs represent a unique therapeutic opportunity. The acid hydrolases targeted for cellular lysosomes are

post-translationally tagged with mannose-6-phosphate residues [115]. Mannose-6-phosphate moieties bind to receptors in a late Golgi compartment and dissociate in the acidic prelysosomal compartment. Due to receptor binding inefficiency, some lysosomal enzyme is secreted. Many different cell types possess surface receptors for mannose-6-phosphate moieties so that secreted lysosomal enzymes are taken up by neighboring cells. This process enables the phenomenon of 'cross-correction' that is integral to gene therapeutic strategies for the LSDs. Cross-correction permits the establishment of overlapping 'spheres of correction' produced from the expression of a lysosomal enzyme in foci of transplanted or endogenously transduced cells [176, 163]. Cross-correction obviates the need to transduce every cell in an affected individual.

Mucopolysaccharidosis VII (MPS VII) is a neurodegenerative LSD caused by ß-glucuronidase enzyme deficiency that first manifests in early childhood [164]. The existence of both small and large animal homologues of human MPS VII [59, 11, 52, 24, 47] makes this disease a valuable model for transplantation therapy of LSDs. Cellular transplantation into the brains of MPS VII-affected mice as a means of gene therapy has comprised both neural and non-neural cell types [176, 84, 101]. To date, two studies have utilized NPCs for therapeutic transplantation into the mouse model of MPS VII [167, 101]. The NPCs engrafted widely throughout the brain and there were therapeutic levels of enzyme expression with resultant clearance of cell storage material in the regions of engraftment [167, 101]. These studies are proof of principle that NPC transplantation is therapeutically effective for treatment of CNS disease

associated with MPS VII. However, the brain of a human child is architecturally more complex and nearly 2000-fold larger than that of a mouse. Modelling cell transplantation therapy in the dog brain would allow for the architectural complexities of the human brain with a difference in brain size of only 10-fold.

Materials and Methods

Experimental animals. Dogs were raised in the animal colony at the University of Pennsylvania School of Veterinary Medicine according to NIH and USDA guidelines for the use of animals in research and were approved by the Institutional Animal Care and Use Committee of the University of Pennsylvania. Screening for MPS VII dogs was performed by evaluating Wright-Giemsa-stained blood films for the presence of storage granules in white blood cells. Normal, carrier, or MPS VII genotype was then established by polymerase chain reaction for the mutation [136].

The SCID mice (C3H/HeOuJ) (The Jackson Labs) were maintained in a breeding colony at the Children's Hospital of Philadelphia. Animal procedures were conducted in strict accordance with the NIH *Guide for the Care and Use of Laboratory Animals* and were approved by the Institutional Animal Care and Use Committee of the Children's Hospital of Philadelphia.

Isolation of canine neural precursor cells. Brains from three MPS VII-affected dogs 2-weeks, 4-weeks, and 6.5-weeks of age were collected on three separated occasions. The dogs were humanely euthanized by intravenous injection of a barbituate solution. The brain was removed, placed into a balanced

salt solution, and then dissected grossly. The olfactory bulbs, cerebellum, and hippocampus were separated from the brain and from each other. Half of the vermis and half of a lobule were removed from the cerebellum. The tissues were minced separately and then digested in 0.25% trypsin (Worthington) in a 37°C water bath for 45 minutes to 1 hour. The enzymatic digestion was stopped with addition of fetal bovine serum (FBS; Hyclone). The tissues were then incubated with DNAse I (Sigma) for fifteen minutes in a 37°C water bath and triturated to a single cell suspension with successively smaller diameter pipettes, ending at a flame-polished Pasteur pipette. The cell suspensions were centrifuged at 700 rpm at 4°C for 8 minutes, resuspended in 10% FBS plating medium (see below), and triturated. The total number of viable cells was determined by manual count on a hemacytometer; cell viability was assessed using trypan blue exclusion (0.4%; Sigma).

Neural precursor cell culture and expansion. The NPCs were plated at a concentration of $4x10^4/cm^2$ in 10% serum-containing plating medium consisting of DMEM:F12 (1:1 ratio; GibcoBRL) supplemented with 10% FBS, 1% N2 supplement (GibcoBRL), 1% antibiotic-antimycotic (PSF)(100 U/mL penicillin; 100 µg/mL streptomycin; 0.25 µg/mL amphotericin B; GibcoBRL), and 1% L-glutamine (2mM; GibcoBRL). After 24-48 hours, the medium was changed to a serum-free feeding medium consisting of DMEM:F12 supplemented with 1% N2 supplement, 1% PSF, and 1% L-glutamine. The standard combination of growth factors consisted of 20 ng/mL epidermal growth factor (EGF) (recombinant murine; Roche), 20 ng/mL basic fibroblast growth factor (bFGF) (recombinant

human; Promega), and heparin (5 µg/mL; Sigma). The NPC cultures were maintained at 37°C in humidified 5% CO_2 tissue culture incubators. Cultures were fed every 3-5 days by changing half of the medium and adding fresh growth factors. The NPCs were plated into 25 cm^2 tissue culture flasks (Corning) coated with 10 µg/mL poly-D-lysine (Sigma). Cultures were passaged at approximately 90% confluence by trypsinizing (0.05% trypsin-EDTA; GibcoBRL) and replating at a concentration of $4x10^4/cm^2$.

Canine neural precursor cell (CNPC) transduction. Canine NPCs were transduced with two different viral vectors containing the human ß-glucuronidase (GUSB) gene driven by the human GUSB promoter. The first vector was an amphotropic retroviral murine leukemia virus vector modified to prevent gene silencing [132] and the second vector was a third-generation self-inactivating (SIN) HIV vector [114]. The SIN vectors are replication deficient and the promoter ability of the LTR is abolished due to a deletion in the 3' U3 region of the LTR. Transgene expression is driven solely by an internal promoter. The cultures were transduced by incubating them with the viral supernatant supplemented with 8 µg/ml hexadimethrinebromide (polybrene) (Sigma) in conditioned NPC medium at a multiplicity of infection (MOI) of at least 10. After 4–6 hours, fresh media was added overnight. For the retroviral transduction, this procedure was repeated for four consecutive days. The cells were then passaged and selected in G418 (0.8 mg/ ml) after two days. Selection was performed for at least two passages [61].

Labelling of CNPCs with micron-sized superparamagnetic iron oxide

particles (MPIOs) for MRI. CNPCs for all of the older dog injections and for two out of the four 23-day old dog injections were labelled with MPIOs. These particles are microspheres comprised of an inert polymer matrix of which magnetite iron oxide and a FITC analog (Dragon Green) are components (Bangs Laboratories). Microspheres average 0.9 µm in diameter. The MPIOs were added to the NPC culture medium at a concentration of 1.5×10^8 particles/mL [158] and incubated overnight in the tissue culture incubator. Cells were harvested the following day for transplantation.

Preparation of CNPCs for transplantation. Prior to transplantation, CNPCs were trypsinized and washed twice in PBS by centrifuging at 700 rpm for 8 minutes at 4°C. After the first wash, the cells were resuspended in 1 mL of PBS and the total number of viable cells was determined by manual count on a hemacytometer; cell viability was assessed using trypan blue exclusion (0.4%; Sigma). The cells were then centrifuged and resuspended in a volume of PBS to yield ~$5x10^4$ cells/µl. The suspension was placed on ice until transplantation.

Intraventricular injection into neonatal SCID mice. Neonatal SCID pups were used for xenografts at the first to second day of postnatal life. The pups were cryoanesthetized for 3-5 minutes and assessed to be properly anesthetized before injections. Injections were performed as described previously [167]. Briefly, 2µl of cell suspension were injected into each lateral ventricle with a finely drawn glass capillary pipette using trans-illumination to guide the injection. Trypan blue (0.04% final concentration) (SIGMA) was added to the cell suspension to facilitate visualization of the injections into the ventricles.

The landmarks for injection were 1 mm lateral from midline and 1 mm rostral from the lambda suture line.

Intracranial CNPC transplantation into dogs. Ten MPS VII-affected dogs were injected with CNPCs. Dogs were 23-days old (n=4), 3-months old (n=1), and 5-months old (n=5) at the time of transplantation. The dogs were divided into two groups by age: The first group comprised the 23-day old dogs (n=4) and the second group consisted of dogs older than 3 months of age (n=6).

Dogs were anesthetized with intravenous propofol (4 mg/kg), intubated, and maintained on isofluorane inhalant anesthesia. The older group of six dogs received a single (n=2) or two injections (n=4) into the right hemisphere via a stereotaxic apparatus. The cells used were canine olfactory bulb NPCs from an MPS VII dog transduced with HIV-GUSB/GUSB (SIN vector containing the human GUSB gene driven by the human GUSB promoter). For these injections, transduction was very low (~1% GUSB). Consequently, cells were labeled with MPIOs and suspended in PBS at a concentration of $5x10^4/\mu l$.

A midline incision in the skin was made and the skull was broached using a burr drill. Cells were injected at one (rostral site) or two sites (caudal and rostral) using the following stereotaxic coordinates: Rostral site: 10 mm right of midline; 25 mm ventral to the pial surface; 23 mm rostral to the interaural line. Caudal site: 10 mm right of midline; 25 mm ventral to the pial surface; 10.5 mm rostral to the interaural line. Cells were injected with a 26g Hamilton syringe. The cells were deposited up the injection tract in 1µl aliquots starting from the most ventral point (25 mm ventral to the pial surface) and every 2mm dorsad.

The aliquots were injected over 1 minute and there was a minute delay between each injection; at the end of the injection series, there was a 5 minute delay before the needle was extracted.

For the younger group of dogs (23-days of age), a single bolus injection into the caudal portion of the left caudate nucleus was performed using ultrasound guidance. The fontanelle of dogs this age is not fully calcified and the brain can be visualized via this site. Canine olfactory bulb NPCs from an MPS VII dog transduced with HIV-GUSB/GUSB were used for injection. The transduction efficiency was ~60% for these cells. For two of the dogs, the cells were also labelled with MPIOs. After a midline skin incision, the skull was broached manually with an 18-gauge needle. The cells were injected into the parenchyma by hand with a 26-gauge Hamilton syringe. One microliter (7×10^4 cells) was injected over the course of five minutes.

Post-transplantation surgery, dogs received 20 mg cyclosporine divided every 12 hours until the day of sacrifice. Dogs also were given an antibiotic (Clavamox 13.75 mg/kg) twice daily for 10 days.

Preparation of the brain. Mice to be sacrificed were deeply anesthetized with 5 mg/kg xylazine and 100 mg/kg ketamine. The mice were then perfused transcardially with cold PBS followed by ice-cold fixative (4% paraformaldehyde; pH 7.4). Brains were removed and put into 4% paraformaldehyde overnight at 4°C. Fixed tissues were cryo-protected overnight in 30% sucrose solution at 4°C. After dehydration, the brains were placed in optimal cutting temperature (OCT) embedding medium. Tissues were then frozen on dry ice.

Dogs were humanely euthanized with an intravenous injection of a barbituate solution. Immediately before death, the dogs were anesthetized and given intravenous heparin (1000U/mL). After death, intracardiac perfusion with cold 0.9% saline followed by 4% paraformaldehyde solution was performed. The brains were removed and fixed in 4% paraformaldehyde for 24 hours. The brains of the 23-day old dogs were divided into right and left hemispheres. The left half of the brain (injected side) was sectioned at the rostral and caudal borders of the lateral ventricle and placed in 30% sucrose solution for 24-48 hours. The sections were then frozen in OCT for cryosectioning in a sagittal plane.

Brains from the six older dogs were separated into right and left hemispheres. The right hemisphere (injected side) was sectioned transversely at the rostral and caudal ends of the lateral ventricle. This section was then sectioned horizontally (dorsal to ventral) into 3 mm slices. The odd slices were embedded in paraffin and the even slices were placed into 30% sucrose solution for freezing in OCT embedding medium.

Enzyme histochemistry. Frozen tissue sections were assayed for enzymatic activity by staining with a naphthol-AS-BI-ß-D-glucuronide substrate as reported previously [192]. Briefly, slides were thawed for 5 min at room temperature and treated with chloral-formal-acetone fixative for 30 min at 4°C. The slides were washed three times with 0.05 M sodium acetate buffer (pH 4.5). Next, 0.25 mM naphthol-AS-BI-ß-D-glucuronide (pH 4.5) was added and the slides incubated at 4°C for 4 h, at which point the solution was removed. Equal volumes of 4% pararosaniline solution in 2 N hydrochloric acid (HCl) and 4%

sodium nitrite solution in deionized water were mixed. This solution was diluted 1 to 500 in 0.25 mM naphthol-AS-BI b-dglucuronide (pH 5.2), placed on slides, and incubated at 37°C overnight.

The third wash in 0.05 M sodium acetate was performed at 65°C for all sections. Heat-inactivation serves to distinguish between the human and canine or murine ß-glucuronidase (GUSB) proteins. Canine and murine GUSB are inactivated at 65°C, whereas the human protein is stable.

Immunohistochemistry. The frozen brain regions were sectioned into 20 µm slices on a cryotome and subjected to immunohistochemical staining. The polyclonal primary antibodies used were rabbit polyclonal anti-nestin, *1:20* dilution (rabbit 130; kind gift of R. McKay, NIH) and rabbit polyclonal anti-glial fibrillary acidic protein (GFAP), *1:100* dilution (Chemicon). Primary monoclonal antibodies consisted of mouse anti-ßtubulin III, *1:100* dilution (IgG; Chemicon); and mouse anti-MAP2ab, *1:100* dilution (IgG; Chemicon). Secondary fluorescent antibodies used were goat anti-rabbit IgG 594 Alexa fluor, *1:300* dilution (Molecular Probes); and goat anti-mouse IgG 594 Alexa fluor, *1:300* dilution (Molecular Probes).

Tissue sections were thawed, then blocked for 1 hour in 10% goat serum (GibcoBRL) with 0.2% Triton X-100 (Sigma) in PBS. Sections labelled with antibodies against cell surface antigens did not receive a blocking step. Primary antibody incubation was performed for 2 hours at room temperature or overnight at 4°C in PBS with 2% goat serum and 0.2% Triton X-100 (Triton X-100 was not used for cell surface marker labelling). The sections were washed three times in

PBS and then incubated with secondary antibody in PBS for 1 hour at room temperature or overnight at 4°C. After another 3 PBS washes, the slides were mounted in Vectashield containing 4',6 diamidino-2-phenylindole (DAPI; Vector Laboratories).

Confocal analysis. Immunolabelled sections were scanned with a Leica DM IRE2 HC fluo TCS 1-B-UV microscope coupled to a Leica TCS SP2 spectral confocal system/UV. The three fluorochromes were then sequentially scanned.

Results

Xenograft transplants. Preliminary experiments were performed using canine hippocampal NPCs (CHNPCs) transduced with a retroviral vector carrying the human ß-glucuronidase (GUSB) transgene driven by the human GUSB promoter and a selectable antibiotic resistance gene [132]. The human GUSB protein, in contrast to murine GUSB, is resistant to heat-inactivation. Following heat-inactivation even the small amount of endogenous GUSB in the brain is eliminated, permitting definitive identification of transduced transplanted cells. Following selection with neomycin and prior to transplanation, eighty-five percent of the CHNPCs were GUSB. Neonatal SCID mice were injected unilaterally into the lateral ventricle on the first day after birth and evaluated at 1- and 4-weeks post-injection (n=2 for each time-point). At 1-week post-injection, cells that expressed human GUSB had engrafted throughout the brain from the olfactory bulb to the cerebellum (Figure 3.1). However, by 4-weeks post-injection, there

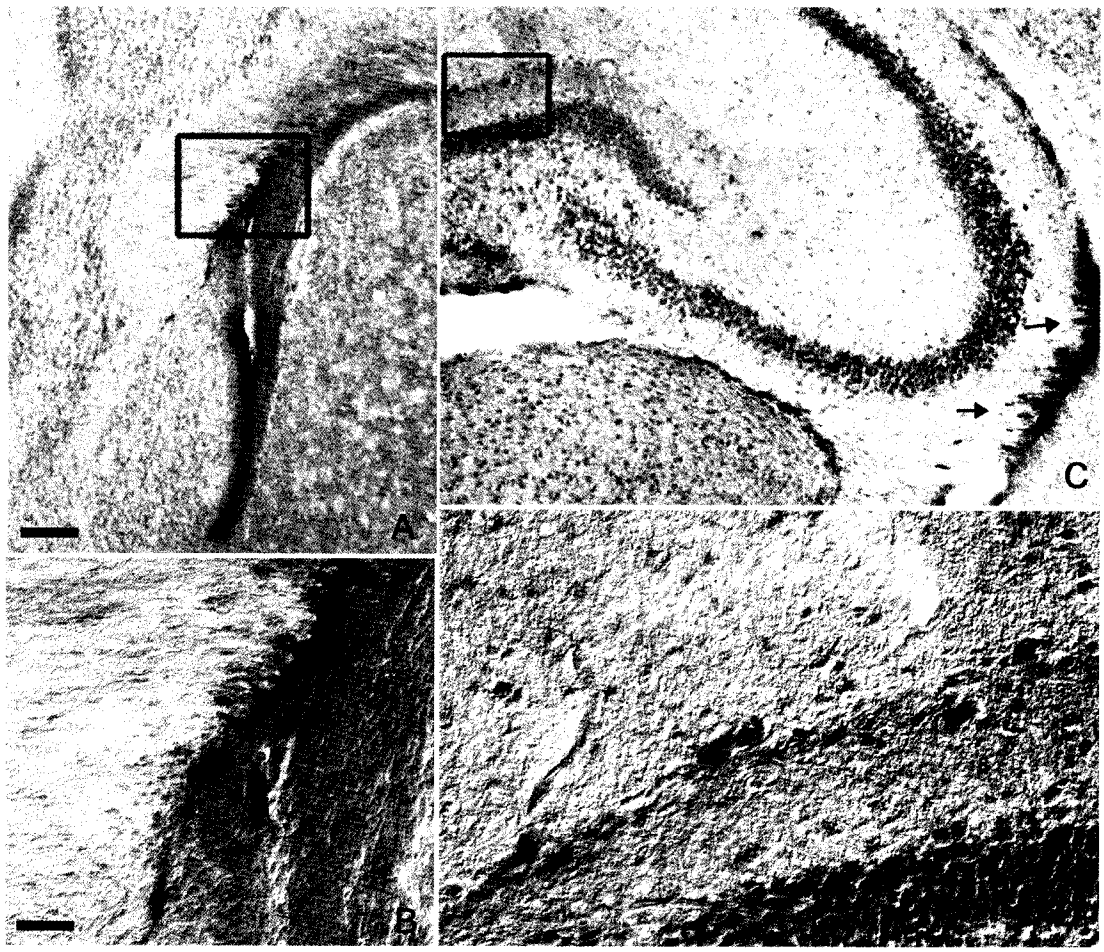

Figure 3.1 Sections of the SCID mouse brain at 1-week post-transplantation. (A) GUSB-positive (red) cells were noted within the ependymal layer of the lateral ventricle and migrating into the corpus callosum. (B) High magnification view of the box in A showing the cells moving along the white matter tract. (C) GUSB-positive cells were present in the dentate gyrus of the hippocampus and were seen migrating out from the lateral ventricle along the corpus callosum (arrows). (D) High magnification view of the box in C showing CHNPCs in the molecular layer of the dentate gyrus. (A,C) Bar= 200μm; (B,D) Bar= 25μm.

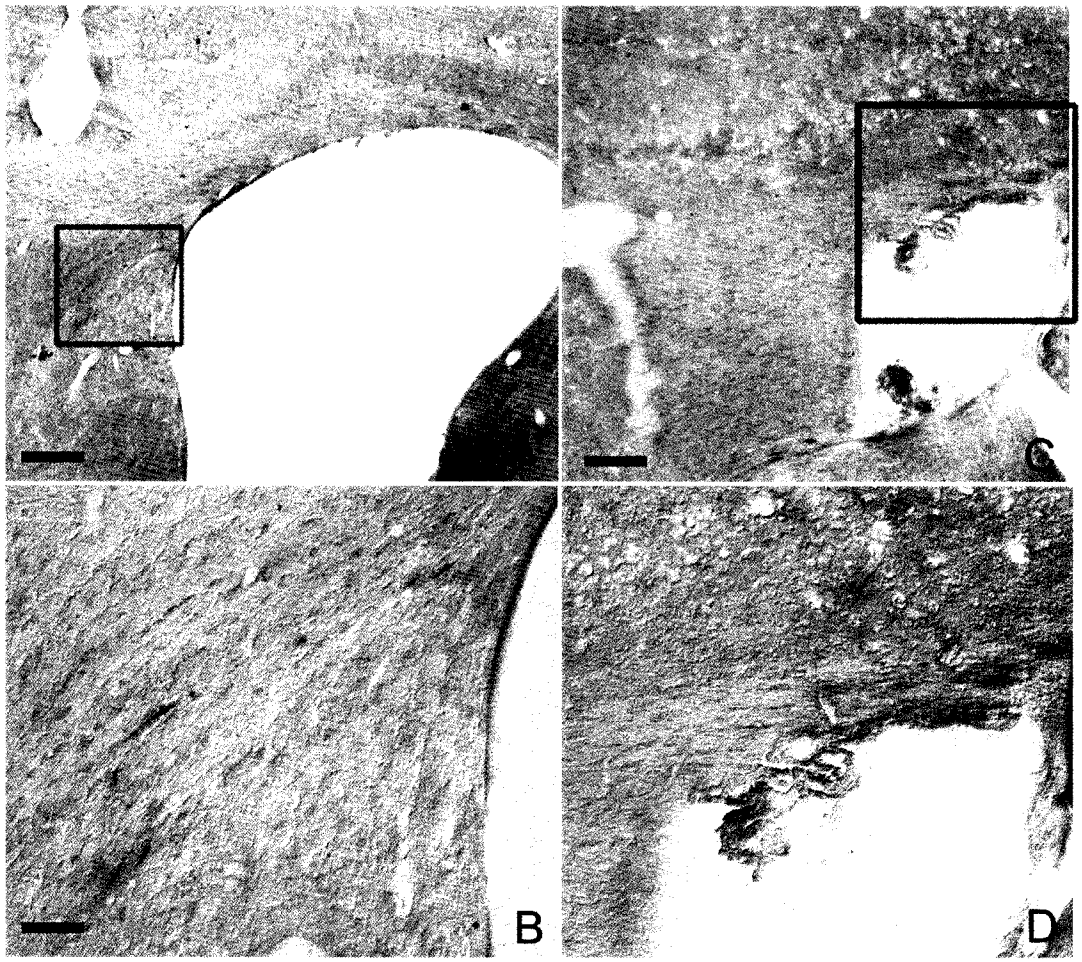

Figure 3.2 Sections of the SCID mouse brain at 4-weeks post-transplantation. (A) Small numbers of GUSB-positive cells remained in the septum and corpus callosum. Bar= 200μm. (C) GUSB-positive cells remaining in the hippocampus were present within the corpus callosum immediately adjacent to the lateral ventricle. Bar= 100μm. (B, D) High magnification view of the boxes in A and C, respectively. Bar= 25μm.

were many fewer GUSB positive cells in fewer regions throughout the brain (Figure 3.2).

The second xenograft experiments were performed using cerebellar-derived CNPCs (Cb-CNPCs) transduced with a lentiviral vector containing the human GUSB gene driven by the human GUSB promoter. Approximately 60% of the Cb-CNPCs were GUSB-positive prior to transplantation. The Cb-CNPCs were injected bilaterally into the lateral ventricles in six neonatal pups. Brains were evaluated at 1- and 6-weeks post-transplantation (n=3 for each time-point). Small numbers of cells positive for GUSB were seen in the olfactory bulb and engraftment extended caudally to the rostral hippocampus (Figure 3.3). No GUSB-positive cells were observed in the caudal part of the brain, including the cerebellum and colliculi. The amount of GUSB staining and number of cells was similar in the first and sixth weeks post-transplantation.

Murine allograft transplants. In order to determine whether the difference in species accounted for the sparse CNPC engraftment, primary mouse NPCs were injected into the lateral ventricles of neonatal SCID mice. The mouse NPCs were isolated from the forebrain of neonatal mice transgenic for the human GUSB gene [86]. Engraftment was assessed by expression of human GUSB. Overall, the engraftment of primary mouse NPCs was greater than that of the canine lentivirally transduced xenograft (Figure 3.4 and Figure 3.5).

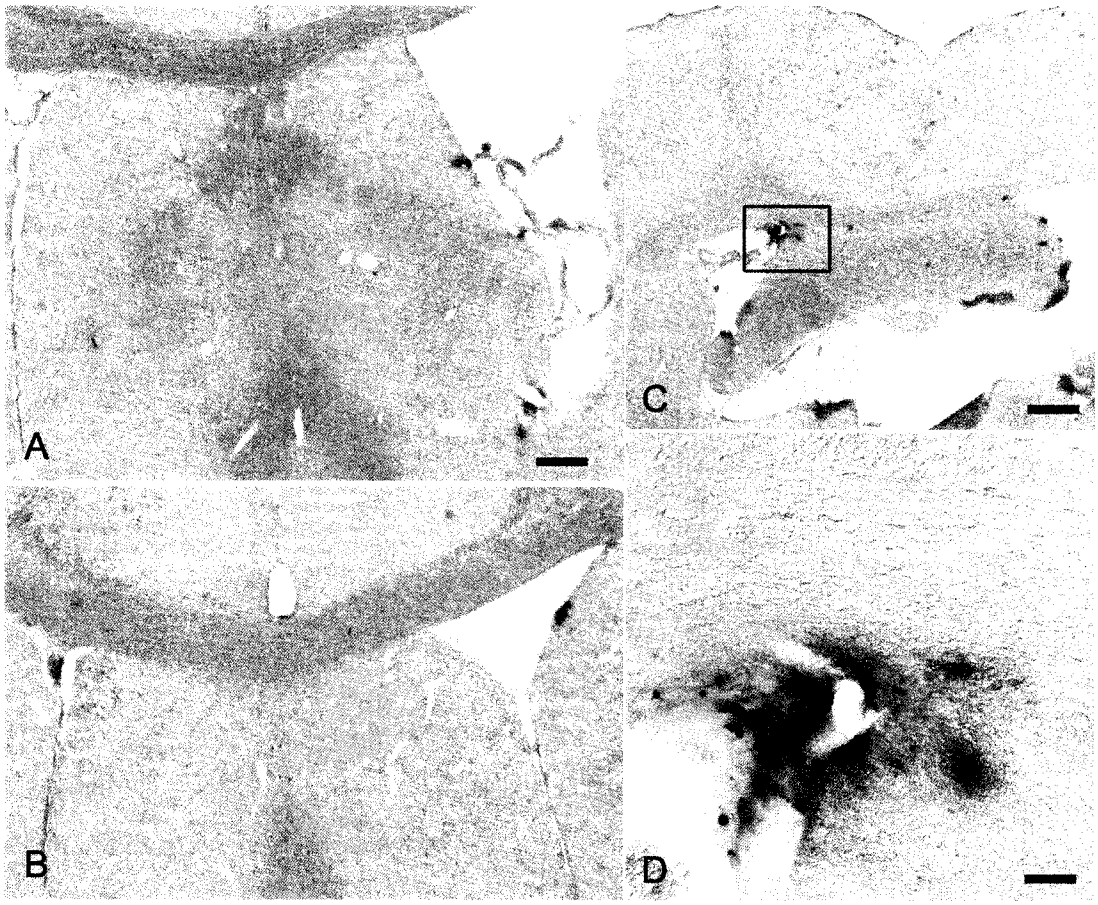

Figure 3.3 Cb-CNPC engraftment 6-weeks post-transplantation. GUSB-positive cells were observed in the subventricular zone of the (A) septum, (B) caudate nucleus, and (C) the corpus callosum and fimbria. (D) A higher magnification view of the box in C is shown. (A,B) Bar= 200μm; (C) Bar= 400μm; (D) Bar= 50μm.

Figure 3.4 Engraftment of primary transgenic human GUSB mouse NPCs at 7-weeks post-transplantation. GUSB-positive cells were detected in small numbers throughout the brain beginning in the olfactory bulbs and extending caudally (see Figure 3.5). Bar= 400μm.

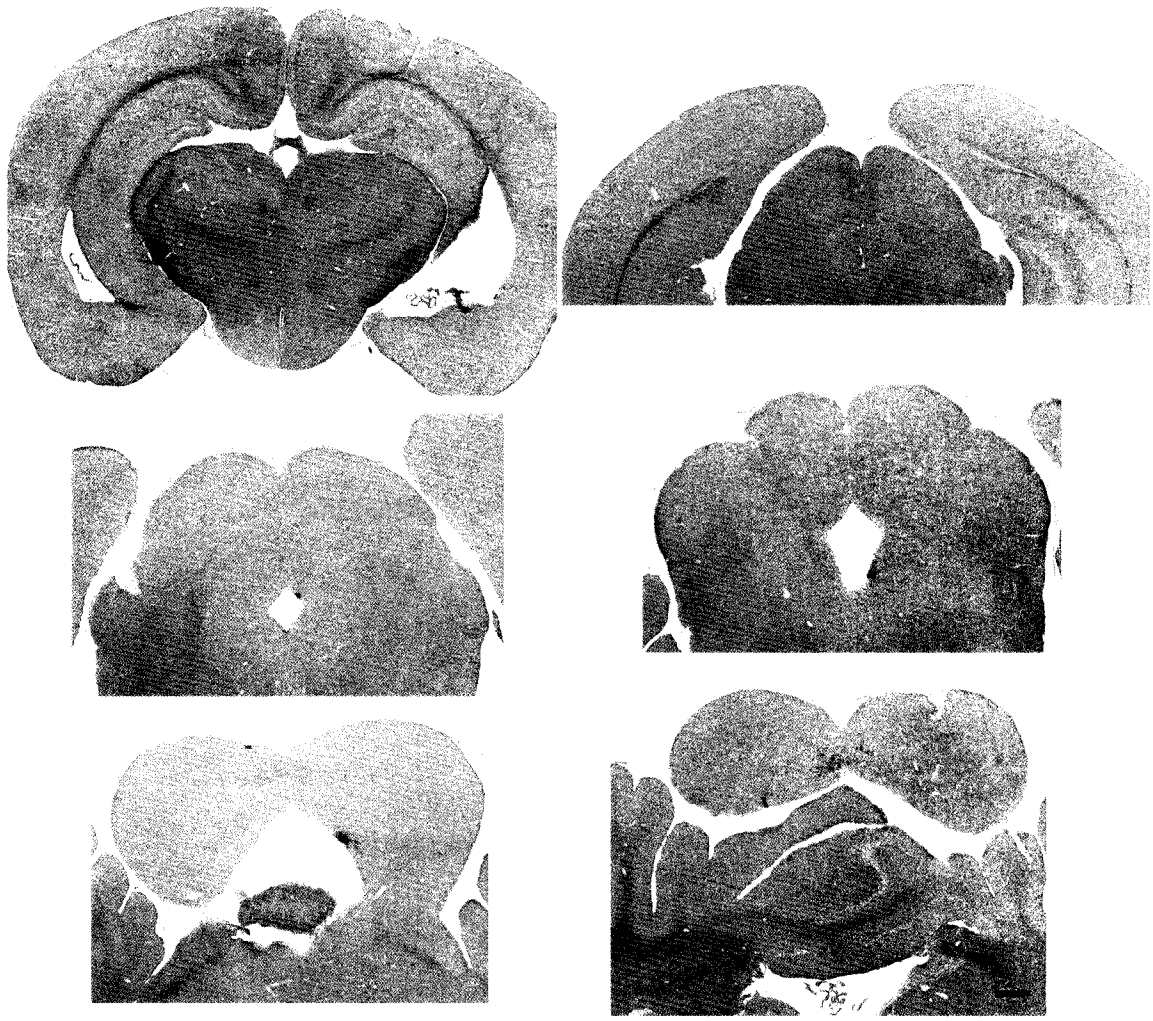

Figure 3.5 Engraftment of primary transgenic human GUSB mouse NPCs at 7-weeks post-transplantation. The GUSB-positive mouse NPCs were observed as far caudal as the colliculi and the cerebellum, but only small numbers of cells were present. Bar= 400µm.

In a separate experiment, neonatal SCID mice also received intraventricular injections of mouse NPCs transduced with the modified retrovirus. Beta-glucuronidase-positive mouse NPCs were observed at 1-, 4-, and 14-weeks post-transplantation in numbers similar to the transgenic mouse NPC allograft (data not shown). The pattern of GUSB staining did not dramatically decrease as was seen with the retrovirally transduced CNPCs, but was only slightly lower over time.

Canine allografts. Canine olfactory-bulb-derived NPCs (OB-CNPCs) were isolated from an MPS VII-affected dog, expanded, and transduced ex vivo with a lentiviral vector containing the human GUSB gene. The cells were approximately 60% GUSB-positive prior to transplantation. Using ultrasound guidance, transduced OB-CNPCs (GUSB-OB-CNPCs) were introduced as a single bolus into the caudal part of the caudate nucleus and thalamus of 3-week old dogs (n=4) (Figure 3.6). In two of the dogs, GUSB-OB-CNPCs were also labelled with micron-sized superparamagnetic iron oxide particles (MPIOs) (Figure 3.7). The MPIOs contained a FITC-like dye to permit identification of the cells by magnetic resonance imaging (MRI) [159, 158] and to visualize engrafted cells in the event of reporter gene silencing. Micron-sized superparamagnetic particles are taken up by cells via endocytosis and have been used previously to label non-neural stem cells with no adverse effects [63, 159].

One of the dogs that received MPIO-labelled GUSB-OB-CNPCs died from anesthetic complications during in vivo MRI one week after transplantation. The

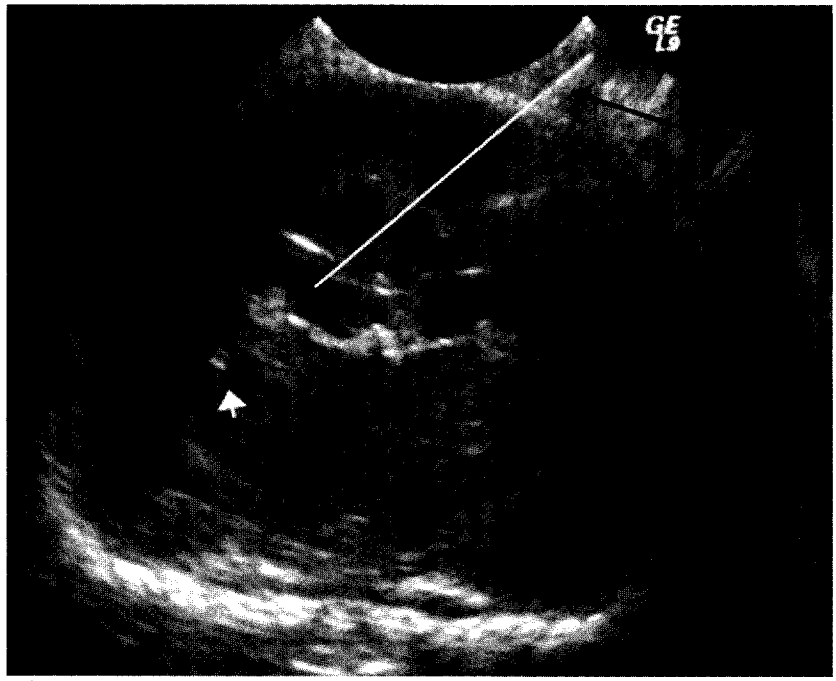

Figure 3.6 Ultrasound image of the canine brain. The section represents a transverse slice through the brain. The white line is superimposed upon the needle seen entering the brain from the upper right corner (black arrow). The cells were injected into the caudal caudate nucleus/thalamus (arrowhead). The oval hypoechoic space that the needle passes through represents the left lateral ventricle.

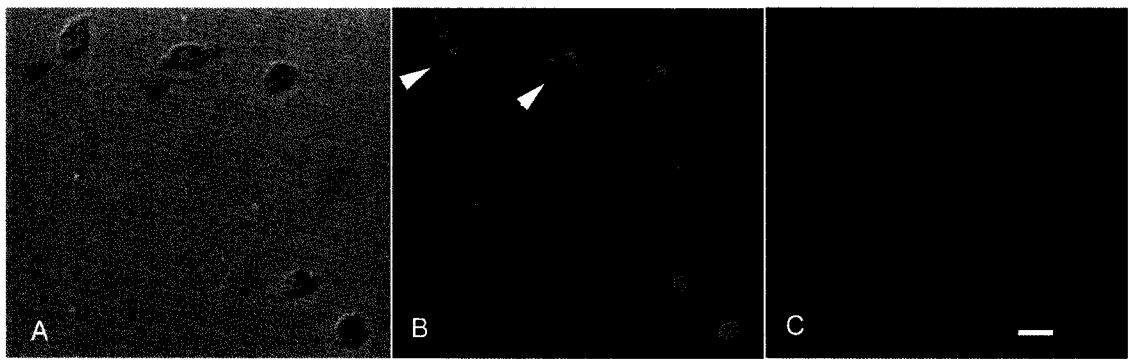

Figure 3.7 GUSB-OB-CNPCs labelled with MPIOs. (A) MPIOs were present in a paranuclear pattern in cells (Nomarski optics). (B) The same field visualized with fluorescent microscopy. The cells labelled with black arrowheads in A correspond to those labelled with white arrowheads in B. (C) Merged image of A and B. Bar= 25μm.

remaining three dogs were sacrificed 4 weeks post-transplantation. The graft site was located in three out of four transplanted dogs: In both of the dogs that received MPIO-labelled GUSB-OB-CNPCs and in one dog that received only GUSB-OB-CNPCs. Visualization of the graft site was accomplished with the aid of red-staining GUSB-positive cells and the large MPIO particles within cells (Figure 3.8). Of the three dogs in which grafts were identified, GUSB-positive cells were present in two. One of the two dogs with GUSB-positive cells received MPIO-labelled GUSB-OB-CNPCs; the MPIO particles hampered visualization of the red GUSB staining (Figure 3.8).

The second group of dogs, ranging in age from 3-6 months, was injected with untransduced OB-CNPCs labelled with MPIOs. Two dogs were sacrificed at 2 weeks after injection and four dogs at 8 weeks post-transplantation. Stereotaxic coordinates based on normal, adult dogs were used for graft placement. Because MPS VII disease results in boney abnormalities that affect skull shape and size and because the age of the dogs, the coordinates were known not to be accurate, but merely approximations of the site locations. The sites chosen were the caudate nucleus (striatum) and the hippocampus/thalamus. Identification of the grafts was dependent upon visualization of intracellular MPIOs. At two weeks post-transplantation, grafts were identified in the two dogs evaluated (Figure 3.9). The eight-week time-points have not been analyzed at this time.

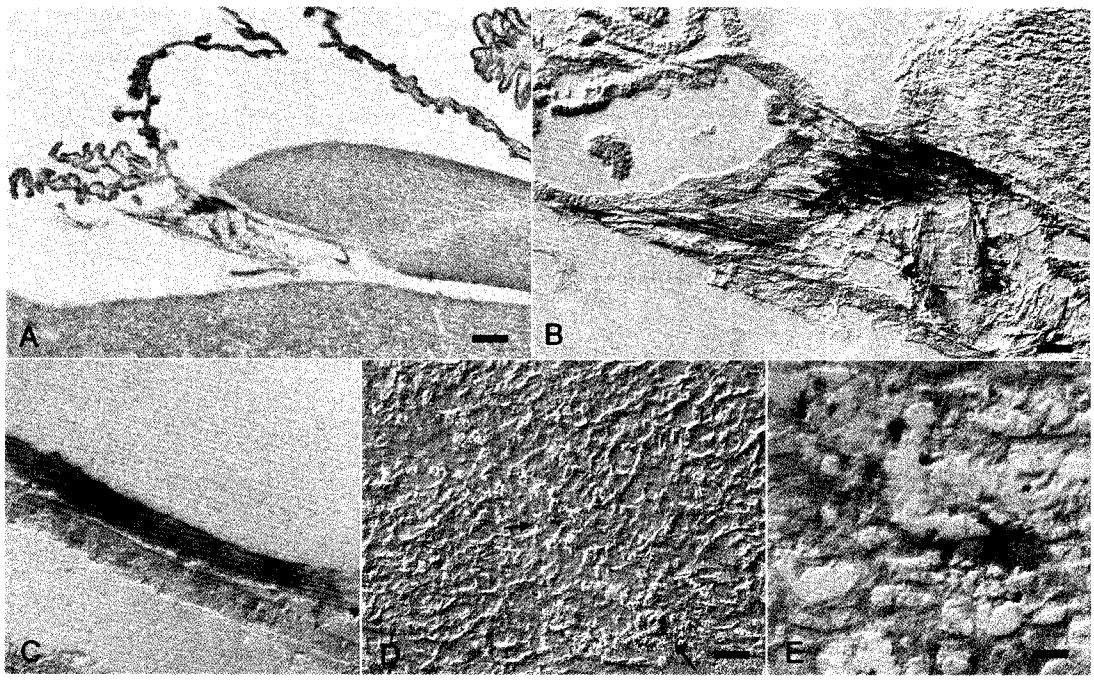

Figure 3.8 Canine olfactory bulb NPCs transduced with human GUSB. GUSB-positive cells were detected in the (A) choroid plexus and in the (C) ependyma at 4 weeks post-transplantation. (B) High magnification view of the positive cells in A. (D) MPIO-labelled OB-CNPC graft. Faint GUSB staining (arrows) was seen in cells with MPIOs. (E) High magnification view of another field with GUSB staining. The arrow points to an MPIO particle in a GUSB-positive area. (A) Bar= 160μm; (B,C) Bar= 40μm; (D) Bar= 80μm; (E) Bar= 20μm.

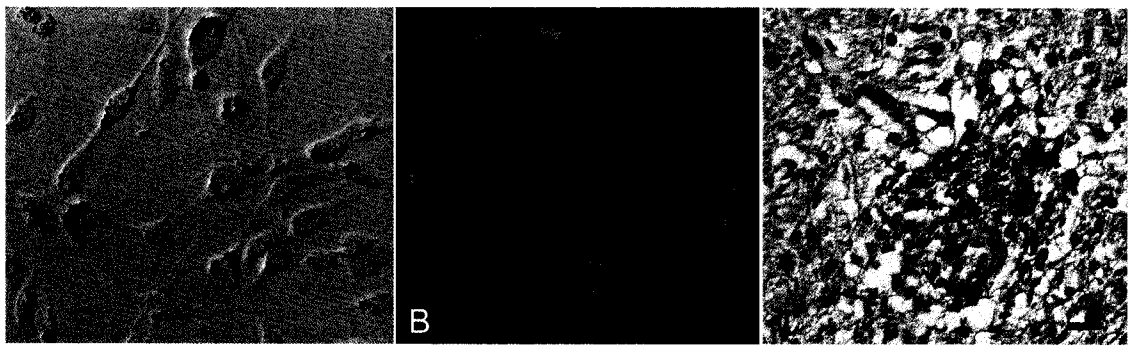

Figure 3.9 OB-CNPCs labelled with MPIOs. (A) Nomarski image of labelled cells in vitro. Individual microspheres can be seen. (B) Fluorescent image of the labelled cells in a graft. (C) Hematoxylin-eosin-stained section of the graft. MPIOs are clearly visible as brown-gold spheres within cells. Bar= 20μm.

Immunophenotyping of MPIO-labelled OB-CNPC grafts. To assess the immunophenotype of transplanted cells, the graft sections were probed with antibodies recognizing markers for neural precursors, astrocytes, and neurons. The phenotypic markers were co-registered with the MPIO-labelled cells with the use of confocal microscopy. The grafts were immunopositive for nestin and glial-fibrillary acidic protein (GFAP)(Figure 3.10). The majority of MPIO-containing cells showed no immunoreactivity, however, small numbers of nestin-positive and GFAP-positive cells were identified (Figure 3.10). In the identification of immunopositive cells with MPIOs, care was taken to localize the MPIOs immediately adjacent to the nucleus. Immunoreactivity for the neuronal markers Map2ab and ß-tubulin III was not seen within the grafts (data not shown).

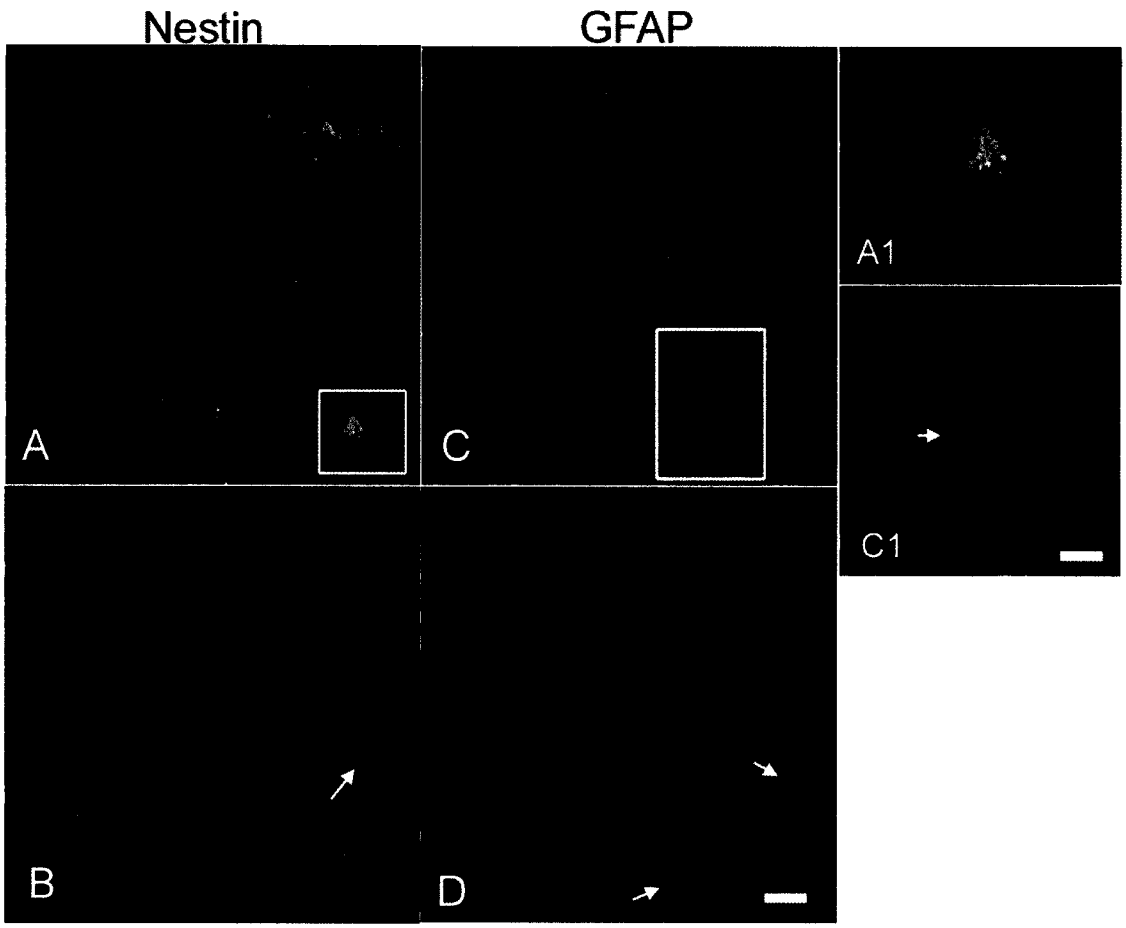

Figure 3.10 Confocal z-stack images of MPIO-labelled OB-CNPC immunostaining. Cells within the graft stained positively for nestin (A, B) and for GFAP (C, D). The arrows indicate non-MPIO-labelled (B) nestin-positive and (D) GFAP-positive cells. (A1) Enlarged view of the box in A showing MPIOs in a nestin-positive cell. (C1) Enlarged view of the box in C indicating a GFAP-positive cell with MPIOs (arrow). The step-size of the sequences was 0.04 µm. (A-D) Bar= 20µm; (A1, C1) Bar= 10µm.

Discussion

Canine neural precursor cells (NPCs) possess characteristics that are advantageous for therapeutic transplantation. They can be expanded ex vivo many-fold and are able to differentiate in vitro into neurons and glia. For autologous transplantation therapy of lysosomal storage diseases (LSDs), three criteria are necessary: efficient transduction of NPCs and engraftment with sustained transgene expression. Canine NPCs could be efficiently transduced or selected using lentiviral and retroviral vectors, respectively. After intraventricular transplantation into neonatal SCID mice, CNPCs transduced with a lentiviral vector were observed in small numbers in the ependyma and adjacent to the lateral ventricles. Transgene expression was observed up to six weeks after transplantation and there were similar numbers of cells at one and 6 week time-points. In contrast, after retroviral transduction with a selectable marker, intraventricular transplantation yielded comparatively robust engraftment and GUSB expression at one week, but at 4 weeks, GUSB staining was significantly less. The results suggest that there is transgene silencing in CNPCs that had been retrovirally transduced. Gene silencing is a phenomenon associated with retroviral vectors that has been attributed to several factors. One of the main factors is thought to be due to reduced transcriptional initiation at the promoter site from binding of *trans*-acting factors to silencer elements in the viral LTRs. Another etiology may be cytosine methylation of CpG sequences in the viral LTRs causing chromatin condensation [174]. The retroviral vector used for these studies was an amphotropic Moloney murine leukemia (L∂4-pQ-HßH) virus that

had been modified by deletion of all long terminal repeat (LTR) transcriptional regulatory elements and inclusion of a permissive primer binding site [132]. With the addition of a eukaryotic housekeeping promoter, transgene expression was sustained in transduced fibroblasts up to six weeks [132]. Although the vector was shown to be refractory to the phenomenon of gene silencing in fibroblasts, it is possible that transgene expression in an undifferentiated cell is affected by factors not present in mature cells. Retroviral transgene silencing has been associated with NPC maturation in vitro and in vivo [182]. However, allograft transplantation of mouse NPCs transduced with the L∂4 vector did not support a hypothesis of gene silencing.

Because the overall engraftment of primary CNPCs in SCID mice was low, we performed murine allograft transplants to determine whether there was an effect of species on engraftment. The microenvironment is essential to the maintenance as well as differentiation of neural precursor cells [127, 69, 31, 77, 21]. It is possible that differences between murine and canine growth factors and cytokines may influence engraftment. The larger number of engrafted murine NPCs in neonatal SCID transplantations, would argue that there is indeed some effect of species on engraftment. It should be noted that these are qualitative assessments and a quantitative analysis is necessary for a definitive conclusion. Furthermore, there are multiple examples of successful human xenografts into mice that would argue against an effect of species on cell engraftment [44, 45, 175, 101, 187].

In the canine allografts of olfactory bulb NPCs transduced with the lentiviral vector (GUSB-OB-CNPC), GUSB expression was detected in only half of the dogs—at 1 week and 4 weeks post-transplantation. Thus, at the 4-week time-point, we detected GUSB staining in only one of three dogs. The GUSB-OB-CNPCs labelled with MPIOs were readily detectable. The MPIOs permitted graft identification of cells that did not express GUSB and provided contrast for MRI studies. The use of the MPIOs is problematic, however. Because these are particles that are readily endocytosed by cells, it is not possible to know whether MPIO-containing cells are indeed graft cells or endogenous cells that have taken up the particles from dead graft cells. Studies using MPIO-labelling have shown no adverse effects of the particles when used with human hematopoietic stem cells or when injected into murine embryos [63, 159]. The nestin-positive and GFAP-positive immunophenotype of cells containing MPIOs would support that at least some cells containing MPIOs are donor-derived, and represent immature progenitors or mature astrocytes.

Assessment of the engraftment potential of CNPCs was limited by not using a canine-specific marker to detect graft cells in the xenograft model. In conjunction with a canine-specific marker, fluorescent in situ hybridization for human GUSB mRNA would determine what proportion of graft cells was expressing the transgene. In this manner it could be determined if the low number of cells (detected by GUSB expression) was due to cell death or to transgene down-regulation. A marked decrease in the number of engrafted

human NPCs in a xenograft transplantation model of MPS VII was determined to be due to apoptotic cell death [101].

The transplantation of CNPCs in xenograft and allograft models did not produce robust engraftment. Transgene expression was not optimal and may either reflect down-regulation of gene expression or progenitor cell death. Further studies to assess for evidence of apoptosis and to identify canine cells in the xenograft model may elucidate whether the paucity of GUSB-positive cells is due to cell death, transgene silencing, or a combination of both.

SUMMARY

Cellular transplantation in the form of bone marrow has been one of the primary treatments of many lysosomal storage diseases (LSDs) [66, 99, 150, 185, 106]. Although CNS disease in some forms of LSD is ameliorated by bone marrow transplantation [185, 106], for many of the LSDs, successful bone marrow transplantation has little impact upon CNS disease. The development of effective cellular transplantation therapy for LSDs with neurodegeneration is therefore desirable and necessary.

The existence of a large animal model of MPS VII affords the opportunity to model CNS transplantation. These studies have provided a characterization of canine neural precursor cells (CNPCs) in vitro and have identified differences in growth and expansion potential attributable to site of origin and culture conditions. In situ studies of the canine brain were also performed. Immunophenotyping of the canine embryonic ventricular zone and postnatal subventricular zone revealed an overlapping pattern of nestin and CD15 positivity in the neuroepithelium and nestin, GFAP, and CD15 positivity in the subependyma that is consistent with findings in rodents and humans. Immunostaining for CD15 in the postnatal cerebellum showed the presence of CD15-positive cells within white matter tracts of the cerebellar folia, a region that has been determined to contain postnatal murine

multipotent NPCs. To our knowledge, this is the first immunocharacterization of postnatal neurogenic regions in the dog.

Preliminary xenograft studies produced sparse engraftment. In canine allografts, cells could be detected up to 4 weeks post-transplantation by GUSB expression and labelling with micron-sized superparamagnetic particles (MPIOs). The number of GUSB-positive cells at 4 weeks post-transplantation was very low and only present in one out of three dogs. Further studies to optimize CNPC engraftment are necessary before this model can provide significant therapeutic effect.

References

1. Aboody KS, Brown A, Rainov NG, Bower KA, Liu S, Yang W, Small JE, Herrlinger U, Ourednik V, Black PM, Breakefield XO, and Snyder EY. (2000) Neural stem cells display extensive tropism for pathology in adult brain: evidence from intracranial gliomas. Proc Natl Acad Sci U S A **97**(23): 12846-12851.
2. Altman J. (1962) Are new neurons formed in the brains of adult mammals? Science **135**: 1127-1128.
3. Altman J and Das GD. (1965) Autoradiographic and histological evidence of postnatal hippocampal neurogenesis in rats. J Comp Neurol **124**(3): 319-335.
4. Anderson DJ. (2001) Stem cells and pattern formation in the nervous system: the possible versus the actual. Neuron **30**(1): 19-35.
5. Ashwell KW and Mai JK. (1997) Developmental expression of the CD15 epitope in the hippocampus of the mouse. Cell Tissue Res **289**(1): 17-23.
6. Bagley RS, Harrington ML, Pluhar GE, Gavin PR, and Moore MP. (1997) Acute, unilateral transverse sinus occlusion during craniectomy in seven dogs with space-occupying intracranial disease. Vet Surg **26**(3): 195-201.
7. Beaudet AL, Scriver CR, Sly WS, and Valle D, *Genetics, biochemistry, and molecular basis of variant human phenotypes*, in *Metabolic Basis of Inherited Disease*, C. Scriver, et al., Editors. 1995, McGraw-Hill: New York. p. 53-118.
8. Belachew S, Chittajallu R, Aguirre AA, Yuan X, Kirby M, Anderson S, and Gallo V. (2003) Postnatal NG2 proteoglycan-expressing progenitor cells are intrinsically multipotent and generate functional neurons. J Cell Biol **161**(1): 169-186.
9. Benedetti S, Pirola B, Pollo B, Magrassi L, Bruzzone MG, Rigamonti D, Galli R, Selleri S, Di Meco F, De Fraja C, Vescovi A, Cattaneo E, and Finocchiaro G. (2000) Gene therapy of experimental brain tumors using neural progenitor cells. Nature Medicine **6**(4): 447-450.
10. Bernfield M, Gotte M, Park PW, Reizes O, Fitzgerald ML, Lincecum J, and Zako M. (1999) Functions of cell surface heparan sulfate proteoglycans. Annu Rev Biochem **68**: 729-777.
11. Birkenmeier EH, Davisson MT, Beamer WG, Ganschow RE, Vogler CA, Gwynn B, Lyford KA, Maltais LM, and Wawrzyniak CJ. (1989) Murine mucopolysaccharidosis type VII. Characterization of a mouse with beta-glucuronidase deficiency. J Clin Invest **83**: 1258-1266.
12. Bonaguidi MA, McGuire T, Hu M, Kan L, Samanta J, and Kessler JA. (2005) LIF and BMP signaling generate separate and discrete types of GFAP-expressing cells. Development **132**(24): 5503-5514.
13. Boockvar JA, Kapitonov D, Kapoor G, Schouten J, Counelis GJ, Bogler O, Snyder EY, McIntosh TK, and O'Rourke DM. (2003) Constitutive EGFR signaling confers a motile phenotype to neural stem cells. Mol Cell Neurosci **24**(4): 1116-1130.

14. Buchet D, Serguera C, Zennou V, Charneau P, and Mallet J. (2002) Long-term expression of beta-glucuronidase by genetically modified human neural progenitor cells grafted into the mouse central nervous system. Mol Cell Neurosci **19**(3): 389-401.
15. Bulte JW, Douglas T, Witwer B, Zhang SC, Strable E, Lewis BK, Zywicke H, Miller B, van Gelderen P, Moskowitz BM, Duncan ID, and Frank JA. (2001) Magnetodendrimers allow endosomal magnetic labeling and in vivo tracking of stem cells. Nat Biotechnol **19**(12): 1141-1147.
16. Bulte JW, Zhang S, van Gelderen P, Herynek V, Jordan EK, Duncan ID, and Frank JA. (1999) Neurotransplantation of magnetically labeled oligodendrocyte progenitors: magnetic resonance tracking of cell migration and myelination. Proc Natl Acad Sci USA **96**(26): 15256-15261.
17. Burns JC, Friedmann T, Driever W, Burrascano M, and Yee JK. (1993) Vesicular stomatitis virus G glycoprotein pseudotyped retroviral vectors: concentration to very high titer and efficient gene transfer into mammalian and nonmammalian cells. Proc Natl Acad Sci U S A **90**(17): 8033-8037.
18. Caldwell MA, Garcion E, terBorg MG, He X, and Svendsen CN. (2004) Heparin stabilizes FGF-2 and modulates striatal precursor cell behavior in response to EGF. Exp Neurol **188**(2): 408-420.
19. Caldwell MA, He X, Wilkie N, Pollack S, Marshall G, Wafford KA, and Svendsen CN. (2001) Growth factors regulate the survival and fate of cells derived from human neurospheres. Nat Biotechnol **19**(5): 475-479.
20. Caldwell MA and Svendsen CN. (1998) Heparin, but not other proteoglycans potentiates the mitogenic effects of FGF-2 on mesencephalic precursor cells. Exp Neurol **152**(1): 1-10.
21. Campos LS, Leone DP, Relvas JB, Brakebusch C, Fassler R, Suter U, and ffrench-Constant C. (2004) Beta1 integrins activate a MAPK signalling pathway in neural stem cells that contributes to their maintenance. Development **131**(14): 3433-3444.
22. Capela A and Temple S. (2002) LeX/ssea-1 is expressed by adult mouse CNS stem cells, identifying them as nonependymal. Neuron **35**(5): 865-875.
23. Carpenter MK, Cui X, Hu ZY, Jackson J, Sherman S, Seiger A, and Wahlberg LU. (1999) In vitro expansion of a multipotent population of human neural progenitor cells. Exp Neurol **158**(2): 265-278.
24. Casal ML and Wolfe JH. (1998) Variant clinical course of mucopolysaccharidosis type VII in two groups of mice carrying the same mutation. Lab Invest **78**(12): 1575-1581.
25. Clancy B, Darlington RB, and Finlay BL. (2001) Translating developmental time across mammalian species. Neuroscience **105**(1): 7-17.
26. Consiglio A, Gritti A, Dolcetta D, Follenzi A, Bordignon C, Gage FH, Vescovi AL, and Naldini L. (2004) Robust in vivo gene transfer into adult mammalian neural stem cells by lentiviral vectors. Proc Natl Acad Sci U S A **101**(41): 14835-14840.

27. Corbeil D, Roper K, Fargeas CA, Joester A, and Huttner WB. (2001) Prominin: a story of cholesterol, plasma membrane protrusions and human pathology. Traffic **2**(2): 82-91.
28. Corbeil D, Roper K, Hellwig A, Tavian M, Miraglia S, Watt SM, Simmons PJ, Peault B, Buck DW, and Huttner WB. (2000) The human AC133 hematopoietic stem cell antigen is also expressed in epithelial cells and targeted to plasma membrane protrusions. J Biol Chem **275**(8): 5512-5520.
29. Craig CG, Tropepe V, Morshead CM, Reynolds BA, Weiss S, and van der Kooy D. (1996) In vivo growth factor expansion of endogenous subependymal neural precursor cell populations in the adult mouse brain. J Neurosci **16**(8): 2649-2658.
30. Doetsch F. (2003) The glial identity of neural stem cells. Nat Neurosci **6**(11): 1127-1134.
31. Doetsch F. (2003) A niche for adult neural stem cells. Curr Opin Genet Dev **13**(5): 543-550.
32. Doetsch F, Caille I, Lim DA, Garcia-Verdugo JM, and Alvarez-Buylla A. (1999) Subventricular zone astrocytes are neural stem cells in the adult mammalian brain. Cell **97**(6): 703-716.
33. Doetsch F, Garcia-Verdugo JM, and Alvarez-Buylla A. (1997) Cellular composition and three-dimensional organization of the subventricular germinal zone in the adult mammalian brain. J Neurosci **17**(13): 5046-5061.
34. Dolman DE, Lawrenson JG, and Abbott NJ. (2004) Cross reactivity of polyclonal GFAP antiserum: implications for the in-vitro characterisation of brain endothelium. Brain Res **1012**(1-2): 185-186.
35. Duittoz AH and Hevor T. (2001) Primary culture of neural precursors from the ovine central nervous system (CNS). J Neurosci Methods **107**(1-2): 131-140.
36. Dunning MD, Lakatos A, Loizou L, Kettunen M, ffrench-Constant C, Brindle KM, and Franklin RJ. (2004) Superparamagnetic iron oxide-labeled Schwann cells and olfactory ensheathing cells can be traced in vivo by magnetic resonance imaging and retain functional properties after transplantation into the CNS. J Neurosci **24**(44): 9799-9810.
37. Einstein O, Karussis D, Grigoriadis N, Mizrachi-Kol R, Reinhartz E, Abramsky O, and Ben-Hur T. (2003) Intraventricular transplantation of neural precursor cell spheres attenuates acute experimental allergic encephalomyelitis. Mol Cell Neurosci **24**(4): 1074-1082.
38. Englund U, Bjorklund A, and Wictorin K. (2002) Migration patterns and phenotypic differentiation of long-term expanded human neural progenitor cells after transplantation into the adult rat brain. Brain Res Dev Brain Res **134**(1-2): 123-141.
39. Eriksson PS, Perfilieva E, Bjork-Eriksson T, Alborn AM, Nordborg C, Peterson DA, and Gage FH. (1998) Neurogenesis in the adult human hippocampus. Nat Med **4**(11): 1313-1317.

40. Falk A, Holmstrom N, Carlen M, Cassidy R, Lundberg C, and Frisen J. (2002) Gene delivery to adult neural stem cells. Exp Cell Res **279**(1): 34-39.
41. Flax JD, Aurora S, Yang C, Simonin C, Wills AM, Billinghurst LL, Jendoubi M, Sidman RL, Wolfe JH, Kim SU, and Snyder EY. (1998) Engraftable human neural stem cells respond to developmental cues, replace neurons, and express foreign genes. Nat Biotechnol **16**(11): 1033-1039.
42. Forutan F, Mai JK, Ashwell KW, Lensing-Hohn S, Nohr D, Voss T, Bohl J, and Andressen C. (2001) Organisation and maturation of the human thalamus as revealed by CD15. J Comp Neurol **437**(4): 476-495.
43. Frederiksen K and McKay RD. (1988) Proliferation and differentiation of rat neuroepithelial precursor cells in vivo. J Neurosci **8**(4): 1144-1151.
44. Fricker RA, Carpenter MK, Winkler C, Greco C, Gates MA, and Bjorklund A. (1999) Site-specific migration and neuronal differentiation of human neural progenitor cells after transplantation in the adult rat brain. J Neurosci **19**(14): 5990-6005.
45. Fricker-Gates RA, Winkler C, Kirik D, Rosenblad C, Carpenter MK, and Bjorklund A. (2000) EGF infusion stimulates the proliferation and migration of embryonic progenitor cells transplanted in the adult rat striatum. Exp Neurol **165**(2): 237-247.
46. Futerman AH and van Meer G. (2004) The cell biology of lysosomal storage disorders. Nat Rev Mol Cell Biol **5**(7): 554-565.
47. Fyfe JC, Kurzhals RL, Lassaline ME, Henthorn PS, Alur PR, Wang P, Wolfe JH, Giger U, Haskins ME, Patterson DF, Sun H, Jain S, and Yuhki N. (1999) Molecular basis of feline beta-glucuronidase deficiency: an animal model of mucopolysaccharidosis VII. Genomics **58**(2): 121-128.
48. Gage F, Ray J, and Fisher L. (1995) Isolation, characterization, and use of stem cells from the CNS. Annu Rev Neurosci **18**: 159-192.
49. Gage FH, Coates PW, Palmer TD, Kuhn HG, Fisher LJ, Suhonen JO, Peterson DA, Suhr ST, and Ray J. (1995) Survival and differentiation of adult neuronal progenitor cells transplanted to the adult brain. Proc Natl Acad Sci U S A **92**(25): 11879-11883.
50. Gaiano N, Nye JS, and Fishell G. (2000) Radial glial identity is promoted by Notch1 signaling in the murine forebrain. Neuron **26**(2): 395-404.
51. Garcia AD, Doan NB, Imura T, Bush TG, and Sofroniew MV. (2004) GFAP-expressing progenitors are the principal source of constitutive neurogenesis in adult mouse forebrain. Nat Neurosci **7**(11): 1233-1241.
52. Gitzelmann R, Bosshard NU, Superti-Furga A, Spycher MA, Briner J, Wiesmann U, Lutz H, and Litschi B. (1994) Feline mucopolysaccharidosis VII due to beta-glucuronidase deficiency. Vet Pathol **31**(4): 435-443.
53. Glaser JH and Sly WS. (1973) Beta-glucuronidase deficiency mucopolysaccharidosis: methods for enzymatic diagnosis. J Lab Clin Med **82**(6): 969-977.
54. Glass EN, Kapatkin A, Vite C, and Steinberg SA. (2000) A modified bilateral transfrontal sinus approach to the canine frontal lobe and

olfactory bulb: surgical technique and five cases. J Am Anim Hosp Assoc **36**(1): 43-50.
55. Goldman S. (2005) Stem and progenitor cell-based therapy of the human central nervous system. Nat Biotechnol **23**(7): 862-871.
56. Goodell MA, Brose K, Paradis G, Conner AS, and Mulligan RC. (1996) Isolation and functional properties of murine hematopoietic stem cells that are replicating in vivo. J Exp Med **183**(4): 1797-1806.
57. Gritti A, Bonfanti L, Doetsch F, Caille I, Alvarez-Buylla A, Lim DA, Galli R, Verdugo JM, Herrera DG, and Vescovi AL. (2002) Multipotent neural stem cells reside into the rostral extension and olfactory bulb of adult rodents. J Neurosci **22**(2): 437-445.
58. Gritti A, Frolichsthal-Schoeller P, Galli R, Parati EA, Cova L, Pagano SF, Bjornson CR, and Vescovi AL. (1999) Epidermal and fibroblast growth factors behave as mitogenic regulators for a single multipotent stem cell-like population from the subventricular region of the adult mouse forebrain. J Neurosci **19**(9): 3287-3297.
59. Haskins ME, Desnick RJ, DiFerrante N, Jezyk PF, and Patterson DF. (1984) Beta-glucuronidase deficiency in a dog: a model of human mucopolysaccharidosis VII. Pediatr Res **18**: 980-984.
60. Herrera DG, Garcia-Verdugo JM, and Alvarez-Buylla A. (1999) Adult-derived neural precursors transplanted into multiple regions in the adult brain. Ann Neurol **46**(6): 867-877.
61. Heuer GG, Skorupa AF, Prasad Alur RK, Jiang K, and Wolfe JH. (2001) Accumulation of abnormal amounts of glycosaminoglycans in murine mucopolysaccharidosis type VII neural progenitor cells does not alter the growth rate or efficiency of differentiation into neurons. Mol Cell Neurosci **17**(1): 167-178.
62. Heyn C, Ronald JA, Mackenzie LT, Macdonald IC, Chambers AF, Rutt BK, and Foster PJ. (2005) In vivo magnetic resonance imaging of single cells in mouse brain with optical validation. Magn Reson Med.
63. Hinds KA, Hill JM, Shapiro EM, Laukkanen MO, Silva AC, Combs CA, Varney TR, Balaban RS, Koretsky AP, and Dunbar CE. (2003) Highly efficient endosomal labeling of progenitor and stem cells with large magnetic particles allows magnetic resonance imaging of single cells. Blood **102**(3): 867-872.
64. Hockfield S and McKay RD. (1985) Identification of major cell classes in the developing mammalian nervous system. J Neurosci **5**(12): 3310-3328.
65. Hoehn M, Kustermann E, Blunk J, Wiedermann D, Trapp T, Wecker S, Focking M, Arnold H, Hescheler J, Fleischmann BK, Schwindt W, and Buhrle C. (2002) Monitoring of implanted stem cell migration in vivo: a highly resolved in vivo magnetic resonance imaging investigation of experimental stroke in rat. Proc Natl Acad Sci U S A **99**(25): 16267-16272.
66. Hopwood JJ, Vellodi A, Scott HS, Morris CP, Litjens T, Clements PR, Brooks DA, Cooper A, and Wraith JE. (1993) Long-term clinical progress in bone marrow transplanted mucopolysaccharidosis type I patients with a defined genotype. J Inherit Metab Dis **16**(6): 1024-1033.

67. Hughes SM, Moussavi-Harami F, Sauter SL, and Davidson BL. (2002) Viral-mediated gene transfer to mouse primary neural progenitor cells. Mol Ther **5**(1): 16-24.
68. Hulspas R and Quesenberry PJ. (2000) Characterization of neurosphere cell phenotypes by flow cytometry. Cytometry **40**(3): 245-250.
69. Hynds DL and Snow DM. (2001) Fibronectin and laminin elicit differential behaviors from SH-SY5Y growth cones contacting inhibitory chondroitin sulfate proteoglycans. J Neurosci Res **66**(4): 630-642.
70. Imura T, Kornblum HI, and Sofroniew MV. (2003) The predominant neural stem cell isolated from postnatal and adult forebrain but not early embryonic forebrain expresses GFAP. J Neurosci **23**(7): 2824-2832.
71. Imura T, Nakano I, Kornblum HI, and Sofroniew MV. (2005) Phenotypic and functional heterogeneity of GFAP-expressing cells in vitro: Differential expression of LeX/CD15 by GFAP-expressing multipotent neural stem cells and non-neurogenic astrocytes. Glia.
72. Jendelova P, Herynek V, Urdzikova L, Glogarova K, Kroupova J, Andersson B, Bryja V, Burian M, Hajek M, and Sykova E. (2004) Magnetic resonance tracking of transplanted bone marrow and embryonic stem cells labeled by iron oxide nanoparticles in rat brain and spinal cord. J Neurosci Res **76**(2): 232-243.
73. Jeyakumar M, Dwek RA, Butters TD, and Platt FM. (2005) Storage solutions: treating lysosomal disorders of the brain. Nat Rev Neurosci **6**(9): 713-725.
74. Jin HK, Carter JE, Huntley GW, and Schuchman EH. (2002) Intracerebral transplantation of mesenchymal stem cells into acid sphingomyelinase-deficient mice delays the onset of neurological abnormalities and extends their life span. J Clin Invest **109**(9): 1183-1191.
75. Jin K, Sun Y, Xie L, Mao XO, Childs J, Peel A, Logvinova A, Banwait S, and Greenberg DA. (2005) Comparison of ischemia-directed migration of neural precursor cells after intrastriatal, intraventricular, or intravenous transplantation in the rat. Neurobiol Dis **18**(2): 366-374.
76. Johansson CB, Momma S, Clarke DL, Risling M, Lendahl U, and Frisen J. (1999) Identification of a neural stem cell in the adult mammalian central nervous system. Cell **96**(1): 25-34.
77. Kearns SM, Laywell ED, Kukekov VK, and Steindler DA. (2003) Extracellular matrix effects on neurosphere cell motility. Exp Neurol **182**(1): 240-244.
78. Kilpatrick T and Bartlett P. (1993) Cloning and growth of multipotential neural precursors: requirements for proliferation and differentiation. Neuron **10**: 255-265.
79. Kim M and Morshead CM. (2003) Distinct populations of forebrain neural stem and progenitor cells can be isolated using side-population analysis. J Neurosci **23**(33): 10703-10709.
80. Kircher MF, Allport JR, Graves EE, Love V, Josephson L, Lichtman AH, and Weissleder R. (2003) In vivo high resolution three-dimensional

imaging of antigen-specific cytotoxic T-lymphocyte trafficking to tumors. Cancer Res **63**(20): 6838-6846.

81. Klassen H, Schwartz MR, Bailey AH, and Young MJ. (2001) Surface markers expressed by multipotent human and mouse neural progenitor cells include tetraspanins and non-protein epitopes. Neurosci Lett **312**(3): 180-182.
82. Klein C, Butt SJ, Machold RP, Johnson JE, and Fishell G. (2005) Cerebellum- and forebrain-derived stem cells possess intrinsic regional character. Development **132**(20): 4497-4508.
83. Kondo T and Raff M. (2000) Oligodendrocyte precursor cells reprogrammed to become multipotential CNS stem cells. Science **289**(5485): 1754-1757.
84. Kosuga M, Sasaki K, Tanabe A, Li XK, Okawa H, Ogino I, Okuda O, Arai H, Sakuragawa N, Kamata Y, Azuma N, Suzuki S, Yamada M, and Okuyama T. (2001) Engraftment of genetically engineered amniotic epithelial cells corrects lysosomal storage in multiple areas of the brain in mucopolysaccharidosis type VII mice. Mol Ther **3**(2): 139-148.
85. Kukekov VG, Laywell ED, Thomas LB, and Steindler DA. (1997) A nestin-negative precursor cell from the adult mouse brain gives rise to neurons and glia. Glia **21**(4): 399-407.
86. Kyle JW, Birkenmeier EH, Gwynn B, Vogler C, Hoppe PC, Hoffmann JW, and Sly WS. (1990) Correction of murine mucopolysaccharidosis VII by a human beta-glucuronidase transgene. Proc Natl Acad Sci U S A **87**(10): 3914-3918.
87. Lacorazza HD, Flax JD, Snyder EY, and Jendoubi M. (1996) Expression of human beta-hexosaminidase alpha-subunit gene (the gene defect of Tay-Sachs disease) in mouse brains upon engraftment of transduced progenitor cells. Nat Med **2**(4): 424-429.
88. Laywell ED, Rakic P, Kukekov VG, Holland EC, and Steindler DA. (2000) Identification of a multipotent astrocytic stem cell in the immature and adult mouse brain. Proc Natl Acad Sci U S A **97**(25): 13883-13888.
89. Lee A, Kessler JD, Read TA, Kaiser C, Corbeil D, Huttner WB, Johnson JE, and Wechsler-Reya RJ. (2005) Isolation of neural stem cells from the postnatal cerebellum. Nat Neurosci **8**(6): 723-729.
90. Lendahl U, Zimmerman LB, and McKay RD. (1990) CNS stem cells express a new class of intermediate filament protein. Cell **60**(4): 585-595.
91. Lewin M, Carlesso N, Tung CH, Tang XW, Cory D, Scadden DT, and Weissleder R. (2000) Tat peptide-derivatized magnetic nanoparticles allow in vivo tracking and recovery of progenitor cells. Nat Biotechnol **18**(4): 410-414.
92. Lillien L and Raphael H. (2000) BMP and FGF regulate the development of EGF-responsive neural progenitor cells. Development **127**(22): 4993-5005.
93. Lim DA, Fishell GJ, and Alvarez-Buylla A. (1997) Postnatal mouse subventricular zone neuronal precursors can migrate and differentiate

within multiple levels of the developing neuraxis. Proc Natl Acad Sci U S A **94**(26): 14832-14836.
94. Liu Z and Martin LJ. (2003) Olfactory bulb core is a rich source of neural progenitor and stem cells in adult rodent and human. J Comp Neurol **459**(4): 368-391.
95. Lois C and Alvarez-Buylla A. (1994) Long-distance neuronal migration in the adult mammalian brain. Science **264**(5162): 1145-1148.
96. Luca T, Givogri MI, Perani L, Galbiati F, Follenzi A, Naldini L, and Bongarzone ER. (2005) Axons mediate the distribution of arylsulfatase A within the mouse hippocampus upon gene delivery. Mol Ther **12**(4): 669-679.
97. Lundberg C, Winkler C, Whittemore SR, and Bjorklund A. (1996) Conditionally immortalized neural progenitor cells grafted to the striatum exhibit site-specific neuronal differentiation and establish connections with the host globus pallidus. Neurobiol Dis **3**(1): 33-50.
98. Magnitsky S, Watson DJ, Walton RM, Pickup S, Bulte JW, Wolfe JH, and Poptani H. (2005) In vivo and ex vivo MRI detection of localized and disseminated neural stem cell grafts in the mouse brain. Neuroimage **26**(3): 744-754.
99. Marechal V, Naffakh N, Danos O, and Heard JM. (1993) Disappearance of lysosomal storage in spleen and liver of mucopolysaccharidosis VII mice after transplantation of genetically modified bone marrow cells. Blood **82**(4): 1358-1365.
100. Meikle PJ, Hopwood JJ, Clague AE, and Carey WF. (1999) Prevalence of lysosomal storage disorders. JAMA **281**(3): 249-254.
101. Meng XL, Shen JS, Ohashi T, Maeda H, Kim SU, and Eto Y. (2003) Brain transplantation of genetically engineered human neural stem cells globally corrects brain lesions in the mucopolysaccharidosis type VII mouse. J Neurosci Res **74**(2): 266-277.
102. Merkle FT, Tramontin AD, Garcia-Verdugo JM, and Alvarez-Buylla A. (2004) Radial glia give rise to adult neural stem cells in the subventricular zone. Proc Natl Acad Sci U S A **101**(50): 17528-17532.
103. Messam CA, Hou J, and Major EO. (2000) Coexpression of nestin in neural and glial cells in the developing human CNS defined by a human-specific anti-nestin antibody. Exp Neurol **161**(2): 585-596.
104. Messing A and Brenner M. (2003) GFAP: functional implications gleaned from studies of genetically engineered mice. Glia **43**(1): 87-90.
105. Milward EA, Lundberg CG, Ge B, Lipsitz D, Zhao M, and Duncan ID. (1997) Isolation and transplantation of multipotential populations of epidermal growth factor-responsive, neural progenitor cells from the canine brain. J Neurosci Res **50**(5): 862-871.
106. Miranda SR, Erlich S, Friedrich VL, Jr., Haskins ME, Gatt S, and Schuchman EH. (1998) Biochemical, pathological, and clinical response to transplantation of normal bone marrow cells into acid sphingomyelinase-deficient mice. Transplantation **65**(7): 884-892.

107. Modo M, Cash D, Mellodew K, Williams SC, Fraser SE, Meade TJ, Price J, and Hodges H. (2002) Tracking transplanted stem cell migration using bifunctional, contrast agent-enhanced, magnetic resonance imaging. Neuroimage **17**(2): 803-811.
108. Morshead CM, Garcia AD, Sofroniew MV, and van Der Kooy D. (2003) The ablation of glial fibrillary acidic protein-positive cells from the adult central nervous system results in the loss of forebrain neural stem cells but not retinal stem cells. Eur J Neurosci **18**(1): 76-84.
109. Morshead CM, Reynolds BA, Craig CG, McBurney MW, Staines WA, Morassutti D, Weiss S, and van der Kooy D. (1994) Neural stem cells in the adult mammalian forebrain: a relatively quiescent subpopulation of subependymal cells. Neuron **13**(5): 1071-1082.
110. Moyer MP, Johnson RA, Zompa EA, Cain L, Morshed T, and Hulsebosch CE. (1997) Culture, expansion, and transplantation of human fetal neural progenitor cells. Transplant Proc **29**(4): 2040-2041.
111. Mueller D, Shamblott MJ, Fox HE, Gearhart JD, and Martin LJ. (2005) Transplanted human embryonic germ cell-derived neural stem cells replace neurons and oligodendrocytes in the forebrain of neonatal mice with excitotoxic brain damage. J Neurosci Res.
112. Muramatsu T and Muramatsu H. (2004) Carbohydrate antigens expressed on stem cells and early embryonic cells. Glycoconj J **21**(1-2): 41-45.
113. Nagato M, Heike T, Kato T, Yamanaka Y, Yoshimoto M, Shimazaki T, Okano H, and Nakahata T. (2005) Prospective characterization of neural stem cells by flow cytometry analysis using a combination of surface markers. J Neurosci Res **80**(4): 456-466.
114. Naldini L, Blömer U, Gallay P, Ory D, Mulligan R, Gage FH, Verma IM, and Trono D. (1996) In vivo gene delivery and stable transduction of nondividing cells by a lentiviral vector. Science **272**: 263-267.
115. Neufeld EF. (1991) Lysosomal storage diseases. Annu Rev Biochem **60**: 257-280.
116. Noctor SC, Flint AC, Weissman TA, Wong WS, Clinton BK, and Kriegstein AR. (2002) Dividing precursor cells of the embryonic cortical ventricular zone have morphological and molecular characteristics of radial glia. J Neurosci **22**(8): 3161-3173.
117. Nunes MC, Roy NS, Keyoung HM, Goodman RR, McKhann G, 2nd, Jiang L, Kang J, Nedergaard M, and Goldman SA. (2003) Identification and isolation of multipotential neural progenitor cells from the subcortical white matter of the adult human brain. Nat Med **9**(4): 439-447.
118. Nurcombe V, Ford MD, Wildschut JA, and Bartlett PF. (1993) Developmental regulation of neural response to FGF-1 and FGF-2 by heparan sulfate proteoglycan. Science **260**(5104): 103-106.
119. Oka S, Honmou O, Akiyama Y, Sasaki M, Houkin K, Hashi K, and Kocsis JD. (2004) Autologous transplantation of expanded neural precursor cells into the demyelinated monkey spinal cord. Brain Res **1030**(1): 94-102.
120. Ostenfeld T, Caldwell MA, Prowse KR, Linskens MH, Jauniaux E, and Svendsen CN. (2000) Human neural precursor cells express low levels of

telomerase in vitro and show diminishing cell proliferation with extensive axonal outgrowth following transplantation. Experimental Neurology **164**(1): 215-226.

121. Ourednik J, Ourednik V, Lynch WP, Schachner M, and Snyder EY. (2002) Neural stem cells display an inherent mechanism for rescuing dysfunctional neurons. Nat Biotechnol **20**(11): 1103-1110.
122. Ourednik V, Ourednik J, Flax JD, Zawada WM, Hutt C, Yang C, Park KI, Kim SU, Sidman RL, Freed CR, and Snyder EY. (2001) Segregation of human neural stem cells in the developing primate forebrain. Science **293**(5536): 1820-1824.
123. Owens GC, Mistry S, Edelman GM, and Crossin KL. (2002) Efficient marking of neural stem cell-derived neurons with a modified murine embryonic stem cell virus, MESV2. Gene Ther **9**(15): 1044-1048.
124. Pagano SF, Impagnatiello F, Girelli M, Cova L, Grioni E, Onofri M, Cavallaro M, Etteri S, Vitello F, Giombini S, Solero CL, and Parati EA. (2000) Isolation and characterization of neural stem cells from the adult human olfactory bulb. Stem Cells **18**(4): 295-300.
125. Palmer TD, Ray J, and Gage FH. (1995) FGF-2-responsive neuronal progenitors reside in proliferative and quiescent regions of the adult rodent brain. Mol Cell Neurosci **6**(5): 474-486.
126. Palmer TD, Takahashi J, and Gage FH. (1997) The adult rat hippocampus contains primordial neural stem cells. Mol Cell Neurosci **8**(6): 389-404.
127. Palmer TD, Willhoite AR, and Gage FH. (2000) Vascular niche for adult hippocampal neurogenesis. J Comp Neurol **425**(4): 479-494.
128. Passini MA, Lee EB, Heuer GG, and Wolfe JH. (2002) Distribution of a lysosomal enzyme in the adult brain by axonal transport and by cells of the rostral migratory stream. J. Neurosci. **22**(15): 6437-6446.
129. Peng WM, Yu LL, Bao CY, Liao F, Li XS, and Zuo MX. (2002) Transplanted neuronal precursors migrate and differentiate in the developing mouse brain. Cell Res **12**(3-4): 223-228.
130. Phemister RD and Young S. (1968) The postnatal development of the canine cerebellar cortex. J Comp Neurol **134**(2): 243-254.
131. Pluchino S, Quattrini A, Brambilla E, Gritti A, Salani G, Dina G, Galli R, Del Carro U, Amadio S, Bergami A, Furlan R, Comi G, Vescovi AL, and Martino G. (2003) Injection of adult neurospheres induces recovery in a chronic model of multiple sclerosis. Nature **422**(6933): 688-694.
132. Prasad Alur RK, Foley B, Parente MK, Tobin DK, Heuer GG, Avadhani AN, Pongubala J, and Wolfe JH. (2002) Modification of multiple transcriptional regulatory elements in a Moloney murine leukemia virus gene transfer vector circumvents silencing in fibroblast grafts and increases levels of expression of the transferred enzyme. Gene Therapy **9**(17): 1146-1154.
133. Raaf J and Kernohan J. (1944) A study of the external granular layer in the cerebellum. American Journal of Anatomy **75**: 151-172.
134. Rakic P. (2003) Elusive radial glial cells: historical and evolutionary perspective. Glia **43**(1): 19-32.

135. Rappa G, Kunke D, Holter J, Diep DB, Meyer J, Baum C, Fodstad O, Krauss S, and Lorico A. (2004) Efficient expansion and gene transduction of mouse neural stem/progenitor cells on recombinant fibronectin. Neuroscience **124**(4): 823-830.
136. Ray J, Bouvet A, DeSanto C, Fyfe JC, Xu D, Wolfe JH, Aguirre GD, Patterson DF, Haskins ME, and Henthorn PS. (1998) Cloning of the canine beta-glucuronidase cDNA, mutation identification in canine MPS VII, and retroviral vector-mediated correction of MPS VII cells. Genomics **48**(2): 248-253.
137. Ray J, Peterson DA, Schinstine M, and Gage FH. (1993) Proliferation, differentiation, and long-term culture of primary hippocampal neurons. Proc Natl Acad Sci U S A **90**(8): 3602-3606.
138. Ray J, Scarpino V, Laing C, and Haskins ME. (1999) Biochemical basis of the beta-glucuronidase gene defect causing canine mucopolysaccharidosis VII. J Hered **90**(1): 119-123.
139. Reynolds BA and Rietze RL. (2005) Neural stem cells and neurospheres--re-evaluating the relationship. Nat Methods **2**(5): 333-336.
140. Reynolds BA and Weiss S. (1992) Generation of neurons and astrocytes from isolated cells of the adult mammalian central nervous system. Science **255**(5052): 1707-1710.
141. Reynolds BA and Weiss S. (1996) Clonal and population analyses demonstrate that an EGF-responsive mammalian embryonic CNS precursor is a stem cell. Dev Biol **175**(1): 1-13.
142. Richards LJ, Kilpatrick TJ, and Bartlett PF. (1992) De novo generation of neuronal cells from the adult mouse brain. Proc Natl Acad Sci U S A **89**(18): 8591-8595.
143. Rietze RL, Valcanis H, Brooker GF, Thomas T, Voss AK, and Bartlett PF. (2001) Purification of a pluripotent neural stem cell from the adult mouse brain. Nature **412**(6848): 736-739.
144. Rosario CM, Yandava BD, Kosaras B, Zurakowski D, Sidman RL, and Snyder EY. (1997) Differentiation of engrafted multipotent neural progenitors towards replacement of missing granule neurons in meander tail cerebellum may help determine the locus of mutant gene action. Development **124**(21): 4213-4224.
145. Roy NS, Wang S, Jiang L, Kang J, Benraiss A, Harrison-Restelli C, Fraser RA, Couldwell WT, Kawaguchi A, Okano H, Nedergaard M, and Goldman SA. (2000) In vitro neurogenesis by progenitor cells isolated from the adult human hippocampus. Nat Med **6**(3): 271-277.
146. Rubio F, Kokaia Z, Arco A, Garcia-Simon M, Snyder E, Lindvall O, Satrustegui J, and Martinez-Serrano A. (1999) BDNF gene transfer to the mammalian brain using CNS-derived neural precursors. Gene Ther **6**(11): 1851-1866.
147. Sahin Kaya S, Mahmood A, Li Y, Yavuz E, and Chopp M. (1999) Expression of nestin after traumatic brain injury in rat brain. Brain Res **840**(1-2): 153-157.

148. Sakurai K, Iizuka S, Shen JS, Meng XL, Mori T, Umezawa A, Ohashi T, and Eto Y. (2004) Brain transplantation of genetically modified bone marrow stromal cells corrects CNS pathology and cognitive function in MPS VII mice. Gene Ther **11**(19): 1475-1481.
149. Sanai N, Tramontin AD, Quinones-Hinojosa A, Barbaro NM, Gupta N, Kunwar S, Lawton MT, McDermott MW, Parsa AT, Manuel-Garcia Verdugo J, Berger MS, and Alvarez-Buylla A. (2004) Unique astrocyte ribbon in adult human brain contains neural stem cells but lacks chain migration. Nature **427**(6976): 740-744.
150. Sands MS, Barker JE, Vogler C, Levy B, Gwynn B, Galvin N, Sly WS, and Birkenmeier E. (1993) Treatment of murine mucopolysaccharidosis type VII by syngeneic bone marrow transplantation in neonates. Lab Invest **68**(6): 676-686.
151. Sawamoto K, Nakao N, Kakishita K, Ogawa Y, Toyama Y, Yamamoto A, Yamaguchi M, Mori K, Goldman SA, Itakura T, and Okano H. (2001) Generation of dopaminergic neurons in the adult brain from mesencephalic precursor cells labeled with a nestin-GFP transgene. J Neurosci **21**(11): 3895-3903.
152. Schinstine M and Iacovitti L. (1996) Expression of neuronal antigens by astrocytes derived from EGF-generated neuroprogenitor cells. Exp Neurol **141**(1): 67-78.
153. Schwartz PH, Bryant PJ, Fuja TJ, Su H, O'Dowd DK, and Klassen H. (2003) Isolation and characterization of neural progenitor cells from post-mortem human cortex. J Neurosci Res **74**(6): 838-851.
154. Seaberg RM and van der Kooy D. (2002) Adult rodent neurogenic regions: the ventricular subependyma contains neural stem cells, but the dentate gyrus contains restricted progenitors. J Neurosci **22**(5): 1784-1793.
155. Seaberg RM and van der Kooy D. (2003) Stem and progenitor cells: the premature desertion of rigorous definitions. Trends Neurosci **26**(3): 125-131.
156. Sejersen T and Lendahl U. (1993) Transient expression of the intermediate filament nestin during skeletal muscle development. J Cell Sci **106 (Pt 4)**: 1291-1300.
157. Seri B, Garcia-Verdugo JM, McEwen BS, and Alvarez-Buylla A. (2001) Astrocytes give rise to new neurons in the adult mammalian hippocampus. J Neurosci **21**(18): 7153-7160.
158. Shapiro EM, Skrtic S, and Koretsky AP. (2005) Sizing it up: cellular MRI using micron-sized iron oxide particles. Magn Reson Med **53**(2): 329-338.
159. Shapiro EM, Skrtic S, Sharer K, Hill JM, Dunbar CE, and Koretsky AP. (2004) MRI detection of single particles for cellular imaging. Proc Natl Acad Sci U S A **101**(30): 10901-10906.
160. Shihabuddin LS, Horner PJ, Ray J, and Gage FH. (2000) Adult spinal cord stem cells generate neurons after transplantation in the adult dentate gyrus. J Neurosci **20**(23): 8727-8735.
161. Shihabuddin LS, Numan S, Huff MR, Dodge JC, Clarke J, Macauley SL, Yang W, Taksir TV, Parsons G, Passini MA, Gage FH, and Stewart GR.

(2004) Intracerebral transplantation of adult mouse neural progenitor cells into the Niemann-Pick-A mouse leads to a marked decrease in lysosomal storage pathology. J Neurosci **24**(47): 10642-10651.
162. Shimazaki T, Shingo T, and Weiss S. (2001) The ciliary neurotrophic factor/leukemia inhibitory factor/gp130 receptor complex operates in the maintenance of mammalian forebrain neural stem cells. J Neurosci **21**(19): 7642-7653.
163. Skorupa AF, Fisher KJ, Wilson JM, Parente MK, and Wolfe JH. (1999) Sustained production of beta-glucuronidase from localized sites after AAV vector gene transfer results in widespread distribution of enzyme and reversal of lysosomal storage lesions in a large volume of brain in mucopolysaccharidosis VII mice. Exp Neurol **160**(1): 17-27.
164. Sly W, Quinton B, McAlister W, and Rimoin D. (1973) Beta-glucuronidase deficiency: report of clinical, radiological and biochemical features of a new mucopolysaccharidosis. J Pediatr **82**: 249-257.
165. Smith PM and Blakemore WF. (2000) Porcine neural progenitors require commitment to the oligodendrocyte lineage prior to transplantation in order to achieve significant remyelination of demyelinated lesions in the adult CNS. European Journal of Neuroscience **12**(7): 2414-2424.
166. Snyder EY, Deitcher DL, Walsh C, Arnold-Aldea S, Hartwieg EA, and Cepko CL. (1992) Multipotent neural cell lines can engraft and participate in development of mouse cerebellum. Cell **68**(1): 33-51.
167. Snyder EY, Taylor RM, and Wolfe JH. (1995) Neural progenitor cell engraftment corrects lysosomal storage throughout the MPS VII mouse brain. Nature **374**: 367-370.
168. Snyder EY, Yoon C, Flax JD, and Macklis JD. (1997) Multipotent neural precursors can differentiate toward replacement of neurons undergoing targeted apoptotic degeneration in adult mouse neocortex. Proc Natl Acad Sci U S A **94**(21): 11663-11668.
169. Song Y, Morikawa S, Morita M, Inubushi T, Takada T, Torii R, and Tooyama I. (2005) Magnetic resonance imaging using hemagglutinating virus of Japan-envelope vector successfully detects localization of intra-cardially administered microglia in normal mouse brain. Neurosci Lett.
170. Stein CS, Martins I, and Davidson BL. (2005) The lymphocytic choriomeningitis virus envelope glycoprotein targets lentiviral gene transfer vector to neural progenitors in the murine brain. Mol Ther **11**(3): 382-389.
171. Steinert PM, Chou YH, Prahlad V, Parry DA, Marekov LN, Wu KC, Jang SI, and Goldman RD. (1999) A high molecular weight intermediate filament-associated protein in BHK-21 cells is nestin, a type VI intermediate filament protein. Limited co-assembly in vitro to form heteropolymers with type III vimentin and type IV alpha-internexin. J Biol Chem **274**(14): 9881-9890.
172. Suhonen JO, Peterson DA, Ray J, and Gage FH. (1996) Differentiation of adult hippocampus-derived progenitors into olfactory neurons in vivo. Nature **383**(6601): 624-627.

173. Svendsen CN, Clarke DJ, Rosser AE, and Dunnett SB. (1996) Survival and differentiation of rat and human epidermal growth factor-responsive precursor cells following grafting into the lesioned adult central nervous system. Exp Neurol **137**(2): 376-388.
174. Swindle CS, Kim HG, and Klug CA. (2004) Mutation of CpGs in the murine stem cell virus retroviral vector long terminal repeat represses silencing in embryonic stem cells. J Biol Chem **279**(1): 34-41.
175. Tamaki S, Eckert K, He D, Sutton R, Doshe M, Jain G, Tushinski R, Reitsma M, Harris B, Tsukamoto A, Gage F, Weissman I, and Uchida N. (2002) Engraftment of sorted/expanded human central nervous system stem cells from fetal brain. J Neurosci Res **69**(6): 976-986.
176. Taylor RM and Wolfe JH. (1997) Decreased lysosomal storage in the adult MPS VII mouse brain in vicinity of grafts of retroviral vector-corrected fibroblasts secreting high levels of ß-glucuronidase. Nature Medicine **3**(7): 771-774.
177. Tramontin AD, Garcia-Verdugo JM, Lim DA, and Alvarez-Buylla A. (2003) Postnatal development of radial glia and the ventricular zone (VZ): a continuum of the neural stem cell compartment. Cereb Cortex **13**(6): 580-587.
178. Tropepe V, Sibilia M, Ciruna BG, Rossant J, Wagner EF, and van der Kooy D. (1999) Distinct neural stem cells proliferate in response to EGF and FGF in the developing mouse telencephalon. Dev Biol **208**(1): 166-188.
179. Uchida N, Buck DW, He DP, Reitsma MJ, Masek M, Phan TV, Tsukamoto AS, Gage FH, and Weissman IL. (2000) Direct isolation of human central nervous system stem cells. Proceedings of the National Academy of Sciences of the United States of America **97**(26): 14720-14725.
180. Vellodi A. (2005) Lysosomal storage disorders. Br J Haematol **128**(4): 413-431.
181. Vescovi AL, Parati EA, Gritti A, Poulin P, Ferrario M, Wanke E, Frolichsthal-Schoeller P, Cova L, Arcellana-Panlilio M, Colombo A, and Galli R. (1999) Isolation and cloning of multipotential stem cells from the embryonic human CNS and establishment of transplantable human neural stem cell lines by epigenetic stimulation. Exp Neurol **156**(1): 71-83.
182. Vroemen M, Weidner N, and Blesch A. (2005) Loss of gene expression in lentivirus- and retrovirus-transduced neural progenitor cells is correlated to migration and differentiation in the adult spinal cord. Exp Neurol **195**(1): 127-139.
183. Walkley SU. (1998) Cellular pathology of lysosomal storage disorders. Brain Pathol **8**(1): 175-193.
184. Walkley SU. (2004) Secondary accumulation of gangliosides in lysosomal storage disorders. Semin Cell Dev Biol **15**(4): 433-444.
185. Walkley SU, Thrall MA, Dobrenis K, Huang M, March PA, Siegel DA, and Wurzelmann S. (1994) Bone marrow transplantation corrects the enzyme defect in neurons of the central nervous system in a lysosomal storage disease. Proc Natl Acad Sci U S A **91**(8): 2970-2974.

186. Watson DJ, Kobinger GP, Passini MA, Wilson JM, and Wolfe JH. (2002) Targeted transduction patterns in the mouse brain by lentivirus vectors pseudotyped with VSV, Ebola, Mokola, LCMV, or MuLV envelope proteins. Mol Ther **5**(5 Pt 1): 528-537.
187. Watson DJ, Longhi L, Lee EB, Fulp CT, Fujimoto S, Royo NC, Passini MA, Trojanowski JQ, Lee VM, McIntosh TK, and Wolfe JH. (2003) Genetically modified NT2N human neuronal cells mediate long-term gene expression as CNS grafts in vivo and improve functional cognitive outcome following experimental traumatic brain injury. J Neuropathol Exp Neurol **62**(4): 368-380.
188. Weissman IL, Anderson DJ, and Gage F. (2001) Stem and progenitor cells: origins, phenotypes, lineage commitments, and transdifferentiations. Annu Rev Cell Dev Biol **17**: 387-403.
189. Whittemore SR, Morassutti DJ, Walters WM, Liu RH, and Magnuson DS. (1999) Mitogen and substrate differentially affect the lineage restriction of adult rat subventricular zone neural precursor cell populations. Exp Cell Res **252**(1): 75-95.
190. Wilson MT and Snow DM. (2000) Chondroitin sulfate proteoglycan expression pattern in hippocampal development: potential regulation of axon tract formation. J Comp Neurol **424**(3): 532-546.
191. Wolfe JH, Deshmane SL, and Fraser NW. (1992) Herpesvirus vector gene transfer and expression of beta-glucuronidase in the central nervous system of MPS VII mice. Nature Genetics **1**: 379-384.
192. Wolfe JH and Sands MS, *Murine Mucopolysaccharidosis Type VII: A Model System for Somatic Gene Therapy of the Central Nervous System*, in *Protocols for Gene Transfer in Neuroscience: Towards Gene Therapy of Neurological Disorders*, P.R. Lowenstein and L.W. Enquist, Editors. 1996, John Wiley & Sons Ltd.: New York. p. 263-274.
193. Wolfe JH, Schuchman EH, Stramm LE, Concaugh EA, Haskins ME, Aguirre GD, Patterson DF, Desnick RJ, and Gilboa E. (1990) Restoration of normal lysosomal function in mucopolysaccharidosis type VII cells by retroviral vector-mediated gene transfer. Proc Natl Acad Sci U S A **87**(8): 2877-2881.
194. Wu P, Ye Y, and Svendsen CN. (2002) Transduction of human neural progenitor cells using recombinant adeno-associated viral vectors. Gene Ther **9**(4): 245-255.
195. Yandava BD, Billinghurst LL, and Snyder EY. (1999) "Global" cell replacement is feasible via neural stem cell transplantation: evidence from the dysmyelinated shiverer mouse brain. Proc Natl Acad Sci U S A **96**(12): 7029-7034.
196. Zelivyanskaya ML, Nelson JA, Poluektova L, Uberti M, Mellon M, Gendelman HE, and Boska MD. (2003) Tracking superparamagnetic iron oxide labeled monocytes in brain by high-field magnetic resonance imaging. J Neurosci Res **73**(3): 284-295.

197. Zhang L and Goldman JE. (1996) Developmental fates and migratory pathways of dividing progenitors in the postnatal rat cerebellum. J Comp Neurol **370**(4): 536-550.
198. Zhang L and Goldman JE. (1996) Generation of cerebellar interneurons from dividing progenitors in white matter. Neuron **16**(1): 47-54.
199. Zhang SC. (2001) Defining glial cells during CNS development. Nat Rev Neurosci **2**(11): 840-843.
200. Zhang SC, Lipsitz D, and Duncan ID. (1998) Self-renewing canine oligodendroglial progenitor expanded as oligospheres. J Neurosci Res **54**(2): 181-190.
201. Zhang ZG, Jiang Q, Zhang R, Zhang L, Wang L, Arniego P, Ho KL, and Chopp M. (2003) Magnetic resonance imaging and neurosphere therapy of stroke in rat. Ann Neurol **53**(2): 259-263.
202. Zhu G, Mehler MF, Mabie PC, and Kessler JA. (1999) Developmental changes in progenitor cell responsiveness to cytokines. J Neurosci Res **56**(2): 131-145.
203. Zhu G, Mehler MF, Zhao J, Yu Yung S, and Kessler JA. (1999) Sonic hedgehog and BMP2 exert opposing actions on proliferation and differentiation of embryonic neural progenitor cells. Developmental Biology (Orlando) **215**(1): 118-129.